Analysis of Quality Factor and Resonance Frequency Measurements of RFID Transponders

Verification and comparison of RFID measurement methods

Bachelor Thesis

Submitted in Fulfillment of the Degree
Bachelor of Science

University of Applied Sciences Vorarlberg

Carried Out at
Omicron Lab

Submitted to
DI Dr. Reinhard Schneider

Handed in by
Martin Dietmar Bitschnau

Dornbirn, June 18, 2016

Abstract

The thesis is regarding the quality factor measurement and the resonance frequency measurement of RFID transponders. For the measurement of this two characteristics, several methods are available. Some of them are even based on different definitions. In professional literature the difference of the methods is hardly explained. Also the theoretical background of the measurement is described sparsely. The purpose of this thesis is to examine these measurement methods and their background. The assumptions and simplifications that are made get revealed. The measurement methods are applied, and physical measurements are conducted. The results are documented and analyzed in order to detect possible trends and dependencies. Based on the gained knowledge of this measurement methods, computer aided programs are used to assess the error made with the different measurement methods. Additionally, the influence of the parasitic coupling capacitance between an RFID antenna and the reader coil is analyzed. This examination is also performed with physical measurements as well as simulations.

Kurzreferat

Diese Bachelorarbeit beschäftigt sich mit der Gütemessung sowie mit der Resonanzfrequenzmessung von RFID Transpondern. Für diese zwei Merkmale gibt es mehrere mögliche Messmethoden. Einige davon basieren sogar auf unterschiedlichen Definitionen. In der Fachliteratur sind die Unterschiede dieser Methoden bzw. deren Hintergrund auf dem sie beruhen, nur sehr vage beschrieben. Eines der Ziele dieser Arbeit ist diese Messmethoden zu analysieren, das heißt, herauszufinden unter welchen Voraussetzungen diese gültig sind und mit welchen Vereinfachungen diese arbeiten. Die Messungen werden physikalisch durchgeführt und die Ergebnisse dokumentiert und analysiert, um eventuelle Abhängigkeiten von Parametern und Einflüssen feststellen zu können. Mit Hilfe einer computergestützten Simulation werden potentielle Fehler der unterschiedlichen Messmethoden aufgedeckt. Der Einfluss einer parasitären Koppelkapazität, die zwischen RFID Antenne und Lesespule wirkt, wird ebenfalls untersucht. Dies geschieht ebenso mit physikalischen Messungen sowie mit Simulationsprogrammen.

Table of Contents

List of Figures

List of Tables

List of Abbreviations and Symbols

ECD	Equivalent Circuit Diagram
PCB	Printed Circuit Board
Q	Quality Factor, Q Factor or Q Value
RFID	Radio-Frequency Identification
DUT	Device under Test
k	Coupling Factor
M	Mutual Inductance
N	Number of Windings
AC	Alternating Current
RMS	Root Mean Square or Quadratic Mean Value
PICC	Proximity Integrated Circuit Card

1 Introduction

RFID measurements are interesting for chip manufacturers, card manufacturers and systems integrators dealing with RFID systems. For chip manufacturers it is interesting for an obvious reason. Card manufacturers need the same measurements to adjust the added components to the RFID chip. The lamination process, for instance, also affects the quality factor of the used chip. (“CQM Requirements” 2013, 196) The integration of RFID components into another system can affect the characteristics too. Therefore, a system integrator also needs to verify the RFID systems parameters after the integration process. Relevant measurements are for example the respond field strength measurement, the resonance frequency measurement and the quality factor measurement.

Measurements are often conducted with assumptions and simplifications. This results from the fact that parameters often cannot be measured directly. That applies to the resonance frequency and quality factor measurement too. Furthermore, for the quality factor measurement, several methods do exist. Due to the assumptions, simplifications and method diversity the obtained results differ. For OMICRON electronics’ network analyzer Bode 100, an add-on device, capable of measuring RFID antennas’ characteristics, has been designed. For this reason, it is desirable to have sufficient know-how about the measurements regarding the accuracy, practicability and their sensitivity under certain conditions. In established literature this issue is not discussed. Therefore, the thesis is regarding this point to gain knowledge in this field. The goal is to investigate if statements about the mentioned points can be made in order to make a decision between the possible measurement methods and be aware of the possible measurement errors. The detailed definition of the thesis’ scope is stated in chapter 2 “Definition of Task”. The required background knowledge is explained in chapter 3 “Technical Background”. Chapter 4 “Approach” mentions the way of proceeding. In chapter 5 “Execution” the required tasks are performed and the way of performing is described in detail. The outcomes of the thesis are evaluated in chapter 6 “Results”. Chapter 7 “Concluding Chapter” summarizes the gained key data and facts.

2 Definition of Task

The outcome of this thesis is a comparison of the different measurement methods. This is done physically as well as theoretically. On the one hand it should be evaluated how good the physical measurements coincide with the measurement theory. On the other hand, the measurement methods get theoretically analyzed in order to obtain a statement about their accuracy depending on different conditions. The goal of the thesis is to analyze the accuracy of the measurement methods under different conditions. This provides an opportunity to choose the best suitable measurement methods for certain conditions.

The thesis deals with the quality factor (Q-factor) measurement and the resonance frequency measurement evaluation. Measurement evaluations of other RFID-transponder characteristics are not considered. Furthermore, just RFID transponders using the magnetic field for coupling are regarded. RFID systems with capacitive coupling are not considered. The used signal strength has always to be small enough to avoid activating[1] the RFID-chip. Only the most often used 13.56MHz RFID cards (Finkenzeller 2008, 175) with a passive[2] voltage supply are measured. However, the findings derived from the simulations also apply for other frequency ranges which use the same ECD (equivalent circuit diagram) as shown in Figure 3. As a DUT (device under test), an ID-1 card, defined in ISO/IEC 7810:2003, is used if not specified otherwise. An ID-1 card has the standard dimension of approximately 85.60mm x 53.98mm - like a debit card for example. The design process of the RFID reader coils is not covered in this thesis. However, important details concerning it are addressed.

All important findings are displayed in appropriate tables and diagrams and are described.

[1] By speaking of “activating the RFID-chip”, activating the RFID-chips load modulation is meant, which is a process for transmitting information from the chip to the reading device. A small overview about this load modulation is provided in section 3.3 on page 7

[2] The type of the RFID-transponders voltage control can be active and passive. An RFID-chip on a transponder with a passive supply voltage is solely supplied with the energy transmitted by the reading device. More information about the transponders supply voltage is given in section 3.4 on page 8

3 Technical Background

This chapter provides the required knowledge to understand this thesis. Here just the basics are explained. The more detailed analyses are carried out in the corresponding sections in the subsequent chapters.

3.1 Inductive coupling

As this thesis concerns inductively coupled RFID antennas, it is standing to reason that the theory of magnetic coupling is necessary for describing the principle. In all the derivations used in this thesis it is assumed that the magnetic flux Φ through a coil is the same in all windings. Inductive coupling is based on the common magnetic flux Φ. Figure 1 supports and visualizes the following explanation.

Assuming that a current I_1 is flowing through a single winding loop with the winding area A_1, then it causes a magnetic flux Φ_1. Φ_{12} is the part of this magnetic flux Φ_1 which is going through a second single winding loop with the area A_2. If two windings have a common magnetic flux they are inductively coupled. Furthermore, it is assumed that the current $\underline{I_1}$ through winding 1 is alternating. In this case the law of induction [3.1] causes a voltage $u(t)$ in the second winding which leads to the current $\underline{I_2}$. N in equation [3.1] is the number of windings. This equation, however, only is valid if the same magnetic flux Φ goes through all windings.

$$u(t) = -N \cdot \frac{d\Phi}{dt} \qquad [3.1]$$

The part of the overall magnetic flux Φ_1, which is not inductively coupled with the second winding, is called stray flux and is referred to as Φ_{10}. The relative amount of the common magnetic flux is described with the so called k-factor or coupling factor k. Therefore, the overall magnetic flux Φ_1 ,produced in the winding 1, can be separated into two parts using the coupling factor k. (equation [3.2])

$$\Phi_1 = \Phi_{10} + \Phi_{12} = \Phi_1 \cdot (1 - k_1) + \Phi_1 \cdot k_1 \qquad [3.2]$$

Of course it would work as well if an alternating current in the winding two would cause a magnetic flux Φ_2 and a certain part $\Phi_{21} = k_2 \cdot \Phi_2$ would cause a current $\underline{I_1}$ in winding one.

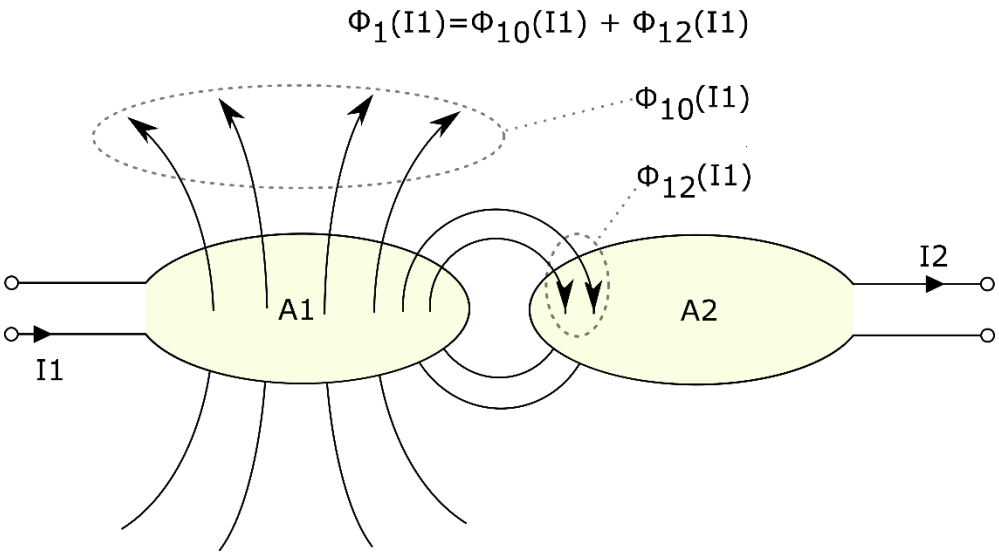

Figure 1: Theory of Inductive Coupling

Source: (based on Finkenzeller 2008, 77)

For an easier calculation it is common to use the mutual inductance M. In the calculation M is handled in the same way as an inductance L is. However, physically it is not existing. Hence, it can be seen as an imaginary inductance between two inductively coupled coils like shown in Figure 2. $L_1 - M$ and $L_2 - M$ are the stray inductances. The common magnetic flux Φ_{12} goes through M and the magnetic stray flux Φ_{10} respectively Φ_{20} goes through the stray inductances.

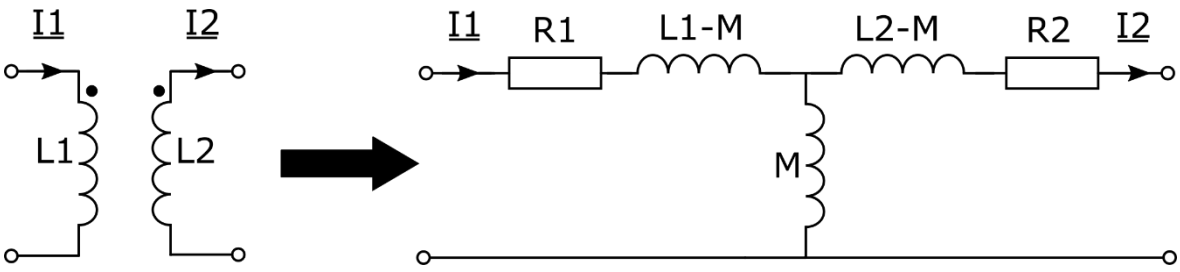

Figure 2: Two Views of Inductively Coupled Circuits.

On the left side of the arrow the components of the circuit do all physically exist. The circuit on the right side, however, shows components which do not all have physical character. As mentioned the current $\underline{I_1}$ of the primary winding induces a voltage $\underline{U_2}$ in the secondary winding and vice versa. The mutual inductance M is derived by the equation where both of this variables are mathematically connected in. The common magnetic flux, responsible for the inductive coupling, is calculated by equation [3.3], whereby Λ is a factor only determined

by the geometry of the coil and the environments permeability. Hence it is regarded as a constant as both is considered unchanging.[3]

$$\phi_{12} = \Phi_1 k_{12} = N_1 i_1 \Lambda_1 k_{12} \qquad \text{resp.} \qquad \phi_{21} = \Phi_2 k_{21} = N_2 i_2 \Lambda_2 k_{21} \qquad [3.3]$$

In order to get the induced voltage u, equation [3.3] has to be differentiated with respect to t and multiplied with $-N$ like stated in equation [3.1]. This results in:

$$u_{2_{ind}} = -N_2 N_1 \Lambda_1 k_{12} \frac{di_1}{dt} \qquad \text{resp.} \qquad u_{1_{ind}} = -N_1 N_2 \Lambda_2 k_{21} \frac{di_2}{dt} \qquad [3.4]$$

As it can be seen, equation [3.4] has the pattern of the self-inductance equation $u = L \cdot \frac{di}{dt}$, and therefore the constant factor in front of the differentiated current becomes the mutual inductance M like shown in equation [3.5].

$$u_{2_{ind}} = -M_{12} \frac{di_1}{dt} \qquad \text{resp.} \qquad u_{1_{ind}} = -M_{21} \frac{di_2}{dt} \qquad [3.5]$$

At this point, however, some literature claim that M_{12} is equal to M_{21}. This, however, only is the case for some transformers. If the two coils have different sizes, the magnetic permeance Λ differs as well as the coupling factors k. Only if the geometry of both coils is the same, this is valid. In this thesis this simplification is also used because it does not affect the simulation results. However, it is important to be aware of this fact.

3.2 Equivalent Circuit Diagram

The generally used ECD is displayed in Figure 3.

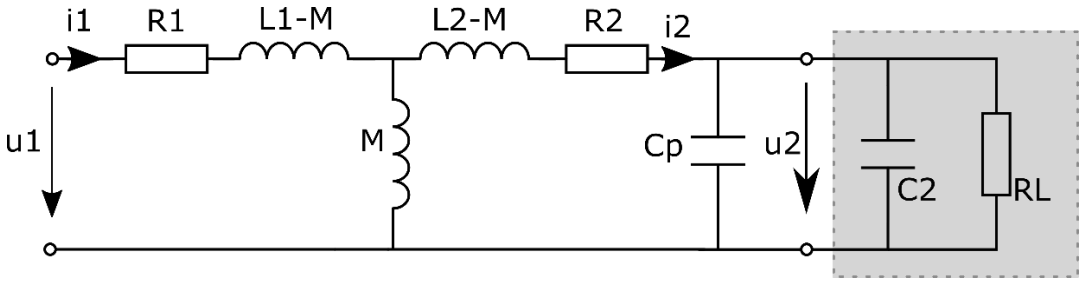

Figure 3: ECD of Magnetic Coupled RFID Transponder and Reader Coil

[3] Some special RFID transponders do use ferrite cores to increase the mutual inductance M. In this case μ_r is dependent on the frequency and the temperature and has to be regarded. Such ferrite RFID transponders are necessary when very small chips are required. As an example, it is used in animal identification chips. (Finkenzeller 2008, 120)

The reader coil can be seen on the left side. It consists of the Inductance L_1 and the parasitic resistance R_1 which constitutes the copper losses. The secondary side (elements to the right of the mutual inductance M) shows the ECD of the RFID card. R_2 also constitutes the copper losses of the RFID antenna. The capacitor C_2 and the resistor R_L in the gray box represent the RFID-chip. The functionality of the chip is not explained in this thesis, as it never gets activated during the measurement. C_2 and the parasitic capacitance C_p in combination with the inductance L_2 are designed in a way to ensure that the circuit has its resonance frequency at about 13.56MHz. Usually the resonance frequency is higher than 13.56MHz for anti-collision reasons. The resonance frequency often is chosen to be 1 to 5 MHz higher in order to keep the performance higher in the event that two or more transponders are in the area of a reading device. Reason for that is the fact that two transponders have a smaller resonance frequency than one transponder. (Finkenzeller 2008, 82)

3.3 Load modulation

In this thesis the load modulation theory is hardly used, yet for some explanations it is required to mention. For that reason, this part is kept short and should just provide an overview.

Among other methods the load modulation is the most often used way for information interchange of RFID systems. When performing load modulation, parameters of the RFID transponder circuit are changed. The variable parameters in the transponder circuit is either the chip resistance R_L or the chip capacitance C_2. In Figure 4 the two capacitances C_p and C_2 have been added up and referred to as C. The gray component represents a capacitance C_{mod} or a resistor R_{mod} depending on the used variant of load modulation. Hence, a distinction is made between resistive and capacitive load modulation (Finkenzeller 2008, 107). If the chip gets activated, the load gets switched on and off. This can theoretical be rated as opening and closing the switch in Figure 4. This happens with the modulation frequency f_M.

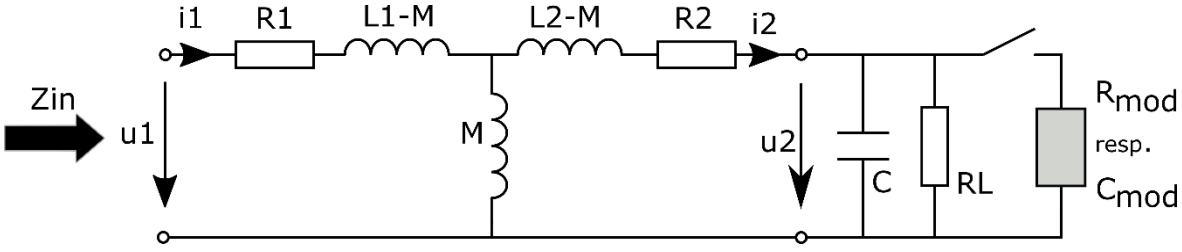

Figure 4: Visualization of a Simple Load Modulation Process.

The change of one of these parameters causes a change of the transponder's impedance. As the transponder and the reader coil are inductively coupled, this change in the impedance is also detectable on the primary side. Figure 5 shows the circuit of the inductively coupled reader coil. $\underline{Z}'$, in this circuit, is the transformed transponder impedance. The evidence that the input impedance is a series connection of the three components shown in Figure 5 is supplied in section 5.2.

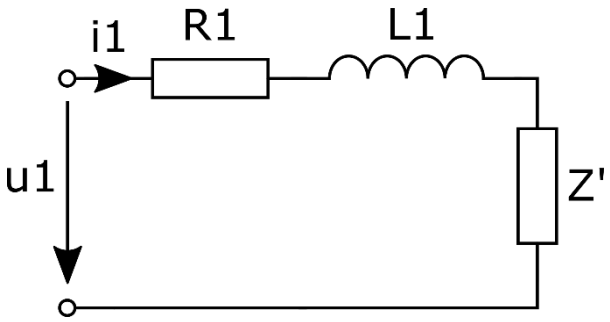

Figure 5: Schematic of the Circuit with the Transformed Impedance $\underline{Z}'$

The transformed transponder impedance $\underline{Z}'$ is changed with the frequency of the data stream f_M. This results in modulation sidebands at $f_0 - f_M$ and $f_0 + f_M$ like shown in Figure 6. The transponders information is in this sidebands. Therefore, it is necessary to ensure that this sidebands' levels are sufficiently high. The displayed curve in this figure is the impedance $\underline{Z}'$. It is common that the peak of $\underline{Z}'$ is not at the center frequency f_c because of the anti-collision precaution which was mentioned in section 3.2. This also affects the levels of the modulation sideband which is also visualized in Figure 6.

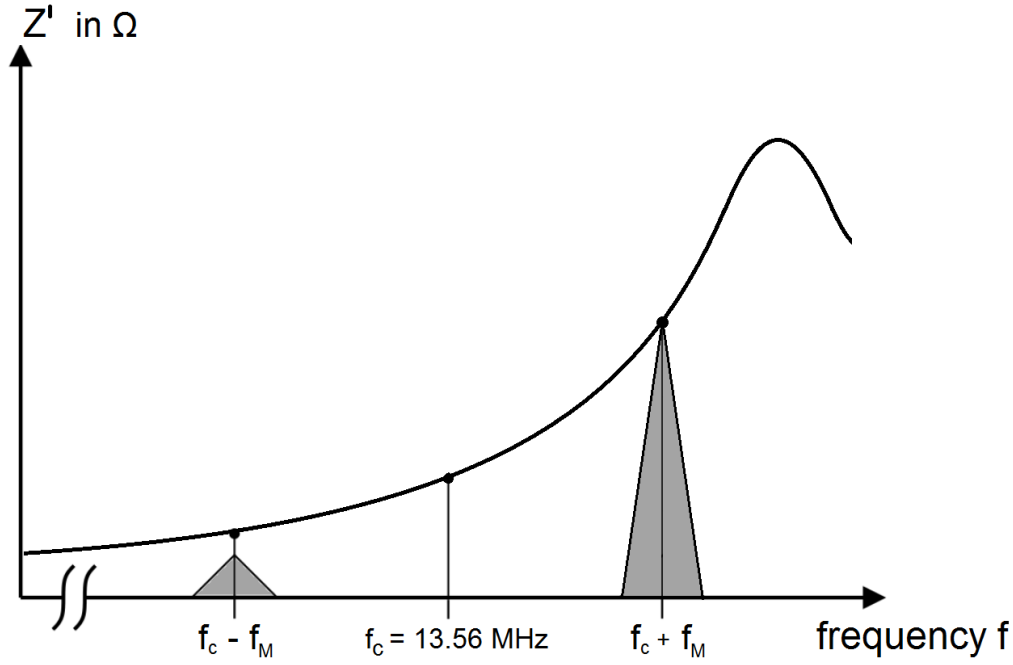

Figure 6: Load modulation with modulation sidebands
Source: (based on Finkenzeller 2008, 112)

3.4 RFID Chip's Supply Voltage

Generally, there are two different types of transponders regarding the supply voltage. The active and the passive ones. Both do require the induced voltage form the reading coil. The active RFID transponder uses the induced voltage just as a wake-up-signal. If the voltage u_2 shown in Figure 3 on page 5 reaches a certain value, the RFID chip gets activated and uses the implemented battery to perform the information transaction. After the information is transmitted or if the induced voltage u_2 drops under a certain limit, the chip again gets into the sleep mode. A passive RFID transponder needs the induced energy for the whole information transmission. For the RFID chip this induced voltage u_2 has to be rectified and kept constant at the voltage level the chip requires. (Finkenzeller 2008, 87)

The basic principle can be seen in Figure 7. The circuit shown in Figure 3 has been modified by just adding a shunt resistance parallel to the RFID chip. The parasitic capacitance C_p and the chips capacitance C_2 have been added up.

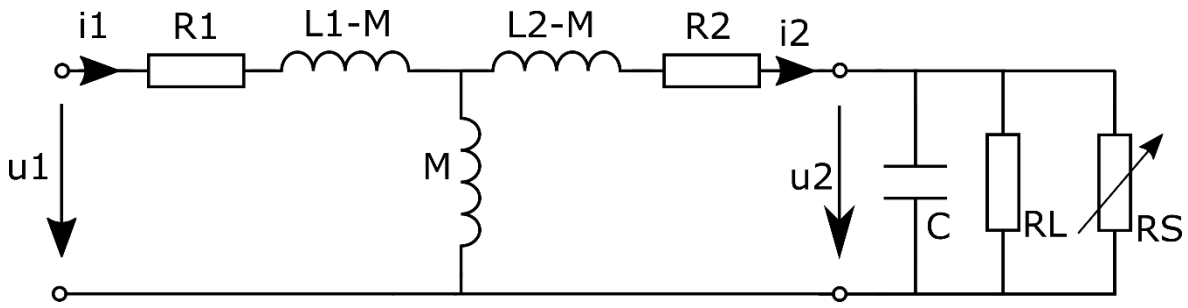

Figure 7: Basic Principle of the Voltage Control with a Shunt

Source: (based on Finkenzeller 2008, 87)

The shunt resistance's purpose is to change its value in order to ensure a constant supply voltage for the RFID chip. In order to do so, R_S ranges from $10^5\Omega$ down to a few 10Ω depending on the coupling factor k. (Finkenzeller 2008, 89)

This of course affects the transponders impedance and hence the quality factor Q. For the Q factor measurement this kind of behavior has to be regarded in order to obtain comparable measurement results. In chapter 4 it is elaborated how this can be ensured.

3.5 Resonance Frequency f_0

The resonance frequency in general is the frequency, where the amplitude in a vibrating system is higher than at adjacent frequencies. In resonant circuits the established definition of this frequency f_0 is the frequency where the impedance is purely resistive. For RFID transponders, the resonance frequency f_0 is defined as the frequency where the voltage across the RFID chip reaches its maximum. This is the voltage of interest because it is crucial for the voltage supply of the RFID chip. (see section 3.4) Hence, the voltage $\underline{U_2}$ across these chip elements has to be mathematically described. For the calculation, the two capacitances C_p and C_2 are combined and referred to as C. The shunt resistor R_s, displayed in Figure 7, has been consolidated with R_L and is considered constant over the frequency. Doing all this, results in the ECD shown in Figure 8 which is used for explanation and calculation purposes in this section if not specified otherwise.

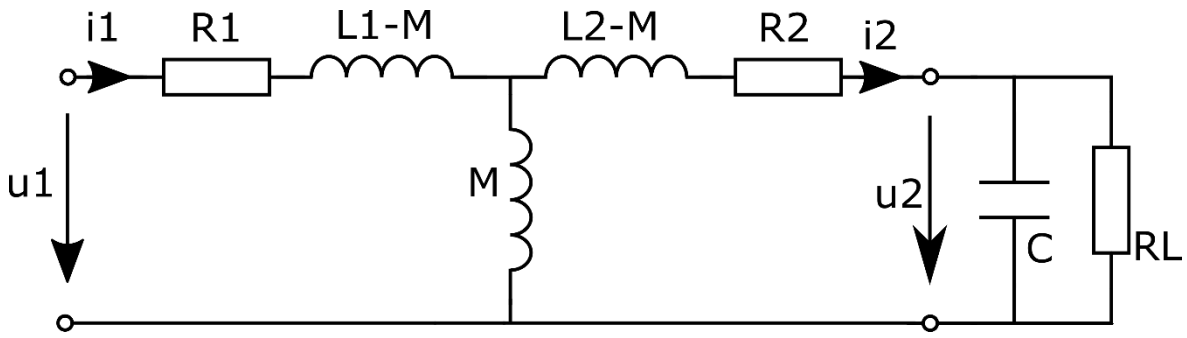

Figure 8: ECD of the Inductively Coupled Reader Coil and Transponder

By using Kirchhoff's voltage law, equation [3.6] is derived.

$$\underline{U_2} = j\omega M I_1 - I_2 \cdot (j\omega L_2 + R_2) \qquad [3.6]$$

To get rid of the current $\underline{I_2}$, the second equation [3.7] is set up.

$$\underline{I_2} = \underline{U_2} \cdot \frac{j\omega C R_L + 1}{R_L} \qquad [3.7]$$

Unifying both, equation [3.6] and [3.7] results in [3.8]

$$\underline{U_2} = \underline{I_1} \cdot \frac{j\omega M}{\left(1 + \frac{R_2}{R_L} - \omega^2 C L_2\right) + j\omega \cdot \left(\frac{L_2}{R_L} + C R_2\right)} \qquad [3.8]$$

At this point, a look should be taken at Figure 9. It shows the ECD of the inductively coupled transponder side. u_{Q2} is the induced voltage $j\omega M\underline{I_1}$. In order to analyze the transponder independently from the reader coil, the current $\underline{I_1}$ is considered to have a constant RMS (root mean square) value independent of the circular frequency ω. This also leads to a voltage u_{Q2} with a constant RMS value. The RMS value of the current $\underline{I_1}$ can only be constant over the frequency if a current source is used to supply the reader coil instead of a voltage source. Even though this usually is not the case, it is considered this way because the common measurement methods are based on this assumption. The consulted literature does not mention this assumption, however, in section 5.2 and 5.3 it is shown that the measurement results are just valid for an $\underline{I_1}$ with a constant RMS value. At the end of this section, on page 12, the voltage $\underline{U_2}$ is calculated again assuming that a common voltage source is used to supply the reader coil.

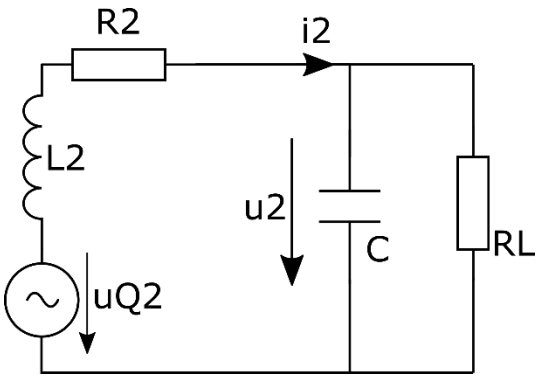

Figure 9: ECD of the Inductively Coupled Transponder

To get the frequency f_0 where the voltage $\underline{U_2}$ reaches its maximum, the absolute value of $\underline{U_2}$ in equation [3.9] has to be differentiated with respect to the circular frequency ω ([3.10]). This equation has to be set equal to zero in order to find the maximum ([3.11]). Finally, it is solved for ω to get the circular resonance frequency ω_0 ([3.12]).

The absolute value $\left|\underline{U_2}\right|$ is:

$$\left|\underline{U_2}\right| = \frac{\omega M |\underline{I_1}|}{\sqrt{\left(1 + \frac{R_2}{R_L} - \omega^2 C L_2\right)^2 + \omega^2 \cdot \left(\frac{L_2}{R_L} + C R_2\right)^2}}$$

$$= \frac{\omega M |\underline{I_1}|}{\sqrt{\omega^4 \cdot (C^2 L_2^2) + \omega^2 \cdot \left(\frac{L_2^2}{R_L^2} + C^2 R_2^2 - 2CL_2\right) + \left(1 + \frac{2R_2}{R_L} + \frac{R_2^2}{R_L^2}\right)}} \qquad [3.9]$$

$$For\ more\ clearness\ the\ auxiliary\ variables\ D, E, F\ and\ G\ are\ used$$

$$= \frac{\omega M |\underline{I_1}|}{\sqrt{\omega^4 \cdot D + \omega^2 \cdot E + F}} = \frac{\omega M |\underline{I_1}|}{\sqrt{G}}$$

After the differentiation it results in:

$$\frac{d\left|\underline{U_2}\right|}{d\omega} = \frac{M\underline{I_1} \cdot \sqrt{G} - \frac{\omega M \underline{I_1} \cdot (4\omega^3 D + 2\omega \cdot E)}{2 \cdot \sqrt{G}}}{G} \qquad [3.10]$$

Setting equal to zero and changing the variable name ω to ω_0 as it is the circular resonance frequency, yields in:

$$\frac{d|\underline{U_2}|}{d\omega} := 0 = G - (2\omega_0^4 D + \omega_0^2 \cdot E) = -\omega_0^4 \cdot D + F =$$

$$= -\omega_0^4 (C^2 L_2^2) + \left(1 + \frac{2R_2}{R_L} + \frac{R_2^2}{R_L^2}\right) =$$

$$= \omega_0^4 - \frac{1}{C^2 L_2^2} + \frac{2R_2}{R_L C^2 L_2^2} + \frac{R_2^2}{R_L^2 C^2 L_2^2} =$$

$$= \omega_0^4 - \frac{(R_L + R_2)^2}{C^2 L_2^2 R_L^2} \qquad [3.11]$$

Solving for ω_0:

$$\omega_0 = \sqrt{\frac{R_L + R_2}{C L_2 R_L}} = \sqrt{\frac{1 + \frac{R_2}{R_L}}{C L_2}} \qquad [3.12]$$

The parasitic resistance R_2 is several orders of magnitude lower than the chip resistance R_L. Hence, the resonance circular frequency $\omega_0 = 2\pi f_0$ can be simplified to equation [3.13].

$$\omega_0 \approx \sqrt{\frac{1}{C L_2}} \qquad [3.13]$$

The relative error made with the simplification in equation [3.13] is not constant, but rather dependent on the magnetic field strength available for the transponder. Depending on this strength, the chip resistance R_L is changing because of either the load modulation, (explained in section 3.3) or the RFID chip's voltage control (explained in section 3.4). The RFID chip's voltage control is initiated at a much lower field strength than the load modulation. Additionally, the capacitance C is also dependent on the signal strength due to parasitic semiconductor effects. (Finkenzeller 2008, 103)

Now, it is analyzed how an AC voltage source with a constant RMS influences the voltage $\underline{U_2}$. As the current source gets replaced by a voltage source, the current $\underline{I_1}$ is not constant anymore, but rather depending on the impedance connected to the source. For that reason, equation [3.8] has to be modified. The current $\underline{I_1}$ in this equation has to be expressed by the supply voltage $\underline{U_1}$. By applying mesh analysis at the reader coil loop, $\underline{I_1}$ is calculated with equation [3.14]

$$\underline{I_1} = \frac{\underline{U_1} + \underline{I_2} \cdot j\omega M}{j\omega L_1 + R_1} \qquad [3.14]$$

Together with equation [3.7] for $\underline{I_2}$, $\underline{I_1}$ can be expressed as a function of $\underline{U_1}$ and $\underline{U_2}$ (equation [3.15]).

$$\underline{I_1} = \frac{\underline{U_1} + \underline{U_2} \cdot \frac{j\omega C R_L + 1}{R_L} \cdot j\omega M}{j\omega L_1 + R_1} \qquad [3.15]$$

Inserting the formula for $\underline{I_1}$ in equation [3.8] and rearranging it for $\underline{U_2}$, results in equation [3.16]. This equation states the correct value of the voltage across the chip resistor R_L if the reader coil consists of a series connection of an AC voltage source $\underline{U_1}$, a series resistance R_1 and the inductance of the reader coil L_1.

$$\underline{U_2} = \frac{j\omega M R_L \underline{U_1}}{\left(\left(1 + \frac{R_2}{R_L} - \omega^2 C L_2\right) + j\omega \cdot \left(\frac{L_2}{R_L} + C R_2\right)\right)(j\omega L_1 + R_1)R_L + \omega^2 M^2 (j\omega C R_L + 1)} \qquad [3.16]$$

The frequency where $\underline{U_2}$ of equation [3.16] gets maximal cannot be derived analytically with generally valid assumptions. In the appendix on page 68 and 69, it is shown that the derivation of ω_0 is not successful. For this purpose, a simulation or other numerical methods have to be used. Unlike equation [3.8], where $\underline{I_1}$was assumed to be constant, equation [3.16] is now dependent on the reader coil circuit elements and the mutual inductance M. Hence, the frequency where the voltage $\underline{U_2}$ gets maximal depends on the whole RFID system consisting of the reader coil and the transponder. The derived equations [3.9] to [3.13] that assume the use of an AC current source are relevant for the measurement, even though no such current source is used. The Bode 100 also does not use a current source, but still the measurement results obtain the theoretical resonance frequency. By speaking of “theoretical resonance frequency”, the frequency describing the resonance frequency of an equal system, however, supplied by an AC current source with a constant RMS value, is meant. In section 5.2, it is explained how the theoretical resonance frequency can be measured. How meaningful this theoretical resonance frequency of the transponder is in a system with a voltage source, is analyzed and explained in chapter 6.

3.6 Quality factor Q

The quality factor Q, in general, provides information about how damped an oscillator is. A high Q goes along with a higher resonance peak value and a smaller bandwidth and vice versa. Figure 10 shows the frequency response of a random oscillating system. In general, no statement about the ideal Q factor can be made because it always depends on the purpose of the system. By taking a look at the quality factor of RFID transponders in

particular, the ideal Q factor is still dependent on the purpose. Section 3.6.2 provides more information about this issue.

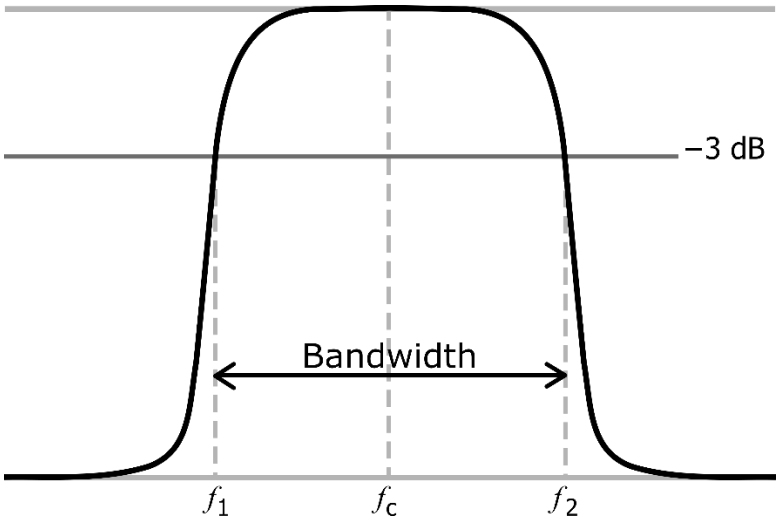

Figure 10: Graph of a Damped Oscillator
Source: (Wikipedia 2016)

3.6.1 Definitions

Generally, there are two common but different definitions for the Q factor. In German literature this two definitions are often used without differentiating, however, they are not equivalent. One definition is the resonance frequency to bandwidth ratio. (equation [3.17])

$$Q = \frac{f_0}{f_{BW}} = \frac{\omega_0}{\omega_{BW}} \qquad [3.17]$$

The bandwidth is the frequency range between the two frequencies where the observed signal's power is half the size of the maximum power at resonance frequency. A reduction of the power by $1/2$ of the value is approximately $-3dB$ like it is shown in Figure 10.

The other definition of the quality factor is the ratio of the maximal energy stored in the resonance circuit to the energy dissipated per cycle. (equation [3.18]) (Wikipedia 2016)

$$Q = 2\pi \cdot \frac{Energy\ stored}{Energy\ dissipated\ per\ Cycle} = 2\pi f_0 \cdot \frac{Energy\ stored}{Power\ loss} \qquad [3.18]$$

The two definitions get approximately equivalent for high Q values (Wikipedia 2016)

3.6.2 Expressiveness in Terms of RFID Systems

To ensure that an RFID transponder receives enough energy to operate, a high Q is beneficial because the maximum voltage at resonance is higher in that case. The problem, however, is that the concomitant smaller bandwidth requires that the frequency the reading coil sends is fine-tuned with the transponders resonance frequency. On the other hand, however, there are several things that require a lower Q factor. The anti-collision precaution mentioned in 3.2 requires the transponders resonance frequency to be above the reader coils frequency of $13.56\ MHz$. Hence, the possible Q factor is already limited for bandwidth reasons. The other limiting factor is the transmission of the information from the RFID transponder to the reader coil. Even if the chip gets enough energy form the reader coil to work, it is unclear if the information the transponder sends is received at the reader coil side. To ensure this, the modulation sideband levels, shown in Figure 6, have to be big enough so that they can be received. Therefore, the bandwidth has to be sufficiently high. In Figure 6, it also can be seen that the levels of the sidebands are also dependent on the transponder's resonance frequency. Obviously the Q factor has to be a trade-off between the maximal distance for the energy supply of the transponder and the maximal communication distance. Ideally, the Q factor is chosen to be in the middle so that both distances are equal. (Finkenzeller 2008, 113)

4 Approach

The framework conditions of this thesis are already mentioned in section 2 on page 2. This chapter provides a more exact scheme of the thesis' methodology.

As a first step, information about all the possible measurement methods are gathered and examined theoretically. That means, the thoughts behind the methods have to be fully comprehensible. This goes along with revealing all the made assumptions and simplifications. All these methods are based on an ECD that is used in the common RFID literature (Figure 7). This ECD is assessed in terms of correspondence between a simulation model and a real DUT. This is done by ascertaining if a simulation of the ECD with parameters of an existing DUT results in the same frequency response. The parameter values for the ECD have to be obtained from a real RFID transponder. To measure this discrete elements, a contact measurement with an RFID transponder is performed. For that reason, an RFID transponder, able to be physically contacted, like shown in Figure 11, is used.

Figure 11: Transparent Foil with RFID Antenna and Chip

After the ECD verification, a standard ID-1[4] card is used. Measurements are performed with all the gathered measurement methods. Parameters that can physically be varied, like the coupling factor k, are changed in order to detect trends and possible influences. Other

[4] According to ISO/IEC 7810:2003 the ID-1 has the dimensions of approximately 85.60mm x 53.98mm like a debit card

variable parameters are the signal strength and the parasitic coupling capacitance. It is important to keep in mind that the signal strength also affects the impedance of the transponder due to the voltage control mentioned in section 3.4 on page 8 and other parasitic effects. Hence, it is mandatory to think about which measurements can be compared in what kind of way. The physical measurements also give a feedback about the measurement's repeatability and therefore their practicability. The trends and deviations of the practicable methods get compared to the simulation. The parasitic coupling capacitance is not considered at first. To create an ECD simulation model with nominal values, this values get measured in advance. Information about how these measurements are performed is provided in chapter 5 when it is actually conducted. The simulation fully relies on the used ECD and shows the theoretically exact values according to their definition. Furthermore, the measurement methods are also simulated and their results get compared to the results according to the definitions. The advantage of the simulation is the variable parameters. The measurement methods are repetitively simulated with different parameter values. This is done in order to expose possible dependencies of the measurement methods. It also gets assessed if these dependencies change when other parameters of the ECD are changed too. After that, the parasitic coupling capacity is added to the ECD to see the possible influence while performing a close coupled measurement. A close coupled measurement is a measurement where the RFID card lies directly on top of the reader coil.

The simulation is divided into two parts and uses two programs. First the network analysis of the ECD is performed with the spice program Qucs. An AC analysis is performed in order to obtain the frequency response of the RFID system. The generated data afterwards gets processed in a MATLAB script to calculate all measurement results. The reason why this is separated in those two steps instead of calculating everything in MATLAB, is that the ECD can simply be changed in the spice program without the need to adapt the MATLAB script. A detailed description of the different simulations is given in chapter 5. The comparison of the measurement methods is done in chapter 6.

5 Execution

In this chapter the things mentioned in chapter 4 are put into operation. A detailed explanation of the measurement and simulation steps is provided. These explanations just have an exemplary character. If several measurements of the same type are conducted it is mentioned, however, not explained again. Results are descriptively presented in chapter 6. All the obtained measurement plots can be seen in the appendix.

5.1 Used Equipment and Tools

For the physical measurements, the Bode 100 vector network analyzer is used. All measurements that require an inductive coupling are conducted with self-designed reader coils. (Figure 12) The topic of this thesis does not regard the design of this reader coils, however, at this point, an overview of the ideas behind such a reader coil design is presented.

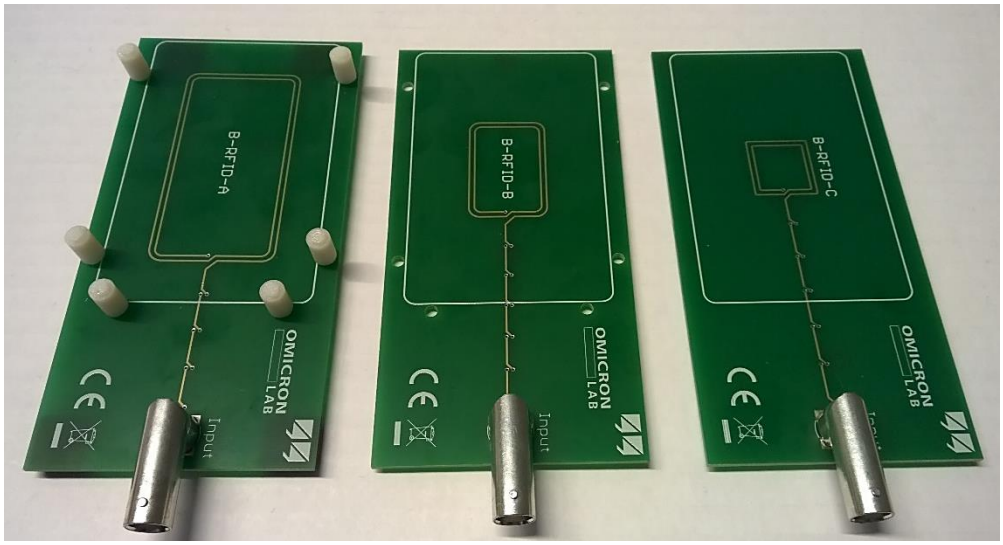

Figure 12: Used RFID Reader Coils

The ideal coupling coil would have an area congruent with the transponders coil. In this case a maximum mutual inductance is possible, and therefore, less power is required. However, the reading coils have been designed to be suitable for different antenna classes[5]. Therefore, the area of the reading coil is a trade-off, so that they are suitable for more classes. To determine how many turns the coupling coil should have, as well trade-offs

[5] There are six different antenna classes defined in ISO/IEC 14443-1. The classes define the size and the shape of the RFID antennas.

have to be made. On the one hand, many turns would generate a stronger magnetic field at the same signal power level[6]. On the other hand, however, more turns go along with a higher parasitic capacitance, due to the capacitive coupling between the windings. This has to be avoided because this decreases the reader coils resonance frequency and this in turn would affect the measurement. According to Infineon Technologies, two turns are a good trade-off. The reading coils do have six card spacers mounted on it, in order to hold an ID-1 card in a defined place. The card can be placed directly on the print for a close coupled measurement or it can be placed 10mm above the print. The material of those spacers requires a low permeability, in order to not disturb the magnetic field. For the same reason the BNC connector is not placed right next to the windings. Instead, it is placed at the edge of the PCB. The signal leads between the BNC connector and the windings are placed closely to each other to minimize the area and keep the parasitic inductance of this leads small. Due to the fact that parallel running signal leads create a parasitic capacitance, this leads are twisted to minimize this parasitic too. (Figure 13)

Figure 13: Twisted Signal Leads

During all measurements where the inductive coupling between the RFID reader coil and the transponder is required care of the environment around the DUT has to be taken. In the close environment of the DUT there must not be materials with high permeability or materials with a high electrical conductivity. This actions have to be taken to ensure a consistent magnetic field and to minimize eddy currents.

The reading coils are three in number. Actually, just one of them is designed for measuring an ID-1 card. However, all of them are used in the subsequent sections in order to see how different coupling factors do affect the results. The three reader coils are referred to as B-RFID-A, B-RFID-B and B-RFID-C. B-RFID-A is the one which is actually designed for an ID-1 card and therefore has the highest coupling factor. The coupling factor k between an ID-1 card and the B-RFID-C reader coil is the lowest one. Also the parasitic capacitance, which is topic of 5.7, is different. This is because the overlapping of the reader coil's windings and the windings of the DUT is different. For the used ID-1 card, it already can be

[6] The signal power level is given in dBm. When performing measurements with the Bode 100, this is the parameter that can be adjusted. The maximum signal power level is $13dBm$. The source of the Bode 100 consists of a voltage source in series with a 50Ω resistor.

said that the parasitic coupling capacitance of the B-RFID-A board is the highest and the B-RFID-C board has the lowest. When using another DUT, of course, this can be different.

5.2 Resonance Frequency Measurement

In section 3.5 on page 9, it was already explained what the resonant frequency is in terms of an RFID-transponder. In equation [3.13], the mathematical formulation of this resonance frequency f_0 is stated. As the parameters in this formula cannot be measured individually without modifying the RFID transponder, other solutions have to be found. What can be measured is the impedance. For the purpose of visualization, the RFID system consisting of the inductively coupled transponder and the reader coil can be seen in Figure 14.

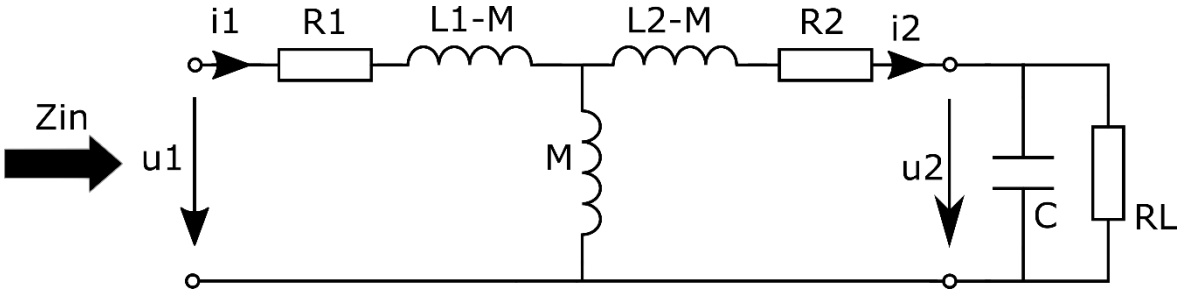

Figure 14: ECD of Inductively Coupled Reader Coil and Transponder

The input impedance can simply be calculated with the mesh analysis. This is done in equation [5.1].

$$a)\ U_1 = I_1 \cdot (R_1 + j\omega L_1) - I_2 \cdot j\omega M$$

$$b)\ U_2 = I_1 \cdot j\omega M + I_2 \cdot (-j\omega L_2 - R_2) = I_2 \cdot \frac{R_L}{1 + j\omega C R_L}$$

$$I_1 \cdot j\omega M = \quad I_2 \cdot \left(\frac{R_L}{1 + j\omega C R_L} + j\omega L_2 + R_2\right)$$

$$get\ I_2\ from\ equation\ \ b)$$

$$c)\ \ I_2 = j\omega M I_1 \cdot \frac{1 + j\omega C R_L}{R_L + R_2 - \omega^2 C L_2 R_L + j\omega \cdot (L_2 + C R_2 R_L)}$$

$$insert\ c)\ into\ a)$$

$$d)\ \ U_1 = I_1 \cdot (R_1 + j\omega L_1) + \frac{I_1 \cdot \omega^2 M^2 (1 + j\omega C R_L)}{R_L + R_2 - \omega^2 C L_2 R_L + j\omega \cdot (L_2 + C R_2 R_L)}$$

$$e)\quad Z_{in} = \frac{U_1}{I_1} = \ (R_1 + j\omega L_1) + \frac{\omega^2 M^2 (1 + j\omega C R_L)}{R_L + R_2 - \omega^2 C L_2 R_L + j\omega \cdot (L_2 + C R_2 R_L)} \qquad [5.1]$$

$$Z' = \frac{\omega^2 M^2 (1 + j\omega C R_L)}{R_L + R_2 - \omega^2 C L_2 R_L + j\omega \cdot (L_2 + C R_2 R_L)} \qquad [5.2]$$

As can be seen in equation [5.1] as well as in Figure 15, the input impedance consists of a series connection of R_1, the parasitic copper resistance of the reader coil, L_1, the inductance of the reader coil and a third term which, from now on, is referred to as $\underline{Z}'$. $\underline{Z}'$ is the transformed transponder impedance and is analytically described in equation [5.2].

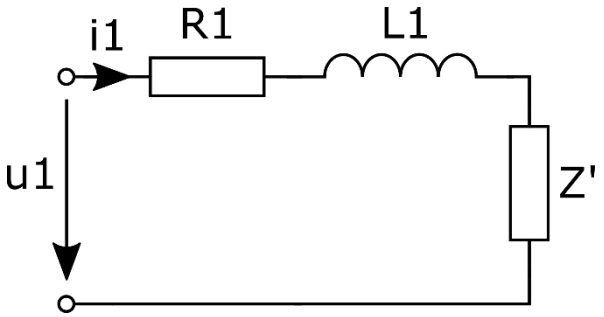

Figure 15: Series Connection of Reader Coil and Transformed Transponder Impedance

If the reader coil is measured without the inductively coupled transponder, the input impedance is the series connection of R_1 and L_1. Hence, it is possible to subtract it from the input resistance $\underline{Z}_{in}$ to just get the transformed transponder impedance $\underline{Z}'$. In section 3.5 on page 9, it was stated that the resonance frequency is where the voltage across R_L reaches the maximum. According to Finkenzeller, this happens when the real part $Re\{\underline{Z}'\}$ of the transformed impedance $\underline{Z}'$ (equation [5.9]) reaches its maximum. Alternatively, the maximum of $|\underline{Z}'|$ can be used. (Finkenzeller 2008, 117) This, however, just can be explained if a current source is used for the reader coil supply. This circumstance hardly gets mentioned in professional literature. A thought experiment helps to understand this.

The transformed impedance $\underline{Z}'$ can be separated in an imaginary and a real part. This two parts can also be seen as a series connection of a resistive part and a reactive part like shown in Figure 16. Both, the reactive as well as the resistive part depend on the frequency.

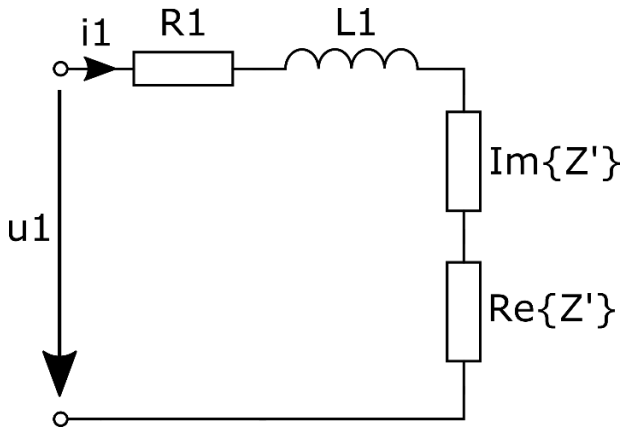

Figure 16: ECD with $\underline{Z}'$ Separated In Reactive and Resistive Part

The power in the circuit can just be consumed by resistive parts. That in turn means that all the power, which dissipates in $Re\{\underline{Z}'\}$, has to be consumed by one of the two resistive parts of the transponder. At this point, it can be assumed that the main part of the power is consumed by the RFID chip. Therefore, the parasitic resistance R_2 can be neglected. This leads to the statement that if the power dissipating in $Re\{\underline{Z}'\}$ gets maximal also the voltage $\underline{U}_2$ across the RFID chip, represented by R_L, gets maximal. At this point, of course, a constant R_L is assumed. The power now gets maximal if the expression [5.3] gets maximal.

$$P(f) = \underline{I}_1^2(f) \cdot Re\{\underline{Z}'(f)\} = \frac{\underline{U}_2^2(f)}{R_L} \qquad [5.3]$$

Equation [5.3] shows that the frequency of the maximum dissipated power $f(P_{max})$ equals the frequency of the maximum chip voltage $f(\underline{U}_{2_{max}})$ which is the resonance frequency of

the transponder. The assumption that the power gets maximal for a maximal $Re\{\underline{Z}'(f)\}$ just is true if a current $\underline{I}_1(f)$ with a constant RMS value over frequency is assumed. This also can be seen by taking a look at equation [5.3]. That means, the measurement result is just valid for a current source providing a constant RMS current. If a voltage source is used, then the current as well as the voltage across $Re\{\underline{Z}'(f)\}$ varies over the frequency since X_{L_1} and $\underline{Z}'$ vary over frequency. This means that the measured resonance frequency $f\left(Re_{max}\{\underline{Z}'\}\right)$, when using a voltage source, differs from the actual resonance frequency $f(\underline{U_2}_{max})$. Therefore, the measurement of $f\left(Re_{max}\{\underline{Z}'\}\right)$ just gives information about where the resonance frequency f_0 would be, in case that a current $\underline{I}_1$ with a constant RMS value would supply the reader coil. The expressiveness of this theoretical value gets analyzed in chapter 6.

The reason why $|\underline{Z}'|$ can also be used for the resonance frequency measurement (besides $Re\{Z'\}$) is that the imaginary part is almost zero at this point, and therefore, $Re\{Z'\}$ and $|\underline{Z}'|$ are almost the same at the resonance frequency. To proof that these two methods yield approximately the same result as the theoretical resonance frequency stated in [3.13], the transformed transponder impedance Z' as well as the real part $Re\{Z'\}$ have to be calculated. (equation [5.4] and [5.5])

$$Z' = \omega^2 M^2 \cdot \left(\begin{array}{c} \frac{R_L + R_2 - \omega^2 C L_2 R_L + \omega^2 C R_L (L_2 + C R_2 R_L)}{(R_L + R_2 - \omega^2 C L_2 R_L)^2 + \omega^2 \cdot (L_2 + C R_2 R_L)^2} \dots \\ \dots + j\omega \cdot \frac{C R_L (R_L + R_2 - \omega^2 C L_2 R_L) - (L_2 + C R_2 R_L)}{(R_L + R_2 - \omega^2 C L_2 R_L)^2 + \omega^2 \cdot (L_2 + C R_2 R_L)^2} \end{array} \right)$$

$$= \frac{\omega^2 M^2 \cdot \left(R_L + R_2 + \omega^2 C^2 R_L^2 R_2 + j\omega \cdot (C R_L^2 - \omega^2 C^2 L_2 R_L^2 - L_2) \right)}{\omega^4 \cdot (C^2 L_2^2 R_L^2) + \omega^2 \cdot (C^2 R_2^2 R_L^2 - 2 R_L^2 C L_2 + L_2^2) + (R_L + R_2)^2}$$

$$= Re\{Z'\} + j \cdot Im\{Z'\} \qquad [5.4]$$

$$Re\{Z'\} = \frac{\omega^2 M^2 \cdot (R_L + R_2 + \omega^2 C^2 R_L^2 R_2)}{\omega^4 \cdot (C^2 L_2^2 R_L^2) + \omega^2 \cdot (C^2 R_2^2 R_L^2 - 2 R_L^2 C L_2 + L_2^2) + (R_L + R_2)^2} \qquad [5.5]$$

$$Im\{Z'\} = \frac{\omega^3 M^2 \cdot (C R_L^2 - \omega^2 C^2 L_2 R_L^2 - L_2)}{\omega^4 \cdot (C^2 L_2^2 R_L^2) + \omega^2 \cdot (C^2 R_2^2 R_L^2 - 2 C L_2 R_L^2 + L_2^2) + (R_2 + R_L)^2} \qquad [5.6]$$

In order to get the resonant circular frequency $\omega_{0_{Re}}$ where $Re\{Z'\}$ reaches the maximum, equation [5.5] has to be differentiated with respect to ω (equation [5.9]) and set equal to zero afterwards. (equation [5.8])

$$\frac{dRe\{\underline{Z}'\}}{d\omega} == \frac{2M\omega \cdot \begin{pmatrix} C^2R_L^3\omega^4 \cdot (C^2R_2^3R_L - 2CL_2R_2R_L - L_2^2) \\ +2C^2R_2R_L^2\omega^2 \cdot (R_2+R_L)^2 + (R_2+R_L)^3 \end{pmatrix}}{(\omega^4 \cdot C^2L_2^2R_L^2 + \omega^2 \cdot (C^2R_2^2R_L^2 - 2CL_2R_L^2 + L_2^2) + (R_2+R_L)^2)^2} \qquad [5.7]$$

$$\frac{dRe\{\underline{Z}'\}}{d\omega} = 0$$

$$C^2R_L^3\omega_{0_{Re}}^4 \cdot (C^2R_2^3R_L - 2CL_2R_2R_L - L_2^2) + 2C^2R_2R_L^2\omega_{0_{Re}}^2(R_2+R_L)^2 \ldots$$

$$\ldots + (R_2+R_L)^3 = 0$$

$$\omega_{0_{Re}}^4 + \omega_{0_{Re}}^2 \cdot \frac{2C^2R_2R_L^2 \cdot (R_2+R_L)^2}{C^2R_L^3 \cdot (C^2R_2^3R_L - 2CL_2R_2R_L - L_2^2)} \ldots$$

$$\ldots + \frac{(R_2+R_L)^3}{C^2R_L^3 \cdot (C^2R_2^3R_L - 2CL_2R_2R_L - L_2^2)} = 0$$

$$\omega_{0_{Re}} = \frac{\sqrt{CR_2\sqrt{R_L} \cdot \left(\sqrt{R_2+R_L} + \sqrt{R_L}\right) + L_2} \cdot (R_2+R_L)^{\frac{3}{4}} \cdot \sqrt{-\frac{1}{R_L^{\frac{3}{2}}}}}{\sqrt{C} \cdot \sqrt{C^2R_2^3R_L - 2CL_2R_2R_L - L_2^2}} \qquad [5.8]$$

Equation [5.8] shows the theoretically exact frequency where $Re\{Z'\}$ is maximal. To show that this formula yields approximately the same result as the formula for the theoretically exact resonance frequency derived in equation [3.12] respectively [3.13] does, some assumptions and simplifications have to be applied.

By using the assumption $R_2 \ll R_L$, which was already used for equation [3.13] on page 12, [5.8] gets simplified to [5.9].

$$Assumptions: R_2 \ll R_L$$

$$\omega_{0_{Re}} = \frac{\sqrt{2CR_2R_L + L_2}}{\sqrt{C} \cdot \sqrt{-C^2R_2^3R_L + 2CL_2R_2R_L + L_2^2}} \qquad [5.9]$$

For a further simplification, the order of magnitude of the different terms have to be verified. The typical orders of magnitude of the different parameters of a 13.56MHz RFID transponder are listed in Table 1.

Parameter	Order of magnitude
R_L	$10^2\ to\ 10^4$
R_2	10^0
C	10^{-11}
L_2	10^{-6}

Table 1: Parameter's Order of Magnitude

By taking a look at the numerator of equation [5.9], it turns out that the term $2CR_2R_L$ has an estimated maximum order of 10^{-8}. Because this is two orders lower than the order of L_2, the next made assumption is that this term can be neglected. The same examination is done with the denominator which leads to neglecting the terms $C^2R_2^3R_L$ and $2CL_2R_2R_L$.

After this simplifications, equation [5.9] turns into equation [5.10].

$$\omega_{0_{Re}} = 2\pi f_{0_{Re}} = \frac{1}{\sqrt{CL_2}} \qquad [5.10]$$

This is the formula derived in equation [3.13] on page 12 where the resonance frequency theory was explained. The error factor of this measurement method depends on the parameter values of the ECD because they are responsible for how well the made assumptions suit.

The same goes for the $|\underline{Z}'|$ measurement. For the derivation of this method the same steps have to be taken. First, the absolute value has to be calculated. To save calculation time a trick is employed. For the further calculation, an intermediate stage between equations [5.2] and [5.4] is required. The dominator is adopted from equation [5.4]. It is already multiplied with the complex conjugate. This complex conjugate must also be multiplied with the numerator of equation [5.2]. However, this term will not get expanded in order to apply the trick. Therefore, equation [5.11] is derived.

$$Z' = \frac{\omega^2 M^2 (1 + j\omega C R_L) \cdot (R_L + R_2 - \omega^2 C L_2 R_L - j\omega \cdot (L_2 + C R_2 R_L))}{\omega^4 \cdot (C^2 L_2^2 R_L^2) + \omega^2 \cdot (C^2 R_2^2 R_L^2 - 2R_L^2 C L_2 + L_2^2) + (R_L + R_2)^2} \qquad [5.11]$$

Assuming that the complex conjugate of the denominator is referred to as $a - jb$, then the denominator is $a^2 + b^2$. The numerator without the complex conjugate of the denominator is called G. Then $\underline{Z}'$ is equation [5.12].

$$\underline{Z}' = \frac{G \cdot (a - jb)}{a^2 + b^2} \qquad [5.12]$$

With this form of the equation, the absolute value can be calculated with equation [5.13]

$$|\underline{Z}'| = \frac{|G| \cdot \sqrt{a^2 + b^2}}{a^2 + b^2}| = \frac{|G|}{\sqrt{a^2 + b^2}} \qquad [5.13]$$

By applying this trick, just the absolute value of G has to be calculated because everything else is already given. In the case given, G is the term $\omega^2 M^2(1 + j\omega C R_L)$. Hence, the absolute value of Z' is derived:

$$|\underline{Z}'| = \omega^2 M^2 \cdot \sqrt{\frac{(1 + \omega^2 C^2 R_L^2)}{\omega^4 \cdot (C^2 L_2^2 R_L^2) + \omega^2 \cdot (C^2 R_2^2 R_L^2 - 2R_L^2 C L_2 + L_2^2) + (R_L + R_2)^2}} \qquad [5.14]$$

For a better overview, some auxiliary variables are introduced in Table 2:

Auxiliary variables	Value
E	$C^2 R_L^2$
F	$C^2 L_2^2 R_L^2$
G	$C^2 R_2^2 R_L^2 - 2R_L^2 C L_2 + L_2^2$
H	$(R_L + R_2)^2$

Table 2: Used Auxiliary Variables

With the help of this new variables, $|Z'|$ can be written like [5.15].

$$|\underline{Z}'| = \omega^2 M^2 \cdot \sqrt{\frac{(1 + \omega^2 E)}{\omega^4 \cdot F + \omega^2 \cdot G + H}} \qquad [5.15]$$

Now $\left|\underline{Z}'\right|$ is differentiated with respect to ω which results in equation [5.16].

$$\frac{d\left|\underline{Z}'\right|}{d\omega} = 2\omega M^2 \cdot \sqrt{\frac{(1 + \omega^2 E)}{\omega^4 \cdot F + \omega^2 \cdot G + H}} \ldots$$
$$\ldots - \omega^3 M^2 \cdot \sqrt{\frac{\omega^4 \cdot F + \omega^2 \cdot G + H}{(1 + \omega^2 E)}} \cdot \frac{\omega^4 \cdot EF + \omega^2 \cdot 2F - EH + G}{(\omega^4 \cdot F + \omega^2 \cdot G + H)^2} \qquad [5.16]$$

By setting this equation equal to zero and solving it for ω, the circular frequency ω_{0_Z} is derived. ω_{0_Z} is the circular frequency, where $|\underline{Z}'|$ reaches its maximum. As can be seen in equation [5.17], solving for ω cannot simply be done.

$$\frac{d|\underline{Z}'|}{d\omega} = 0$$

$$\omega_{0_Z}^6 \cdot EF + \omega_{0_z}^4 \cdot (2EG) + \omega_{0_Z}^2 \cdot 3(G + EH) + 2H = 0 \qquad [5.17]$$

Based on the knowledge of an already analyzed ECD with certain parameters, some assumptions, and hence, some simplifications can be made. Beside the values of the circuit's parameters, also the circular frequency ω_{0_Z} is known. An overview of the orders of magnitude of all the used variables and parameters is provided in Table 3. Due to that, a statement about the influences of specific terms in the equation on the end result can be made. Terms with a low influence are neglected, and therefore, equation [5.17] can be solved for ω_{0_Z}.

Variables	Order of magnitude
L_2	$4 \cdot 10^{-6}$
C	$3 \cdot 10^{-11}$
R_2	3
R_L	10000
ω_{0_Z}	$9 \cdot 10^{7}$
E	10^{-13}
F	$2 \cdot 10^{-24}$
G	$-3 \cdot 10^{-8}$
H	10^{+8}

Table 3: Orders of Magnitude of the used Parameters and Variables

With this information, the last term $2H$ of equation [5.17] on the left side can be neglected. Additionally, the term $(G + EH)$ can be simplified to EH. With this assumptions, ω_{0_Z} is described by equation [5.18].

$$\omega_{0_Z} = \sqrt{\frac{-G \pm \sqrt{G^2 - 3HF}}{F}} \qquad [5.18]$$

At this point, the auxiliary variables are not needed anymore. For this reason, they get replaced by their former terms stated in Table 2. When doing that, also additional simplifications are made. The term G is simplified from $C^2R_2^2R_L^2 - 2R_L^2CL_2 + L_2^2$ to $-2R_L^2CL_2$ and term H is simplified from $(R_L + R_2)^2$ to R_L^2 considering the order of magnitude. Regarding all that, equation [5.19] is obtained.

$$\omega_{0_Z} = \sqrt{\frac{2 \pm 1}{CL_2}} \qquad [5.19]$$

The calculation achieves two results depending on the arithmetic operator. The theoretical resonance circular frequency is $\sqrt{\frac{1}{CL_2}}$ as already mentioned. Due to that, the minus operator is the right one. Hence, the final ω_{0_Z}, with all the made simplifications in equation [5.20], equals the theoretical resonance circular frequency ω_0 derived in equation [3.13] on page 12.

$$\omega_{0_Z} = 2\pi f_{0_Z} = \sqrt{\frac{1}{CL_2}} \qquad [5.20]$$

5.3 Quality Factor Measurement Methods

In section 3.6.1, on page 14, two definitions for the Q-factor are stated. For both of this definitions, measurement methods are available. In this section they get explained and analyzed. First, measurement methods for the Q-factor definition stated in equation [3.17] are examined in section 5.3.1. Afterwards, the measurement methods based on the definition in equation [3.18] are analyzed.

5.3.1 Methods, Subject to the Frequency to Bandwidth ratio

$$Q = \frac{f_0}{f_{BW}} = \frac{\omega_0}{\omega_{BW}}$$

For the purpose of visualization, the definition [3.17] used in this section is stated above. According to this definition, the resonance frequency as well as the $-3dB$ bandwidth is required in order to obtain the Q-factor. How the resonance frequency is measured was stated in the prior section 5.2. Hence, now it is necessary to also find a way to measure the bandwidth. In the literature there are two common measurement methods mentioned. Often the background to this measurement method is hardly explained. One measurement method claims that the bandwidth is obtained by taking a look at the impedance $\underline{Z}'$. The upper and the lower limit of the bandwidth is supposed to be at the point where the absolute value $|\underline{Z}'|$ is $\frac{1}{\sqrt{2}}$ times its maximum at resonance frequency. According to Finkenzeller, this is due to the fact that the voltage $\underline{U_2}$ is proportional to the transformed impedance $\underline{Z}'$. (Finkenzeller 2008, 118) Comparing the equation of $\underline{U_2}$ [3.8] to the equation of $\underline{Z}'$ [5.2] indicates that this claimed proportionality is not entirely given. The other method to measure

the bandwidth uses just the real part $Re\{\underline{Z}'\}$. With this method the upper and the lower bandwidth limit is obtained at the points where $Re\{\underline{Z}'\}$ is half of the maximum value $Re\{\underline{Z}'(\omega_{0_{re}})\} = Re_{max}\{\underline{Z}'(\omega)\}$. The background knowledge to these measurement methods is carried out now.

In Figure 16 on page 22, it was explained that the transformed impedance $\underline{Z}'$ can be separated in an imaginary and a real part. The definition in equation [3.17] comprises the power. Power just can be consumed by resistive parts. Therefore, the reactive part $Im\{\underline{Z}'\}$ has not to be regarded. The transponder has two resistive parts which can consume power. One is R_2, the parasitic resistance of the transponder coil and the other is the chips resistance R_L like shown in Figure 14. R_2 is neglected assuming that most of the power is consumed by the RFID chip, rather than by the parasitic resistance. With this assumption, it can be stated that all the power in the transponder is consumed by the RFID chip expressed by R_L. The power dissipating in R_L is calculated with equation [5.21].

$$P = \frac{U_2^2}{R_L} \approx \underline{I}_1^2 Re\{\underline{Z}'\} \qquad [5.21]$$

Like it was done in the section before, it again is assumed that the current flowing through the reader coil has a constant RMS value. This would be ensured by using a current source to supply the reader coil. By using a voltage source, however, the whole reader coil would influence the measurement as $\underline{I}_1$would have to be expressed as a function depending on the frequency. The definition [3.17] now requires the bandwidth limits f_{BW} to be at the point where the power is half the size of its maximum. As equation [5.22] and [5.23] show, this is true when $Re\{\underline{Z}'\}$ is also half its maximum and if the condition of a constant RMS of $\underline{I}_1$ applies.

$$\frac{P_{max}}{2} = \underline{I}_1^2 \cdot \frac{Re_{max}\{\underline{Z}'\}}{2} \qquad [5.22]$$

$$Re\{\underline{Z}'(f_{BW})\} = \frac{Re_{max}\{\underline{Z}'\}}{2} \qquad [5.23]$$

The second measurement method is also based on the same definition of the Q-factor. So, equation [5.23] is still valid which concretely would mean that the absolute value of the transformed transponder impedance $|\underline{Z}'|$ is $\frac{1}{\sqrt{2}}$times $|\underline{Z}_{max}'|$ when $Re\{\underline{Z}'\}$ is $\frac{Re_{max}\{\underline{Z}'\}}{2}$ according to Finkenzeller.

With the aid of the complex vector diagram shown in Figure 17, it can be seen that this just is the case if the reactive part equals the resistive part. This behavior is valid for a simple parallel resonant circuit.

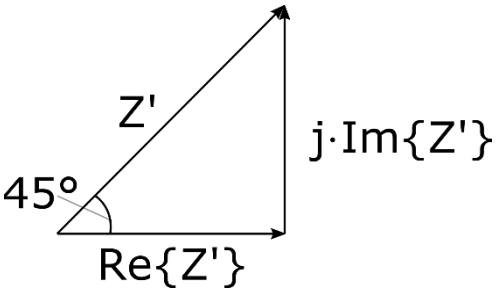

Figure 17: Complex Vector Diagram

As the transformed transponder impedance consists of a more complex circuit than a parallel resonant circuit (Figure 18), the error made by using this method probably is bigger compared to the $Re\{\underline{Z}'\}$ measurement method.

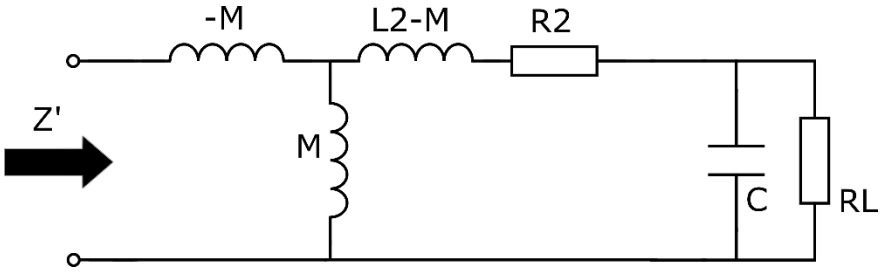

Figure 18: Transformed Impedance ECD

5.3.2 Method Based on the Energy Ratio

$$Q = 2\pi \cdot \frac{Energy\ stored}{Energy\ dissipated\ per\ Cycle} = 2\pi f_0 \cdot \frac{Energy\ stored}{Power\ loss}$$

The definition [3.18] used in this section is stated above for the purpose of visualization.

Besides the difference of the definition for the Q factor, this method has another difference. While the transponder was always regarded as inductively coupled in the prior section, this method here just focuses on the uncoupled transponder circuit. The measured Q factors of this and the prior section cannot be compared. If the transponder isn't inductively coupled, the circuit can be drawn as a parallel circuit shown in Figure 19.

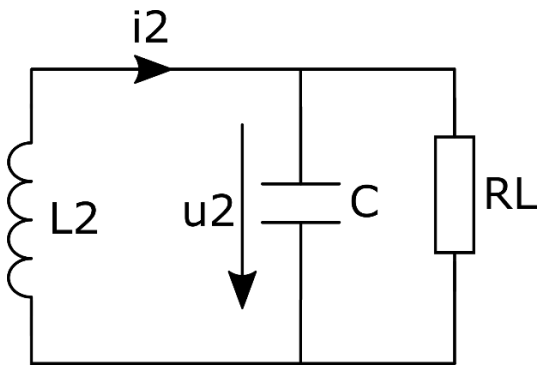

Figure 19: Uncoupled Transponder Circuit

The parasitic resistance R_2 has been neglected. In equation [5.24], the Quality factor of the shown parallel circuit is calculated.

$$Q \overset{\text{def}}{=} 2\pi f_0 \cdot \frac{E_{mag} + E_{el}}{P_{loss}} = \omega_0 \cdot \frac{\frac{L_2 i_2^2}{2} + \frac{C u_2^2}{2}}{\frac{u_2^2}{R_L}}$$
$$= \frac{\omega_0 R_L}{2} \cdot \frac{\frac{L_2 u_2^2}{\omega_0^2 L_2^2} + C u_2^2}{u_2^2} = \frac{R}{2} \cdot \left(\frac{1}{\omega_0 L_2} + C\omega_0\right) \quad [5.24]$$

The resonance circular frequency ω_0 is $\frac{1}{\sqrt{L_2 C}}$. By inserting this into [5.24], the common quality factor formula for a parallel resonance circuit is derived. (equation [5.25])

$$Q = R_L \cdot \sqrt{\frac{C}{L_2}} \quad [5.25]$$

This equation solely describes the quality factor of an uncoupled transponder. For the measurement, of course, the transponder has to be magnetically coupled. So, the task is to get the quality factor of an uncoupled transponder by conducting a measurement using inductive coupling. To do so, the imaginary part of $\underline{Z}'$ [5.6] is required. It is set to zero and solved for ω. (equation [5.26]) This circular frequency at the zero crossing of $Im\{\underline{Z}'\}$ is referred to as $\omega_{0_{Im}}$.

$$Im\{Z'\} = 0$$
$$\omega_{0_{Im}} = 2\pi f_{0_{Im}} = \frac{1}{\sqrt{L_2 C}} \cdot \sqrt{1 - \frac{L_2}{C R_L^2}} \quad [5.26]$$

To get [5.27], equation [5.25] is rearranged for R_L and inserted into equation [5.26]. Additionally, the factor $\frac{1}{\sqrt{L_2 C}}$ is replaced by the symbol ω_0 indicating that this is the resonance circuit's resonance circular frequency.

$$\omega_{0_{Im}} = \omega_0 \cdot \sqrt{1 - \frac{1}{Q^2}} \qquad [5.27]$$

Finally, [5.27] gets rearranged for Q which results in:

$$Q = \sqrt{\frac{1}{1 - \left(\frac{\omega_{0_{Im}}}{\omega_0}\right)^2}} = \sqrt{\frac{1}{1 - \left(\frac{f_{0_{Im}}}{f_0}\right)^2}} \qquad [5.28]$$

The only variables in [5.28] are the frequency at the zero crossing point of the imaginary part of $\underline{Z}'$ as well as the parallel circuit resonance frequency ω_0. As the resonance frequency of the transponder's parallel circuit is approximately the same as the one of the inductively coupled transponder, the same measurement stated in section 5.2 can be conducted. $f_{0_{Im}}$ is simply measured at the zero crossing of $Im\{\underline{Z}'\}$.

5.4 ECD verification

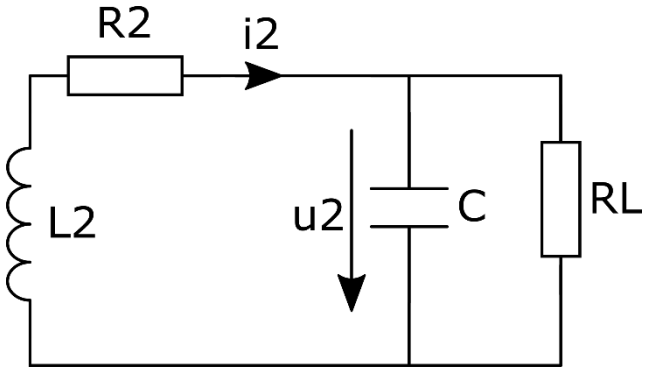

Figure 20: ECD of Transponder

To verify how good the ECD shown in Figure 20 describes the RFID transponder, the parameters are measured and compared to the simulation. As described in chapter 4, for this task the RFID transponder gets contacted. To do so, the foil in Figure 21 is used.

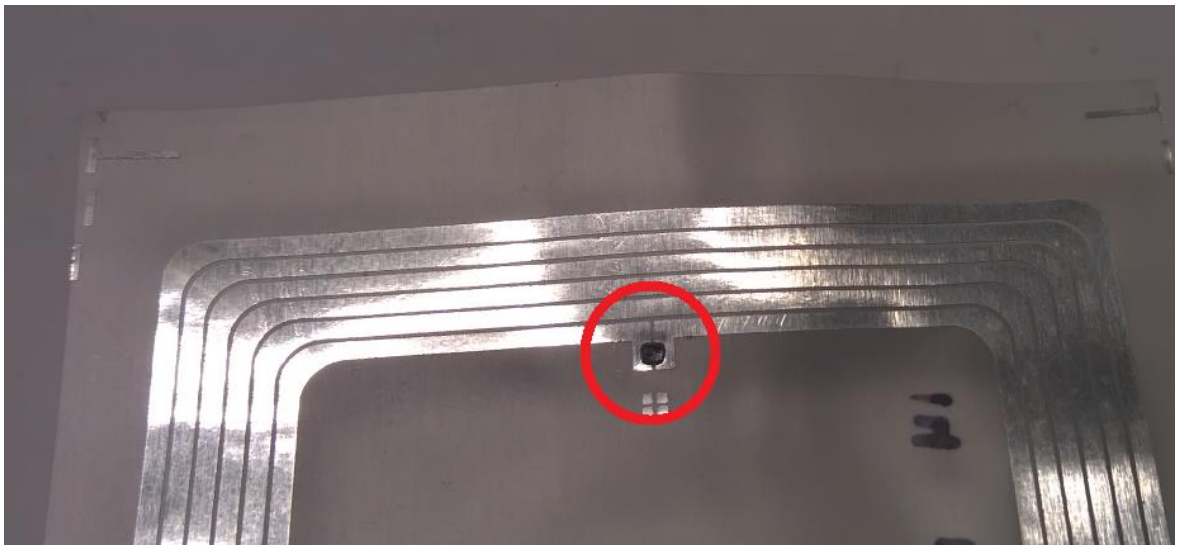

Figure 21: RFID Transponder for Contact Measurement

The frequency response of the impedance is measured while contacting it across the RFID chip which is highlighted in Figure 22. These measurements are conducted with different signal power levels. The obtained results are presented in Figure 22.

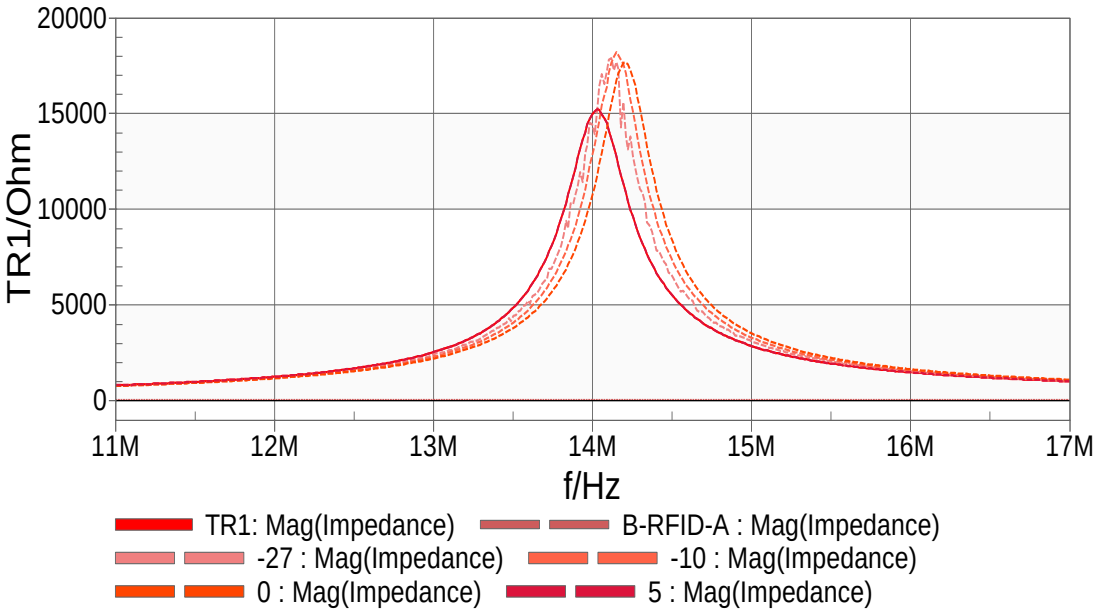

Figure 22: ECD Verification Measurements

After this measurements, the RFID chip shown in Figure 21 is removed to measure the inductance L_2 and the series resistance R_2 of the transponder. The measurement of this parameters is shown in Figure 23 and Figure 24. Surprisingly, the self-resonance of the coil is close to the resonance frequency of the transponder. That means the parasitic coil capacitance C_p is the main part of the overall capacitance C. The value of the inductance

L_2 has to be measured at a point where the parasitic capacitance C_p does not yet affect the measurement. The obtained value for L_2 is approximately $4.4\ \mu H$.

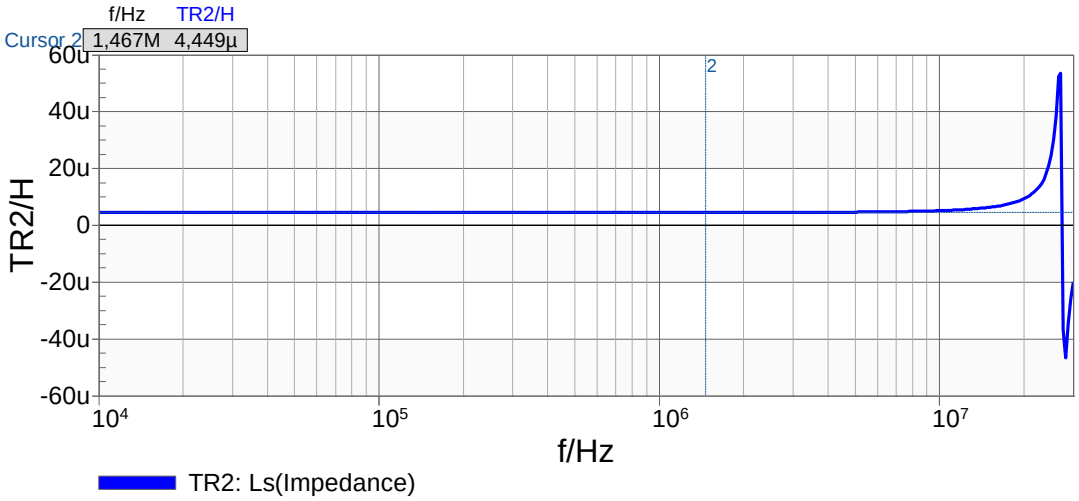

Figure 23: Measurement of Transponder Inductance L_2

The resistance is not constant over the frequency due to the skin effect. Hence, it should be measured at the frequency of interest. However, as the self-resonance is close to the transponders resonance frequency, it is difficult to get the right value for R_2 at this frequency. The resonance of the coil makes this value impractical. Therefore, the parasitic resistance R_2 of the transponder coil is estimated at about $3\ \Omega$.

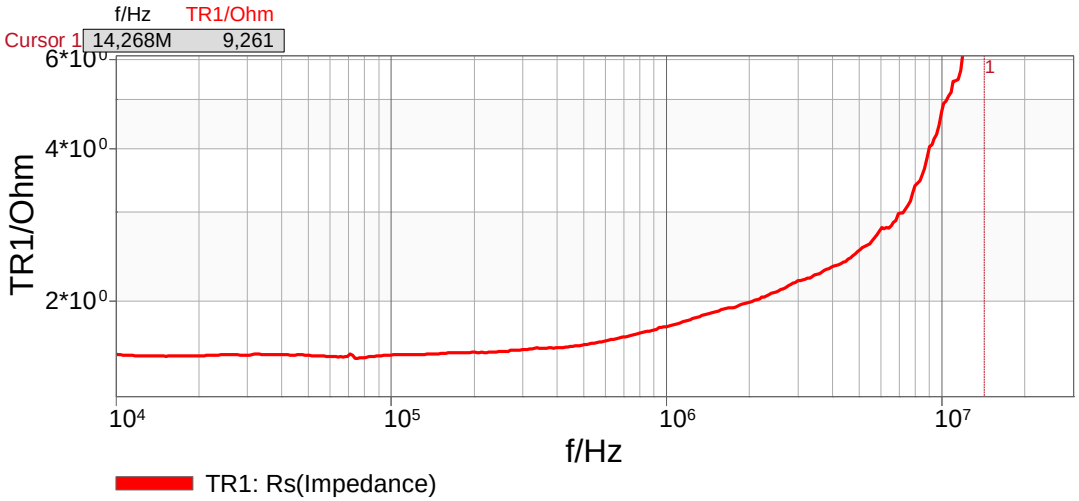

Figure 24: Measurement of the Parasitic Transponder Coil Resistance R_2

The chip's capacitance C and resistance R_L are not measured but calculated instead. The simulation shows if the same frequency responses can be achieved with the ECD and the use of the measured parameters. The measurement results from Figure 22 are loaded into

MATLAB where they get compared to the theoretical frequency response. The theoretical impedance is calculated with the measured parameters R_2 and L_2. The chip capacitance C and R_L get adapted in order to fit the measured frequency responses like shown in Figure 25. The red dashed line is the calculated curve. With adapting C and R_L it is possible to fit the measurements very well. Because of that the used ECD is considered as approved.

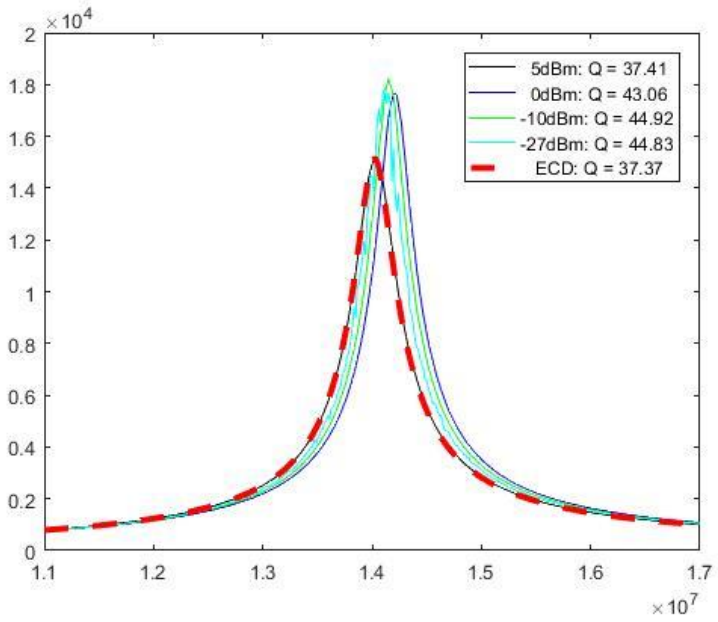

Figure 25: ECD Verification with MATLAB

5.5 Physical measurement

Before the measurement is conducted, the Bode 100 has to be calibrated. This is necessary in order to avoid the influences of the used BNC cables. After the calibration, all the influences of the measurement device, including the cables, are subtracted out so that just the DUT is measured. Most of the measurements are conducted via magnetic coupling. Therefore, it must be ensured that the field does not get disturbed by any interfering signals. In the close environment of the DUT there also must not be materials with high permeability or materials with a high electrical conductivity. This actions have to be taken to ensure a consistent magnetic field and to minimize eddy currents.

5.5.1 Frequency Response and Signal Strength Relation

While conducting measurements involving the RFID chip, it has to be ensured that the signal level does not influence the measurement results. This can happen either due to the chips voltage control mentioned in section 3.4 on page 8 or due to parasitic semiconductor effects.

Depending on the effect, one of the two chip parameters R_L respectively C gets affected. The voltage control affects R_L as described in 3.4. The parasitic semiconductor effect makes the chip capacitance dependent on the voltage $\underline{U_2}$ across the RFID chip. (Finkenzeller 2008, 103) If the magnetic field strength would exceed a certain point, also the load modulation would affect the measurement. However, this effect appears at an even higher signal strength compared to the other two effects. If measurements get compared to each other, this effects always have to be kept in one's mind. For the purpose of illustration, this effect is displayed in Figure 26. Both frequency responses depict the resistive part $Re\{\underline{Z}'\}$ of the transformed transponder impedance $\underline{Z}'$. The red one, however, was measured with a signal power level of $-18\ dBm$ and the blue one was measured with a signal power level of $8\ dBm$.

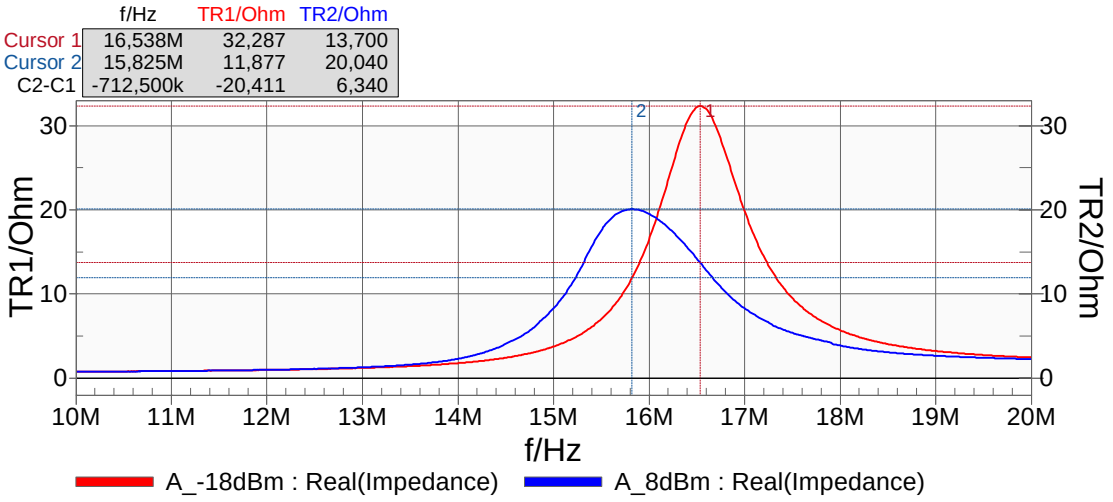

Figure 26: Comparison of two Frequency Responses, Measured with Different Signal Power Levels.

A higher signal level seems to shift the resonance frequency to the left and decrease the peak resistance. Additionally, the frequency response gets asymmetrical, when using a higher signal power to supply the reader coil. In order to ensure comparable measurement results, it is important to avoid these chip parameters to change. To do so, the input signal power level is decreased to the point where the shape of the curve does not change anymore. This signal power level has to be adjusted for each new measurement setup. Choosing the signal power level too low would decrease the measurement accuracy.

5.5.2 Resonance Frequency

As equation [5.1] shows, the measurement device initially measures the coupling coil in series with the transformed impedance $\underline{Z}'$. In order to just measure the impedance $\underline{Z}'$, the coupling coil has to be subtracted. For this reason, first, the uncoupled reader coil is

measured and the impedance is stored in the memory. For visualization, the measured series resistance R_1 and the series inductance L_1 are shown in Figure 27 respectively Figure 28.

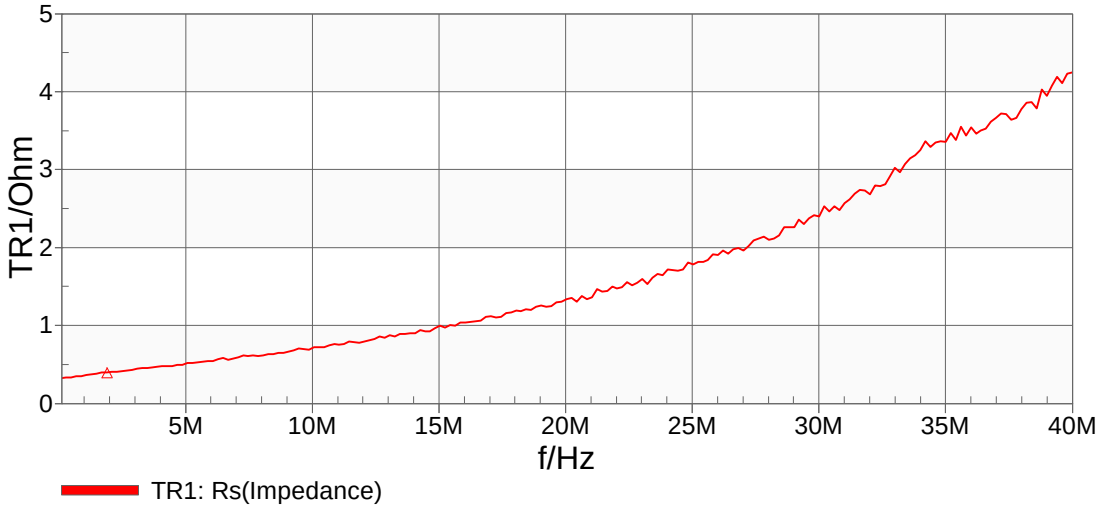

Figure 27: Series Resistance of B-RFID-A Coupling Coil

As can be seen in the two figures, the measured values of the circuit elements are not constant over the frequency. This are parasitic effects which also get subtracted out.

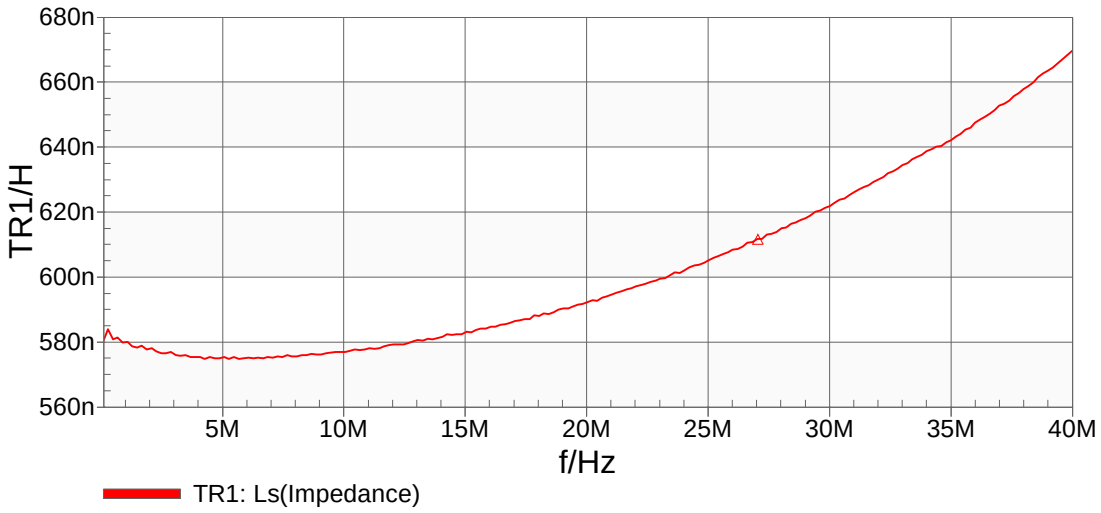

Figure 28: Series Inductance of B-RFID-A Coupling Coil

After getting the parameters of the used reader coil, the resonance frequency can be measured. Therefore, the DUT is placed on the RFID reader coil. The spacers on the reader coil allow to use either a distance of 10mm or 0mm. Measurements using the 0mm distance are hereinafter referred to as close coupled measurements. Next, the input impedance $\underline{Z}_{in}$

is measured again. This time, however, the reader coil is magnetically coupled with the RFID transponder. The stored impedance of the uncoupled reader coil is now subtracted from the measured impedance $\underline{Z}_{in}$ in order to get only $\underline{Z}'$ stated in equation [5.2]. Then, depending on which measurement method is used, either the frequency at the peak of $|\underline{Z}'|$ or at the peak of $Re\{\underline{Z}'\}$ is measured to obtain the resonance frequency f_0. An example of an obtained measurement plot is shown in Figure 29. In this example the method using $|\underline{Z}'|$ is used. To use the $Re\{\underline{Z}'\}$ method, just the format of the plot has to be changed to real.

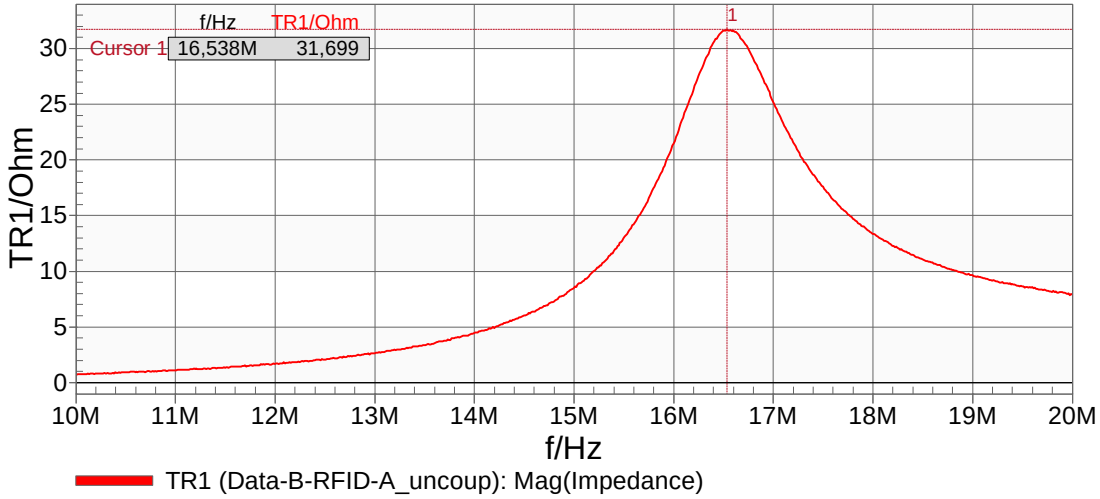

Figure 29: Impedance of Coupled B-RFID-A Coupling Coil

This explained measurements have been conducted with all three reader coils using both available distances. The obtained results shown in Table 4 get analyzed in section 6.1.

	Distance	Resonance Frequency	
		$f_{0_{Re}}$	f_{0_Z}
B-RFID-A	**10mm**	16,538 MHz	16,538 MHz
	0mm	16,213 MHz	16,225 MHz
B-RFID-B	**10mm**	16,550 MHz	16,588 MHz
	0mm	16,250 MHz	16,255 MHz
B-RFID-C	**10mm**	16,513 MHz	16,538 MHz
	0mm	16,283 MHz	16,300 MHz

Table 4: Resonance Frequency Measurement Results

5.5.3 Quality Factor

5.5.3.1 Based on Frequency to Bandwidth Ratio

First, the two measurement methods according to section 5.3.1 are conducted. Besides the resonance frequency, also the bandwidth is required. How the resonance frequency is measured, is explained in the previous section. Hence, in this section it is shown how to get the required bandwidth for calculating the Q factor according to definition [3.17]. The bandwidth can be obtained by measuring $\underline{Z}'$ and having a look at either the resistive part $Re\{\underline{Z}'\}$ or the impedance's absolute value $|\underline{Z}'|$ depending on which measurement method of section 5.3.1 is used. When using $Re\{\underline{Z}'\}$ to measure Q, the bandwidth's range is bounded by the two frequencies where the resistance is half of its maximum $Re\{Z'(\omega_{0_{re}})\}$ occurring at resonant frequency. In the example shown in Figure 30, the measured bandwidth $f_{BW_{Re}}$ is $1.094\ MHz$.

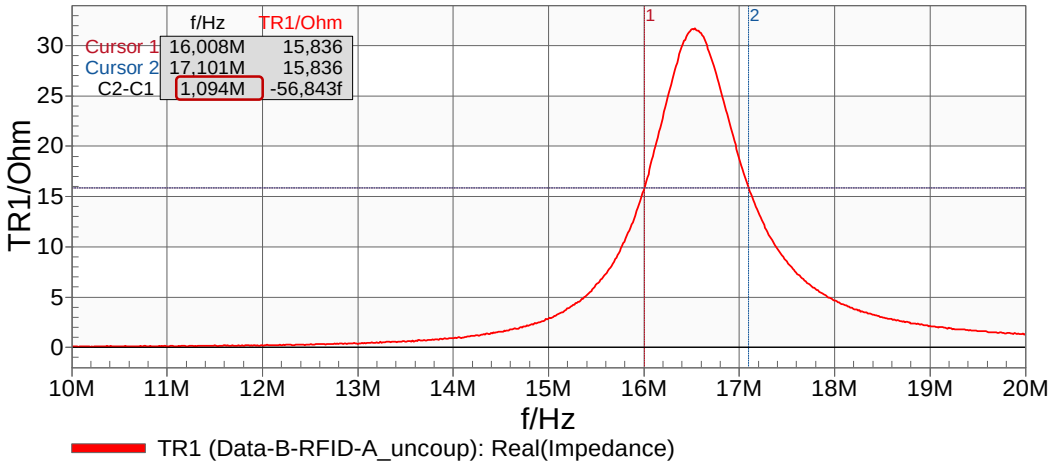

Figure 30: Q Measurement According to Definition 1, using $Re\{\underline{Z}'\}$

When the quality factor is measured with $|\underline{Z}'|$, then the upper and lower bandwidth limits are at the point where $|\underline{Z}'|$ is $\frac{1}{\sqrt{2}}$ times the maximum value $|\underline{Z}'(\omega_{0_Z})|$. This bandwidth is referred to as f_{BW_Z}. The Q factors are calculated as stated in equation [5.29] and [5.30]

$$Q_{re} = \frac{f_{0_{Re}}}{f_{BW_{Re}}} \qquad [5.29]$$

$$Q_Z = \frac{f_{0_Z}}{f_{BW_Z}} \qquad [5.30]$$

Like for the resonance frequency measurements, the explained measurements have been conducted with all three reader coils using both available distances. The obtained results shown in Table 4 get analyzed in section 6.2.

		Quality Factor	
		Q_{Re}	Q_Z
B-RFID-A	**10mm**	15,12	14,90
	0mm	15,46	15,28
B-RFID-B	**10mm**	15,16	14,98
	0mm	15,58	15,45
B-RFID-C	**10mm**	15,15	14,93
	0mm	15,51	15,46

Table 5: Measured Q Factors

5.5.3.2 Based on the Energy Ratio

Now the Q factor measurement is conducted according to the second definition stated in equation [3.18]. The mathematical background of this measurement was discussed in section 5.3.2. The resistance $Re\{\underline{Z}'\}$ and the reactance $Im\{\underline{Z}'\}$ are required for this measurement. $Re\{\underline{Z}'\}$ is needed to obtain the resonance frequency $f_{0_{Re}}$. How this is done is described in section 5.5.2. Additionally, the frequency $f_{0_{Im}}$ at the zero crossing point of the reactance is measured. A measurement example can be seen in Figure 31. Putting the measurement results into equation [5.28] leads to: $Q = \sqrt{\frac{1}{1-\left(\frac{16{,}514MHz}{16{,}538MHz}\right)^2}} = 18{,}57.$

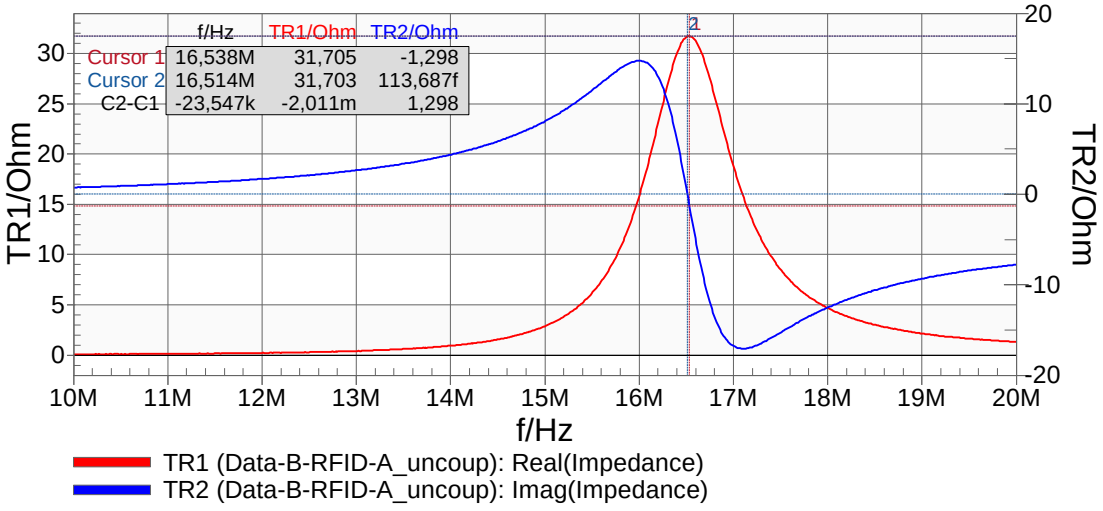

Figure 31: Q Factor Measurement with Reactance and Resistance According to the Energy Ratio Definition

The measurements again have been conducted with all the three different reading coils and with both available distances. The obtained results can be seen in Table 6.

		Q factor
B-RFID-A	10mm	18,57
	0mm	21,84
B-RFID-B	10mm	22,07
	0mm	19,68
B-RFID-C	10mm	24,29
	0mm	25,03

Table 6: Measured Q Factors According to the Energy Ration Definition of 5.3.2

The scattering of this measurement results is very high. This is due to measurement errors. As the two required frequencies $f_{0_{Re}}$ and $f_{0_{Im}}$ occur very close to each other, the precision of the measurement has to be accordingly high. If the accuracy of the measurement is too low, the result also could get imaginary. For the mentioned reasons, this measurement method is not practicable and therefore is not regarded in the further paper.

5.6 Determination of Theoretical Measurement Accuracy

The theoretical accuracy of the measurements is determined by a simulation. The obtained results are based on the used ECD, and hence, also the findings fully rely on the ECD. In the spice program Qucs, the ECD is set up like shown in Figure 32. It is important to note that a current source is used to supply the reader coil. Therefore, the depict circuit does not match the measurement setup. However, the current source is required because the definition of the resonance frequency and the quality factor measurements are based on a constant RMS value of $\underline{I}_1$. This circumstance is explained in section 5.2 on page 22 for the resonance frequency respectively in section 5.3.1 on page 29 for the quality factor.

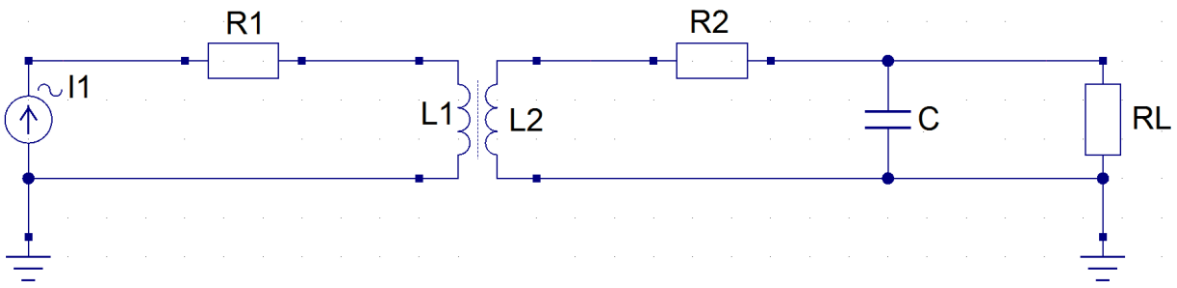

Figure 32: ECD of the Magnetically Coupled Transponder Set Up with Qucs

A parameter sweep is made with the elements of the circuit which influence the transformed transponder impedance $\underline{Z}'$. To ascertain which parameters do have an influence, a look at equation [5.2] has to be taken. All parameters in this equation do affect $\underline{Z}'$, however, the mutual inductance M can be neglected because this constant factor just changes the height of $\underline{Z}'$. That means, it does not have an influence on the resonance frequency or the quality factor measurement methods. Concretely, that means the parameters R_2, R_L, L_2 and C are the parameters which get changed in the simulation. In the spice program, the frequency response of $|\underline{Z}'|$ and $Re\{\underline{Z}'\}$ is obtained for all the parameter values in the parameter sweep. They are required to simulate the measurements. Additionally, the voltage $\underline{U_2}$ across the chip is simulated as a function of the frequency. This voltage is required to get the theoretically exact value of the resonance frequency f_0 and quality factor Q according to the definition. These frequency responses do get processed with MATLAB so that the results for the resonance frequency and the quality factor can be plotted as a function of the changed parameters. To get an idea of how this simulation results look like in the end, it is depicted in Figure 33. The blue lines show the exact resonance frequency f_0 according to the definition. The green lines show $f_{0_{Re}}$ and the red lines f_{0_Z}. The resonance frequency is plotted as a function of the chip resistance R_L. Additionally, this function is plotted for different values of a second circuit parameter. In the displayed example the second parameter is the transponder inductance L_2. Purpose of this is to see how a second parameter affects the dependency on the first parameter. All of the simulations do have a second parameter and all the possible combinations except from $C - L_2$-combinations get analyzed. The simplified resonance frequency in equation [3.13] on page 12 is kept constant and therefore the capacitance C is calculated by using L_2 and vice versa. It is not relevant to change the value of the transponder's inductance L_2 and keep the capacitance C constant. In that case, the resonance frequency would change over a wide range which does not reflect the reality.

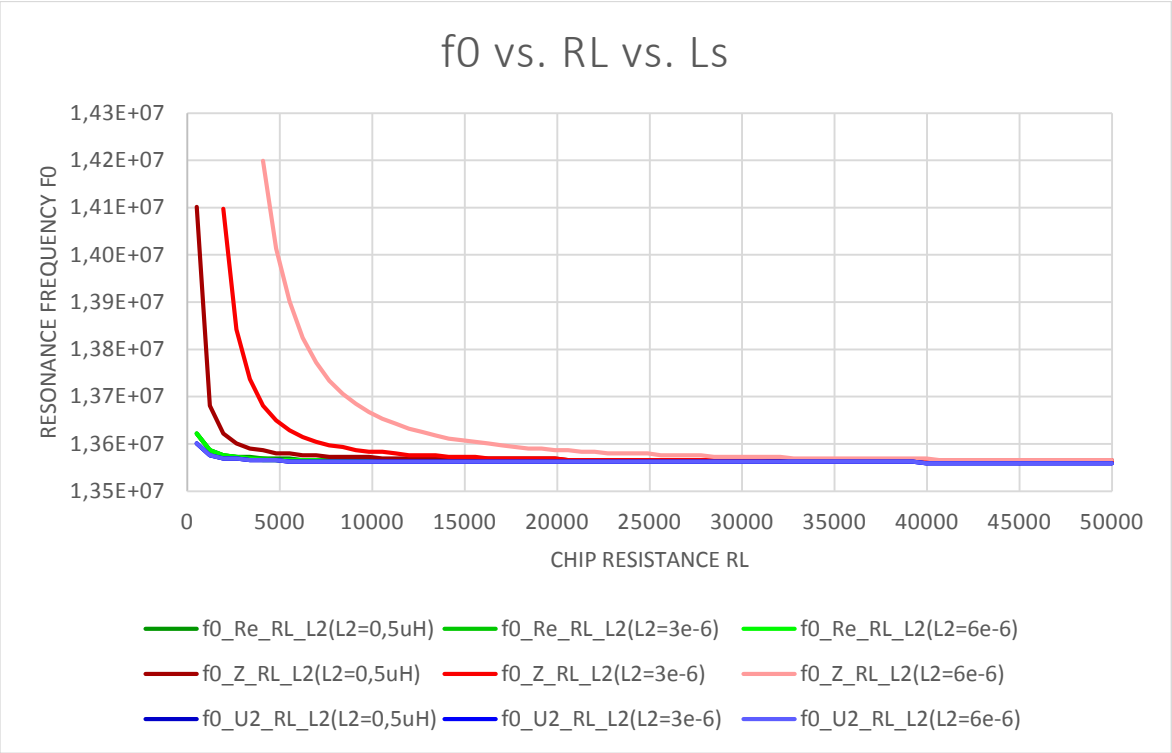

Figure 33: Example of a Simulation Showing f_0 as a Function of R_L

In the example, it can be seen that the theoretical resonance frequency matches $f_{0_{Re}}$ well over the whole range of R_L. For low values of R_L, f_{0_Z} deviates noticeably. Additionally, a higher value for the transponder inductance causes a higher deviation. The ranges of the different parameter sweeps as well as the nominal parameter values can be seen in Table 7. The findings of all these simulations are presented in 6.3.

Circuit Element	Nominal Value	Parameter Sweep Range
C	$31.3pF$	$10pF - 100pF$
L_2	$4.4\ \mu H$	$1.4\ \mu H - 14\ \mu H$
R_L	$10k\Omega$	$500\ \Omega - 10k\Omega$
R_2	3Ω	$0\ \Omega - 6\ \Omega$

Table 7: Ranges and Nominal Values of the ECD Elements

5.7 Influence of a Parasitic Coupling Capacitance

To verify the influence of the parasitic coupling capacitance C_c, a capacitor is connected across the magnetically coupled inductors of the ECD as it can be seen in Figure 34. The

shown capacitor just has the purpose of a model which should depict a simplified variant of the infinitesimal inductor elements. Therefore, no general statement about how these capacitors should be connected can be made. Another option is to place the connections of the capacitor C_c on the other side of R_1 and R_2. The parasitic resistance of an inductance also could be described by two resistances placed on both ends of the coil and the parasitic capacitance also could be represented by two capacitors. Doing so, the second capacitor would be placed on the opposite ends of the coils. In that case, the ground reference on the transponder side has to be removed. The different options do not obtain completely equal results. Hence, to make results replicable it is important to specify the used model.

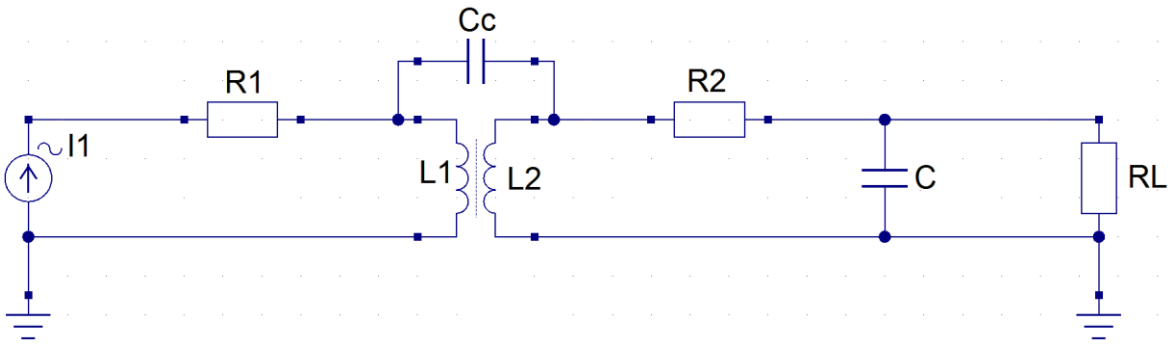

Figure 34: Circuit with Parasitic Coupling Capacitors

The goal is to get information about the error caused by the coupling capacitance C_c when using the reader coils designed for the Bode 100. This error is calculated for the nominal values stated in Table 7. Because the circuit has changed, some more circuit elements do affect the frequency responses. When measuring the resonance frequency or the quality factor, L_1 as well as R_1 is subtracted from the measured impedance. Figure 34, however, shows that this procedure causes an error because not the whole current flows through L_1 anymore. With the used model, R_1 does not affect the result. If the coupling capacitance C_c is connected to the other side of R_1, then it also has an influence on the measurement – however, it is very small. The former $\underline{Z}'$ (equation [5.2]) includes the coupling factor as a constant which just changes the height. Therefore, it does not affect the resonance frequency and the quality factor measurement. Assuming that the ECD with a coupling capacitance in Figure 34 applies, it is different. If a resonance frequency measurement or a quality factor measurement respectively is performed, then the coupling factor also affects the results as it is crucial for the voltage across C_c. The inductance L_1 is chosen to be580nH. This is the inductance value of the reader coil B-RFID-A at 13.56MHz. The measurement can be seen in Figure 28. Both, the coupling factor k as well as the coupling capacitance C_c are strongly dependent on the distance between the reader coil and the DUT. As both of

this parameters do have an influence on the measurement, they are both described as a function of the distance. The coupling capacitor is described with equation [5.31]. (Finkenzeller 2008, 79) This equation is valid for two parallel circular inductances. The radius of the transponder winding is $r_{transp.}$ and the reader coils radius is r_{reader}. The distance between the two inductances is described by the variable x.

$$k = \frac{r_{transp.}^2 \cdot r_{reader}^2}{\sqrt{r_{transp.} \cdot r_{reader}} \cdot \left(\sqrt{x^2 + r_{transp.}^2}\right)^3} \qquad [5.31]$$

Estimating the coupling capacitance is challenging. The capacitance appears between the windings of the two coils, however, the real capacitance can't be simply calculated like a plate capacitor. Nevertheless, this calculation gives information about the capacitance's order of magnitude. The ISO/IEC 14443-1 standard does not define how the antenna of an RFID card exactly has to look like. It is just defined, in which area the antenna is allowed to be placed to meet the standards. Hence, it is difficult to calculate the capacitance. The reader coils have been designed in a way to have minimal overlaps between reader coil and DUT. But as already stated in 5.1, all of the three designed reader coils are designed to meet more than one ISO/IEC 14443-1 antenna class. Because of that the overlaps have been a trade-off. The B-RFID-A reader coil has the biggest winding area and therefore the coupling capacitance is the highest of all three reader coils assuming the worst case scenario. For the worst case scenario, it is assumed that all the coil windings of the B-RFID-A board overlap with the windings of the DUT. The capacitance is then calculated with equation [5.32] where ϵ_0 is the vacuum permittivity, ϵ_r is the relative permittivity, A is the area of the overlapping windings and x is the distance again.

$$C_c = \frac{\epsilon_0 \epsilon_r \cdot A}{x} \qquad [5.32]$$

The winding of the B-RFID-A reader coil has rectangular windings with an average circumference of approximately 60mm x 30mm. The width of the windings is 0.5mm. Therefore, the overlapping area A is about $180mm^2$ large, considering the two windings. To make use of equation [5.31] the reader coil is approximated with a circular coil with the radius $r = 29mm$. The transponder's inductance is approximated with a circular winding with a radius r of $35\ mm$. This approximates a class 1 antenna according to ISO/IEC 14443-1 as depicted in Figure 35. The PICC (proximity integrated circuit card) antenna zone is the area where the antenna is allowed to be placed to meet the standard.

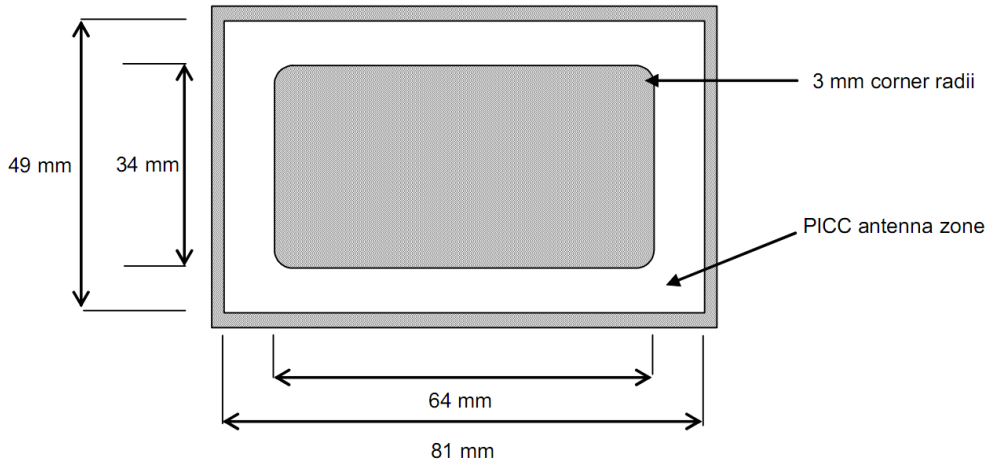

Figure 35: Location of the Antenna of the "Class 1"
Source: ("ISO/IEC 14443-1 Identification Cards - Contactless Integrated Circuit Cards - Proximity Cards" 2008, 79)

The influence of the coupling capacitance is analyzed for a distance of $10\ mm$ and for the close coupled measurement, where the RFID card lies directly on top of the reader coil PCB. That are the two provided measurement distances. Afterwards, it is compared to the result without the influence of C_c. For the $10\ mm$ distance, C_c is calculated with an ϵ_r of 1. For the close coupled measurement, ϵ_r is assumed to be 3. That's the value of PVC (Polyvinylchloride), the card material. The distance x for the close coupled measurement is chosen to be $0.5\ mm$. Within the stated terms and with the made assumptions, the simulation and calculation results in the values shown in Table 8. It is assumed that at a distance of $100\ mm$ no potent influence of a coupling capacitance is present. The resonance frequency $f_{0_{Re}}$ is obtained via the method using $Re\{\underline{Z}'\}$ and f_{0_Z} uses the $|\underline{Z}'|$ method. f_0 is the actual resonance frequency of the simulated circuit according to definition of section 3.5. The indices of the quality factors also indicate the applied measurement method. Q is the resonance frequency according to the definition. Q_{Re} is measured with $Re\{\underline{Z}'\}$ and Q_Z is measured with the frequency response of $|\underline{Z}'|$.

Parameter	$100\ mm$	$10\ mm$ distance	Close coupled
C_c	$0.016\ pF$	$0.16\ pF$	$9.5\ pF$
k	0.028	0.65	0.72
f_0	$13.559\ MHz$	$13.542\ MHz$	$12.551\ MHz$
$f_{0_{Re}}$	$13.560\ MHz$	$13.543\ MHz$	$12.551\ MHz$
f_{0_Z}	$13.572\ MHz$	$13.556\ MHz$	$12.562\ MHz$
Q	21.99	22.02	24.42
Q_{Re}	22.00	22.02	24.42
Q_Z	21.85	21.88	24.30

Table 8: Obtained Results for the Coupling Capacitance Analysis

It can be noted that a smaller distance x leads to a lower resonance frequency as well as a higher quality factor. Furthermore, it can be seen that the results obtained by the measurement methods suit well with the exact results according to the definition. Reason for that is that the theory of the measurement still applies. In section 5.2 the resonance frequency and in 5.3 the quality factor measurement is explained by taking a look at the dissipating power. As no new resistive element has been added in the circuit in Figure 34, the methods using $Re\{\underline{Z}'\}$ still is valid. Using $|\underline{Z}'|$ for the measurement however, causes an additional error. As stated before the reactive part X_{L_1} caused by L_1, theoretically, cannot simply be subtracted from the input impedance as it is done in the measurement. The input impedance of Figure 34 does not consist of a series connection of the parasitic resistance R_1, the reader coil inductance L_1 and the transformed transponder impedance $\underline{Z}'$. Now L_1 is part of $\underline{Z}'$. The relative deviations caused by the coupling capacitance are stated in Table 9. These deviations represent the worst case deviations. The deviation when measuring with a distance of 10mm is very little. As it is the worst case scenario, this error usually can be neglected. However, the error when performing a close coupled measurement could be important. Again, it has to be kept in mind that this are worst case values which probably won't appear.

Ratio in %	
$\frac{f_{0_{10mm}}}{f_{0_{C_c=0}}}$	99.9%
$\frac{f_{0_{close\ coupled}}}{f_{0_{C_c=0}}}$	92.6%
$\frac{Q_{10mm}}{Q_{C_c=0}}$	100,1%
$\frac{Q_{close\ coupled}}{Q_{C_c=0}}$	111,0%

Table 9: Relative Deviation of Measurements using 10mm Distance Respectively Close Coupled Measurements Compared to the Measurement without the Influence of C_c

6 Results

The results achieved in the previous chapter 5 are now analyzed in order to detect trends and dependencies. This is done with the physical measurement results as well as with the simulation results. The physical measurements are also compared to the simulation in order to detect possible discrepancies.

At the beginning of this chapter, it is explained what information the theoretical resonance frequency provides. Until now, it was not explained what this theoretical value reveals. This resonance frequency is also used for the quality factor measurement. Therefore, the explanation also provides background information for all the subsections.

The measured resonance frequency is valid for a constant current $\underline{I}_1$ in the reader coil winding, as stated in section 5.2. However, usually no current source is used to supply a reader coil. Hence, the expressiveness of this theoretical resonance frequency is not obvious. To examine and explain this problem, the following two diagrams in Figure 36 and Figure 37 are used. Figure 36 depicts the measurement of $|\underline{Z}'|$ and $Re\{\underline{Z}'\}$ which are used for the resonance frequency as well as the quality factor measurement. The reader coil is supplied by a voltage source this time. Therefore, the analyzed circuit can be regarded as the ECD stated in Figure 14 with a voltage source at the reader coil side. The AC simulation has been conducted for different values of k. As can be seen in Figure 36, the measured resonance frequency does not change. This is expected because the coupling factor k in equation [5.2] on page 21 does just change the height of $\underline{Z}'$, and therefore, it does not influence the measurement results. The actual resonance frequency is at the point where U_2, the voltage across the RFID chip, is maximal. Equation [3.16] on page 13, however, shows that for a voltage source at the input of the reader coil the coupling factor k does influence the resonance frequency because the mutual inductance M now also appears in a denominator term. ($M = k \cdot \sqrt{L_1 L_2}$). Figure 37 shows the frequency response of the RFID chip's voltage U_2 for several values of the coupling factor k. The height as well as the real resonance frequency increases with the coupling factor k. By comparing the two diagrams, it can be seen that the measured resonance frequency which is valid when a current source supplies the reader coil is also valid when a voltage source supplies the reader coil – however, just for a small coupling factor k. The measured resonance frequency is approximately at 13.56MHz. By just observing this frequency point in Figure 37, it can be seen that the voltage at this certain frequency increases first. If the coupling

factor k increases further, the voltage at $13.56\,MHz$ decreases again. Hence, the RFID reader coil of an RFID system also has to be designed in order to supply the RFID chip with the required voltage for a high coupling factor k. The measured theoretical resonance frequency is the frequency where the transponder requires the lowest magnetic field strength to start working. By using this frequency, the highest required energy to maximal distance ratio can be achieved.

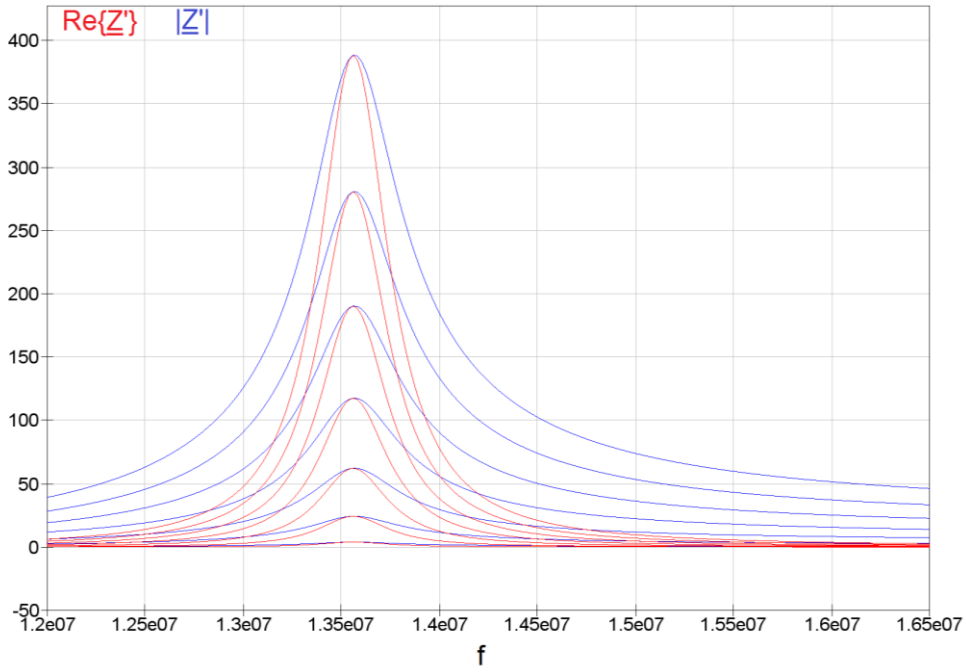

Figure 36: Frequency Response of $Re\{\underline{Z}'\}$ and $|\underline{Z}'|$

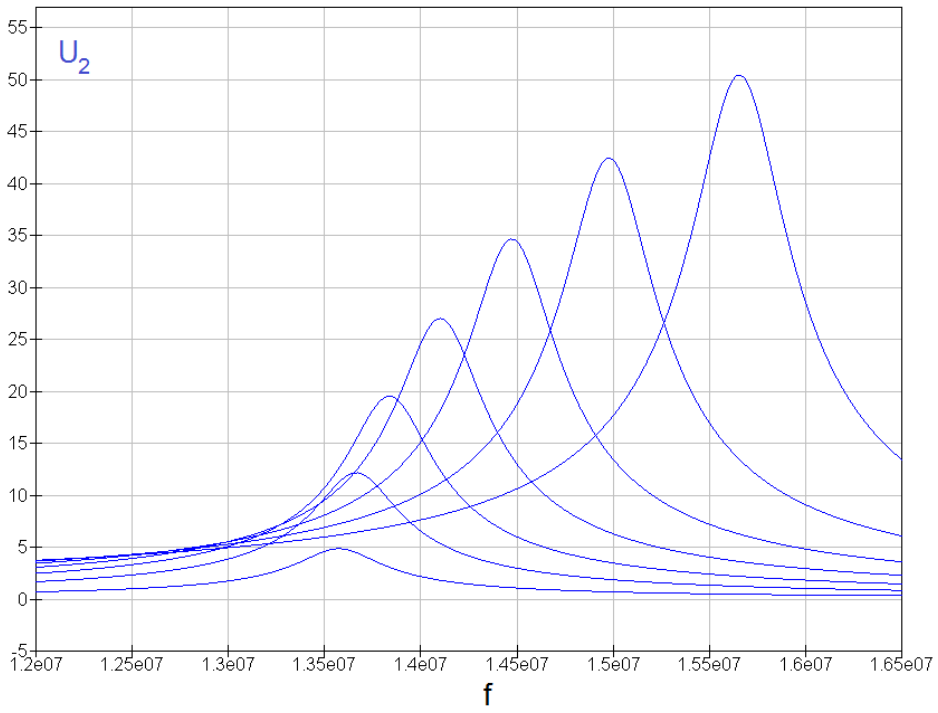

Figure 37: Frequency Response of Voltage U_2 when using a Voltage Source to Supply the Reader Coil.

When using a voltage source, the other circuit elements of the reader coil also influence the frequency response of U_2. ([3.16]). The internal $50\,\Omega$ resistance of the Bode 100, for example, would cause a change of U_2's frequency response like depicted in Figure 38. This internal resistance can be added up with the reader coil resistance R_1. The diagram shows that the additional resistance reduces the level of the frequency responses., and at a certain value for the coupling factor k, the peak level decreases again. But the expressiveness of the theoretical resonance frequency, stated before, still remains. The same goes for the other circuit elements of the reader coil. If the reader coil consists of more or other circuit elements, then the other parts also influence U_2 and [3.16] is not valid anymore

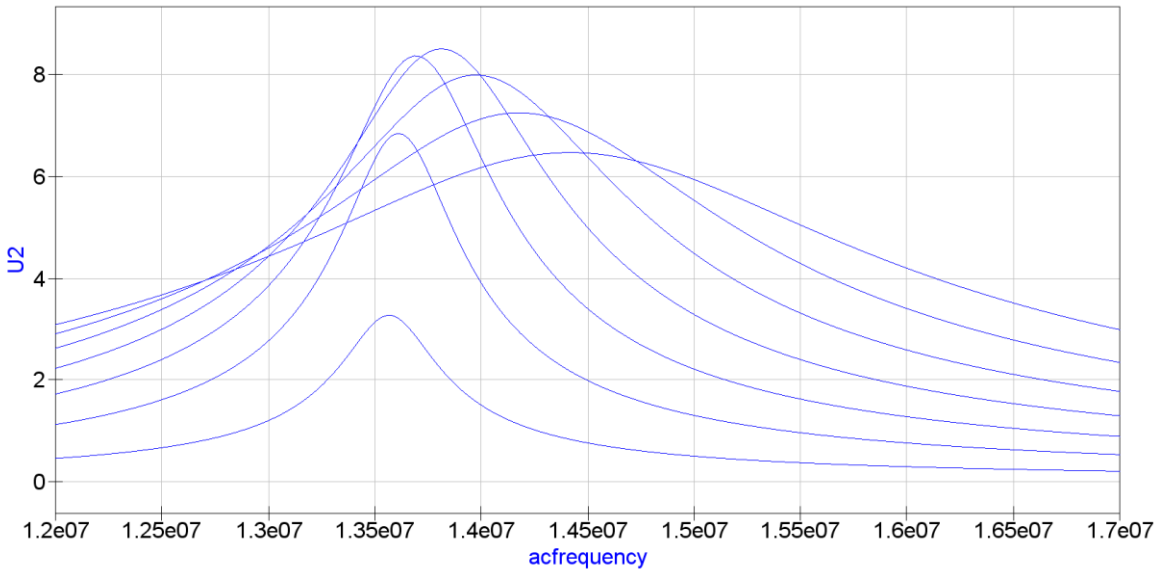

Figure 38: Frequency Response of Voltage U_2 when using a Voltage Source with a 50Ω Internal Resistance to Supply the Reader Coil.

6.1 Resonance frequency measurement

All the measurements and simulations regarding the resonance frequency get analyzed in this section.

6.1.1 Findings of the Physical measurements

The purpose of Figure 39 is to compare the close coupled measurements with the measurements performed at a 10mm distance. The orange bars are the measurement results obtained where the distance between DUT and reader coil was 10mm. The blue bars state the results of the close coupled measurements. The captions on the horizontal axis provide information about the used reader coil and measurement method. Obviously, the close coupled measurements result in lower resonant frequencies. When performing a close coupled measurement, the coupling factor k as well as the parasitic coupling capacitance C_c increases. The signal level power always has been adapted in order to avoid changes of the transformed transponder impedance $\underline{Z}'$ caused by the chips voltage control mentioned in section 3.4 or the load modulation explained in section 3.3 respectively. As the resonance frequency measurement initially is not depending on the coupling factor k as can be explained with equation [5.2], the decrease in resonance frequency is caused due to the parasitic coupling capacitance C_c. If a coupling capacitance operates, also the

coupling factor influences the result. As already shown in section 5.7, the resonance frequency decreases if the coupling capacitance increases.

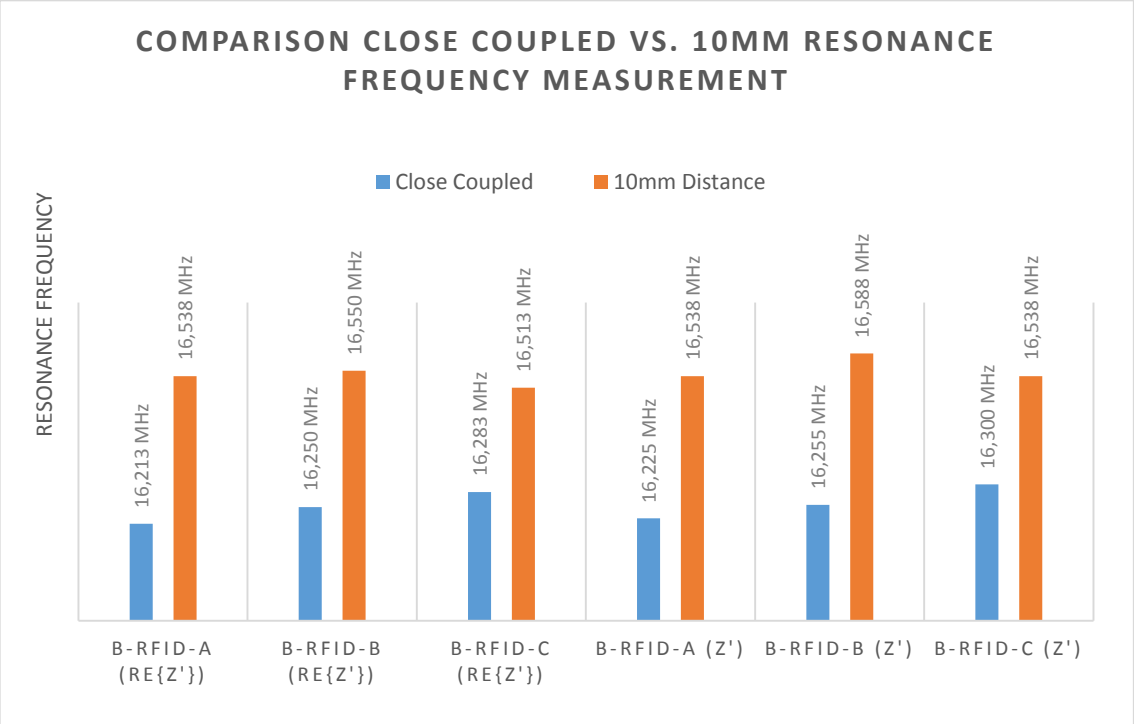

Figure 39: Comparison between Close Coupled Measurements and 10 mm Distance Measurements

In section 5.7, it is shown that the measurement with a distance of 10mm causes no mentionable errors. Therefore, this value is taken as the correct value in order to state the ratio $\frac{f_{0_{close\ coupled}}}{f_{0_{10mm}}}$ as it was done in section 5.7. This, of course, does not regard the potential measurement errors. In Table 10 the relative deviation of the close coupled measurement compared to 10mm distance measurement is stated. The worst case value for the relative deviation stated in Table 9 on page 48 is 7.4%. The values of Table 10 are lower.

Method	Reader Coil	$1-\frac{f_{0_{close\ coupled}}}{f_{0_{10mm}}}$
$Re\{\underline{Z}'\}$	B-RFID-A	2%
	B-RFID-B	1.8%
	B-RFID-C	1.4%
$\lvert\underline{Z}'\rvert$	B-RFID-A	1.9%
	B-RFID-B	2%
	B-RFID-C	1.4%

Table 10: Relative Deviation of Close Coupled Measurements Compared to the 10mm Measurements

Both, Figure 40 and Figure 41 compare the two measurement methods for the resonance frequency. Figure 40 shows the results obtained by the close coupled measurement and Figure 41 the results provided by the 10mm distance measurement. The results that have been obtained with the method using $Re\{\underline{Z}'\}$ are depicted with the blue bars. The orange bars are measured with the method that uses $\lvert\underline{Z}'\rvert$. The $\lvert\underline{Z}'\rvert$ measurement results tend to be higher than the results obtained by $Re\{\underline{Z}'\}$ method. This is generally valid according to the simulation results. It also can be seen in section 6.3.

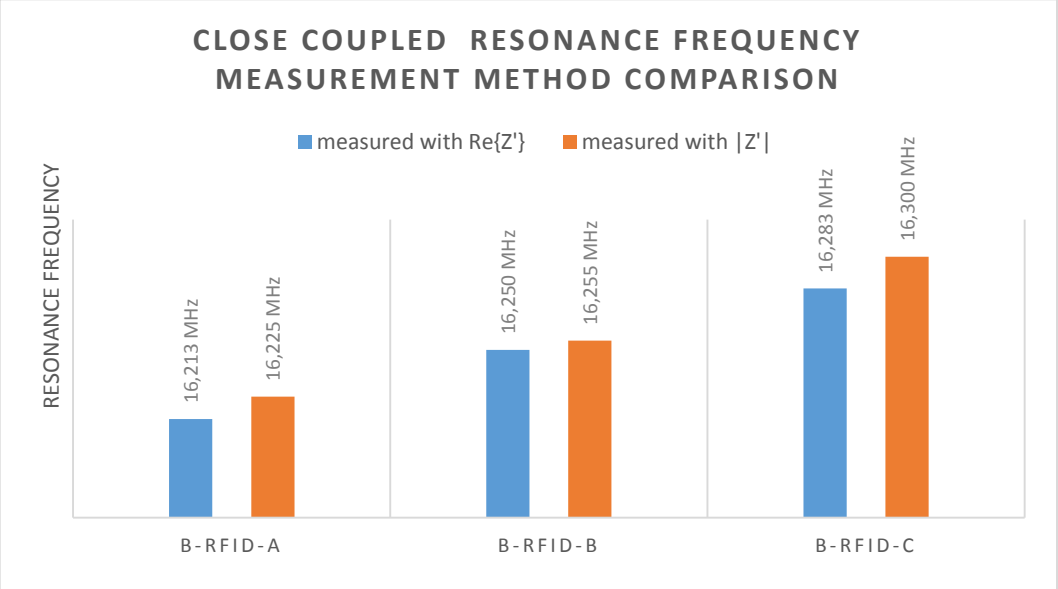

Figure 40: Comparison of the two Resonance Frequency Measurement Methods for Close Coupled Measurements

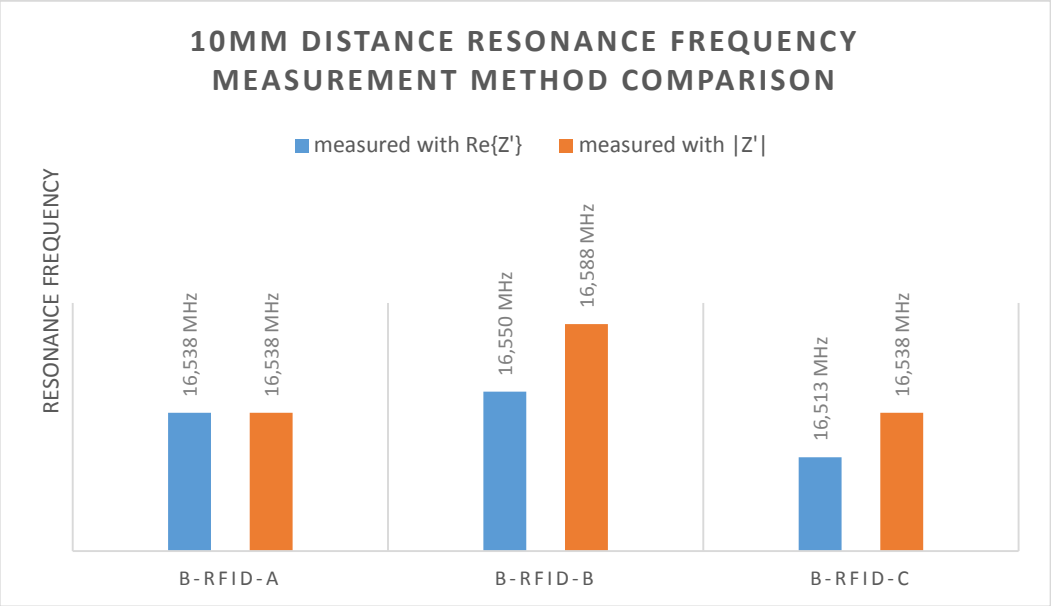

Figure 41: Comparison of the two Resonance Frequency Measurement Methods for 10mm Distance Measurements

6.2 Q-factor measurements

All the measurements and simulations regarding the quality factor get analyzed in this section.

6.2.1 Findings of the Physical measurements

Figure 42 shows a comparison of the close coupled measurement and the measurement with a 10mm distance between DUT and the reader coil. As stated in the prior section, the coupling capacitance and the coupling factor change when the distance is changed. The coupling factor, however, does not influence the measurement results if no parasitic coupling capacitance C_c is present. The bar chart definitely show that the quality factor of the close coupled measurement is higher than the result obtained with a $10\ mm$ distance between reader coil and DUT. That is a sign that the parasitic coupling capacitance is present. The results correspond with the simulation from section 5.7. An increase of the coupling capacitance goes along with an increase of the quality factor despite the fact that the resonance frequency is decreasing. That means that the effect of the bigger getting bandwidth is influencing the quality factor more than the decreasing resonance frequency.

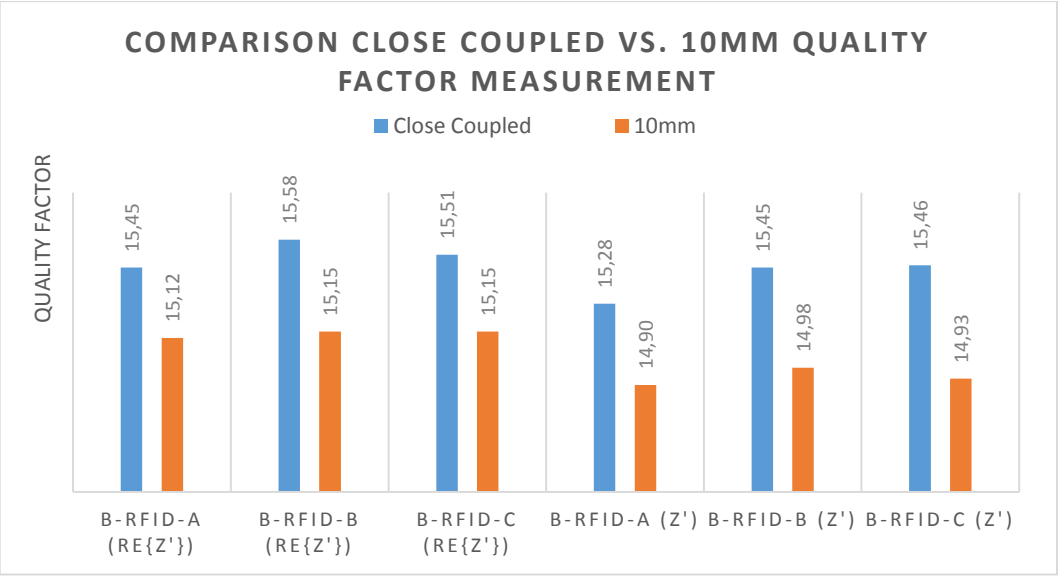

Figure 42: Comparison of Close Coupled and 10 mm Distance Measurement

Figure 43 and Figure 44 compare the two measurement methods. In Figure 43 the close coupled measurements are pictured whereas Figure 44 shows the results of the measurement with a 10mm distance between DUT and reader coil. Independent of the used distance, it generally can be said that the measurements using $Re\{\underline{Z}'\}$ achieved higher quality factors. In most cases, this is also valid in the simulation results. It also can be seen in section 6.3.

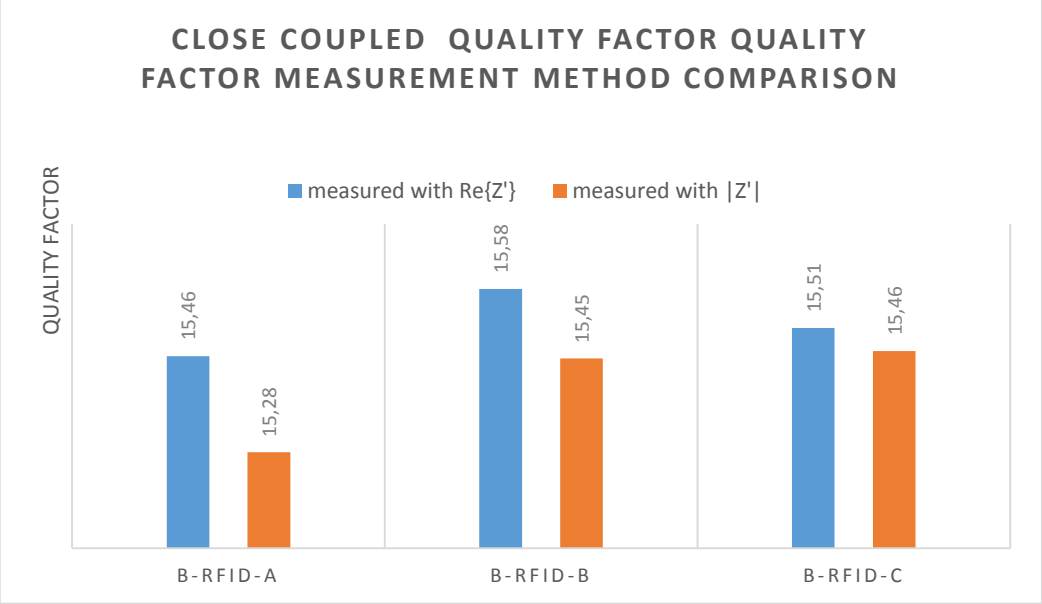

Figure 43: Comparison of the two Quality Factor Measurement Methods for Close Coupled Measurements

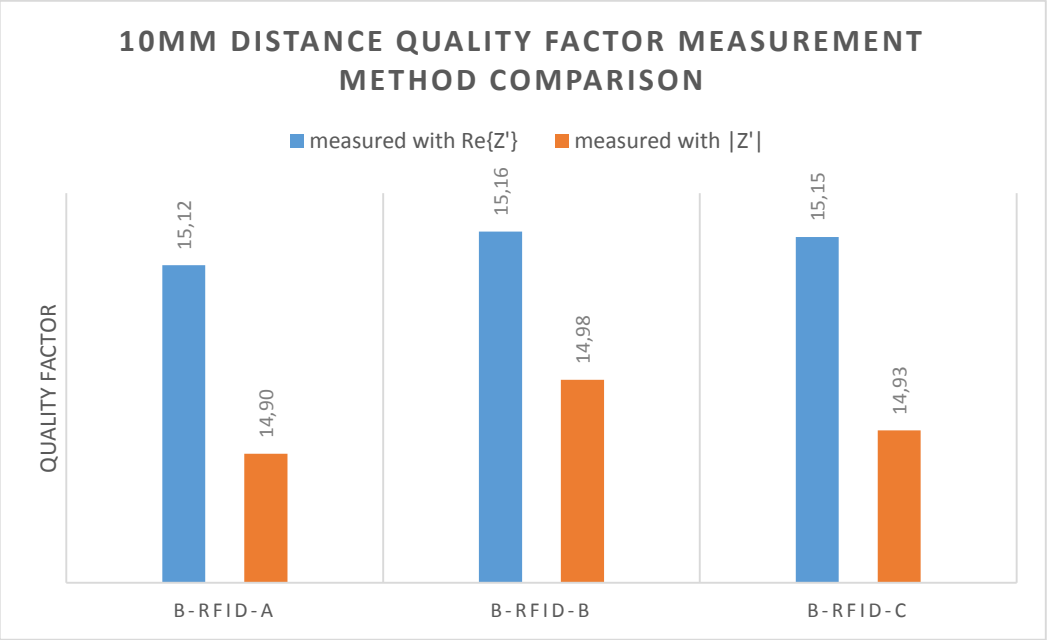

Figure 44: Comparison of the two Quality Factor Measurement Methods for 10mm Distance Measurements

6.3 Measurement Errors According to the Simulation

The simulation is able to show the error made with the different measurement methods. Both, the resonance frequency as well as the quality factor measurement are covered here. The nominal values and the examined ranges of the parameter elements are stated in Table 7 on page 43. This are not all the values of the ECD but that are all values that influence the results. However, just the parameters that cause an error of more than 1% are mentioned here. For the simulation, the ECD of the magnetically coupled reader coil and transponder is used. As the theory, the measurements are based on, requires a current source at the reader coil side, the circuit used for the simulation looks like shown in Figure 45.

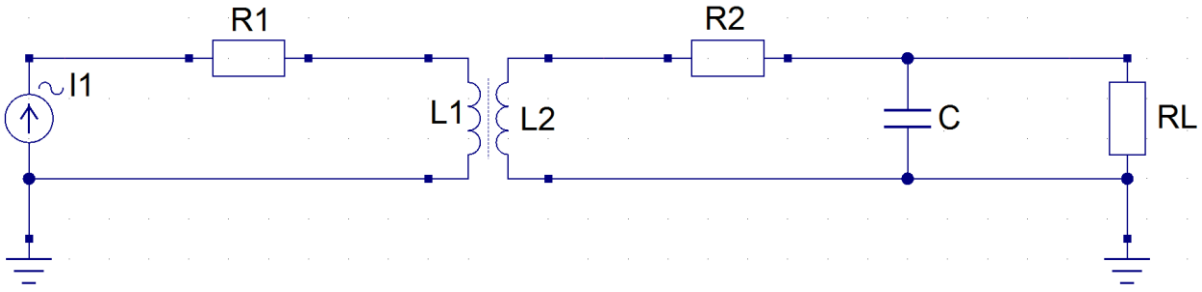

Figure 45: Used ECD for the Error Analysis

In section 3.4, it is stated that the chip resistance R_L is changing over several orders of magnitude. This behavior also affects the measurement accuracy for a certain value range. For small values of R_L, the $|\underline{Z}'|$ measurement method causes an error at the resonance frequency measurement as can be seen in Figure 46. The red line represents the $|\underline{Z}'|$ measurement method. The blue line is the actual resonance frequency and the green line is the resonance frequency obtained with the $Re\{\underline{Z}'\}$ measurement method. This color code also applies for the quality factor measurements. Blue is the actual value, red is the result obtained with the $|\underline{Z}'|$ measurement method and green is the result achieved by using the $Re\{\underline{Z}'\}$ measurement method.

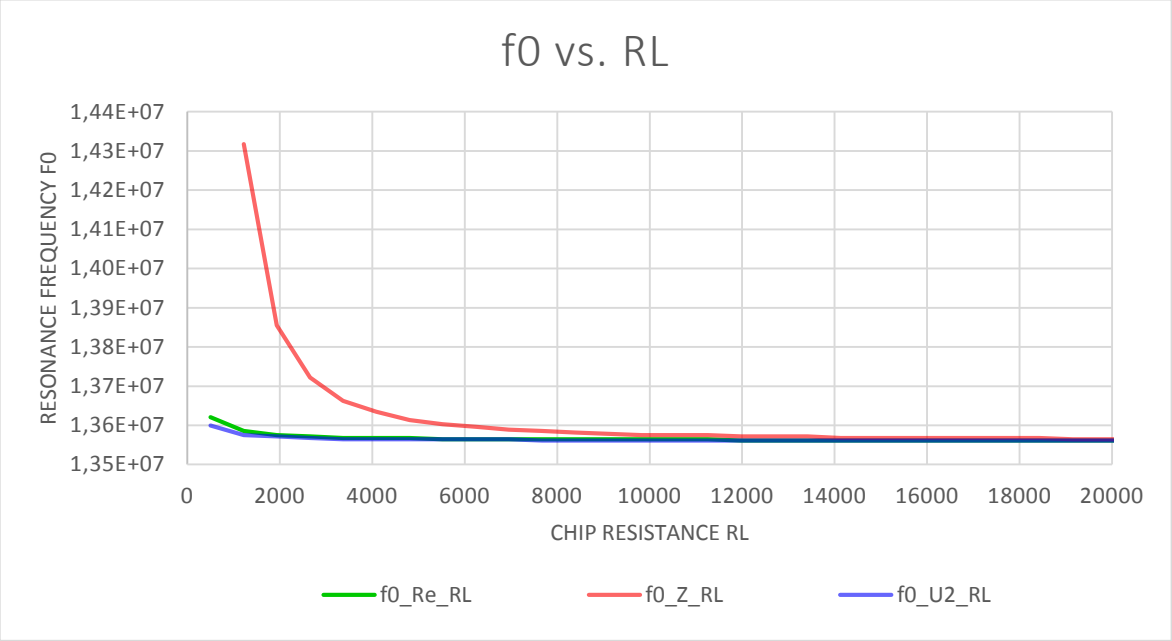

Figure 46: Influence of R_L on the Resonance Frequency Measurement

The relative deviation of the result achieved by the $|\underline{Z}'|$ measurement method goes up to 5.5% in the observed range of R_L. This value, however, depends on the nominal values. It also could be about 10%. This, for example, is true when the capacitance C additionally is changed to $60\ pF$. However, the purpose is not to give detailed numbers but rather to show which parameters of the ECD do affect the measurement methods noticeably. R_L is the only element in the circuit that influences a resonance frequency measurement method in a noticeable way. Therefore, it has to be regarded that the $|\underline{Z}'|$ measurement method is inapplicable for low values of R_L.

The quality factor measurement is on one hand dependent on the resonance frequency and on the other hand on the bandwidth. The RFID chip's resistance can also cause an error

when performing a quality factor measurement. Figure 47 shows this error. The green and the blue line are almost equal in the diagram. Therefore, just two lines can be seen. The $|\underline{Z}'|$ measurement method, again, differs from the actual value. Please, note that it was zoomed in for the purpose of visualization. The x-axis does not show the full range of R_L. The error, again, is noticeable for small values of R_L.

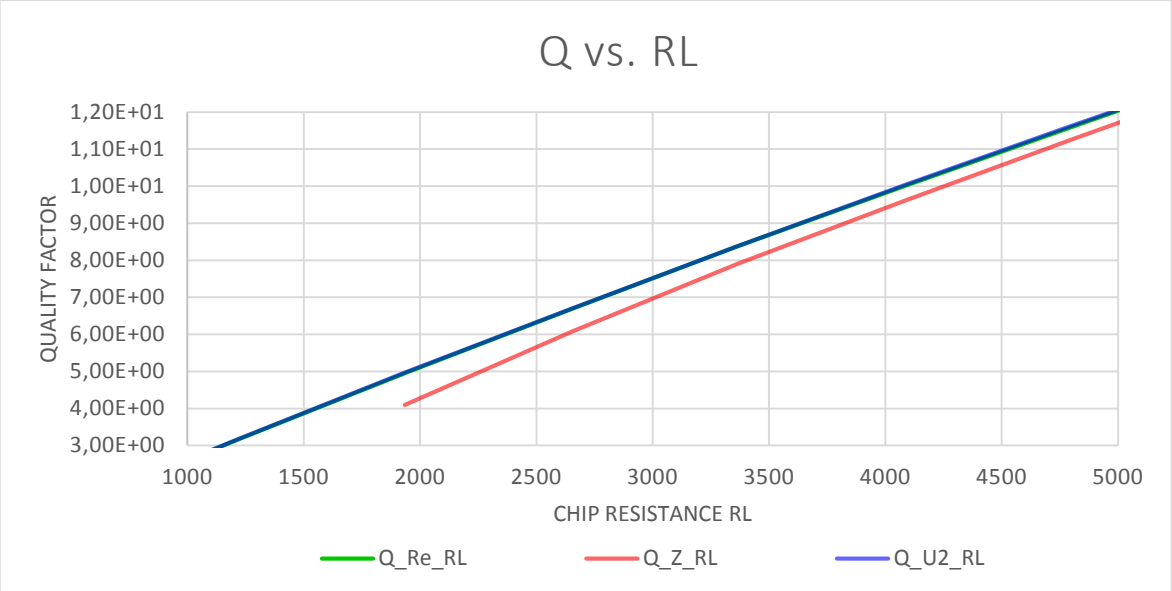

Figure 47: Influence of R_L on the Quality Factor Measurement

In Figure 48, the variable parameter is the chip capacitance C: The green and the blue line are, again, almost equal in the diagram. For small values of C, the $|\underline{Z}'|$ measurement method causes noticeable errors too. Again note that not the whole range of C is displayed in the diagram.

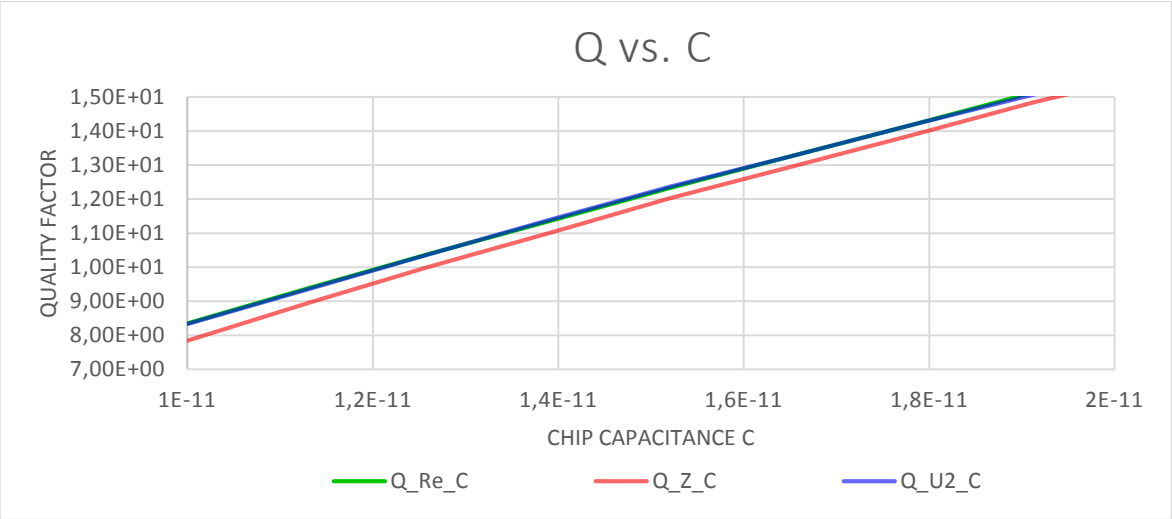

Figure 48: Influence of C on the Quality Factor Measurement

The third parameter that causes noticeable errors is the transponder inductance L_2 for high values. (Figure 49) The horizontal axis does just show the upper end of L_2's range. The $Re\{\underline{Z}'\}$ measurement method matches the line of the real quality factor well. However, the $|\underline{Z}'|$ measurement method has a noticeable deviation. As mentioned, the resonance frequency of the simulated circuit is described with $\frac{1}{\sqrt{L_2 C}}$. This term is kept constant. Therefore, the simulation result shown in Figure 48 and Figure 49 are related to each other. The error made is dependent on the ratio of $\frac{L_2}{C}$. If it is high, the error also is high.

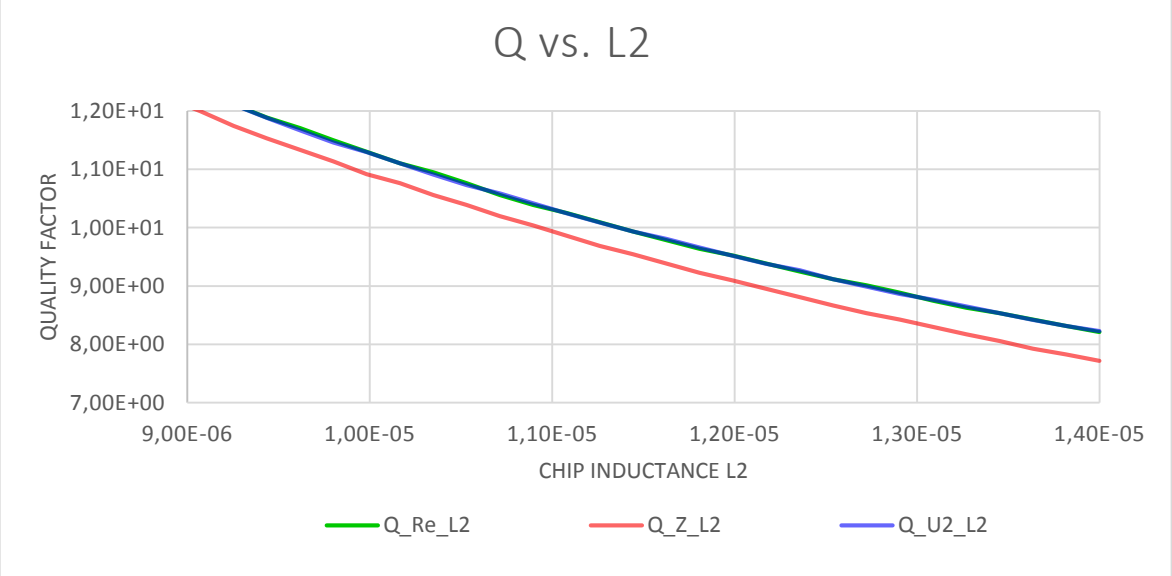

Figure 49: Influence of L_2 on the Quality Factor Measurement

Additionally, it should be mentioned that it is not always possible to measure the resonance frequency or the quality factor with the $|\underline{Z}'|$ measurement method. For example, in Figure 47 on page 59 the red line starts at a higher value of R_L than the other lines do. In the mentioned case, the quality factor cannot be measured for lower values of R_L because the shape of $|\underline{Z}'|$ over the frequency does not have a peak anymore like visualized in an example in Figure 50.

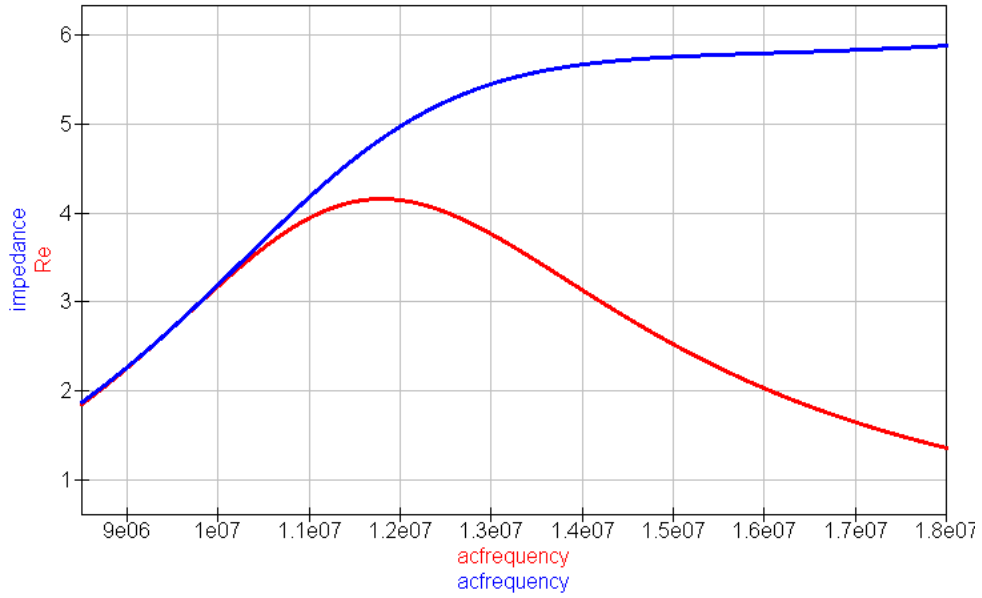

Figure 50: $Re\{\underline{Z}'\}$ and $|\underline{Z}'|$ as a Function of f Show that there is not necessarily a Peak, where the Resonance Frequency can be Measured.

According to the mentioned simulation results, it can be stated that the $Re\{\underline{Z}'\}$ measurement generally obtains more precise results. Therefore, it is preferable to use this measurement method. The measurements that use the absolute value of $\underline{Z}'$ cause an error of more than 1% relative to the actual value for certain conditions: If the value of the chip resistance R_L, is lower than 2.9kΩ, the resonance frequency measurement's error is more than 1%. For the Q measurement, this happens when either R_L is less than 8.5kΩ or the ratio $\frac{L_2}{C}$ is greater than $1.8 \cdot 10^5 \ \frac{kg^2m^4}{A^4 \cdot s^6}$. This is valid for the nominal values that are used for the simulation. (Table 7, page 43)

7 Concluding Chapter

The thesis shows that the measurement methods stated in professional literature are applicable for certain conditions. However, this conditions are often not explained sufficiently. In common literature, there is no difference made between the two measurement methods. The thesis could clarify this conditions and verify the expressiveness of this methods and their results. The derived background of the measurement methods already shows what the simulation approves, namely the greater error that is made with the $|\underline{Z}'|$ measurement methods. The obvious recommendation is to always use the $Re\{\underline{Z}'\}$ measurement method, as the definition that have been explained are primarily based on the resistive $Re\{\underline{Z}'\}$.

Not all of the explained measurement methods are practicable. The method explained in 5.3.2 is not practicable because of the scattering in the results. This method requires a too high measurement accuracy.

The influence of the coupling capacitance could also be verified. However, this results are bound to the used reader coils. Nevertheless, with the explanation in 5.7 the influence of the coupling capacitance also can be assessed for other systems.

References

"CQM Requirements." 2013. MasterCard Worldwide. http://www.smart-consulting.com/wp-content/uploads/2016/03/CQM-Requirements-2013.pdf.

Finkenzeller, Klaus. 2008. *RFID-Handbuch: Grundlagen und praktische Anwendungen von Transpondern, kontaktlosen Chipkarten und NFC*. 5., Aktualisierte und Aufl. München: Hanser.

"ISO/IEC 14443-1 Identification Cards - Contactless Integrated Circuit Cards - Proximity Cards." 2008. ISO copyright office.

Wikipedia. 2016. *Q Factor*. Wikipedia. Accessed May 27. https://en.wikipedia.org/wiki/Q_factor.

Appendix

Table of Appendix Contents

List of Appendix Illustrations

1 Derivation of ω_0 at $\underline{U}_{2_{max}}$ for an inductively coupled transponder and AC voltage source.

In section 3.5 on page 13 the equation [3.16] is derived. This equation describes mathematically the voltage $\underline{U}_2$ across the RFID-chip. Here, it is shown that the resonance frequency where $\underline{U}_2$ gets a maximum cannot be derived analytically.

Initial point of the calculation is the already derived formula for $\underline{U}_2$ in equation [3.16] on page 13.

$$\underline{U}_2 = \frac{j\omega M \underline{U}_1 R_L}{R_L(j\omega L_1 + R_1) + (j\omega C R_L + 1)(j\omega L_2 + R_2)(j\omega L_1 + R_1) + \omega^2 M^2 (j\omega C R_L + 1)} \qquad [0.1]$$

$$\underline{U}_2 = \frac{j\omega M \underline{U}_1 R_L}{\begin{pmatrix}(j\omega L_1 R_L + R_1 R_L) + (-\omega^2 C L_2 R_L + j\omega(L_2 + C R_2 R_L) + R_2) \cdot (j\omega L_1 + R_1) \\ + j\omega^3 C M^2 R_L + \omega^2 M^2\end{pmatrix}}$$

$$\underline{U}_2 = \frac{j\omega M \underline{U}_1 R_L}{\begin{pmatrix} j\omega L_1 R_L + R_1 R_L - j\omega^3 C L_1 L_2 R_L - \omega^2 L_1 (L_2 + C R_2 R_L) + j\omega L_1 R_2 \\ -\omega^2 C L_2 R_1 R_L + j\omega R_1 (L_2 + C R_2 R_L) + R_1 R_2 + j\omega^3 C M^2 R_L + \omega^2 M^2 \end{pmatrix}}$$

$$\underline{U}_2 = \frac{j\omega M \underline{U}_1 R_L}{\begin{pmatrix} -\omega^2 L_1 (L_2 + C R_2 R_L) - \omega^2 C L_2 R_1 R_L + \omega^2 M^2 + R_1 R_L + R_1 R_2 \\ +j \cdot \left(-\omega^3 C L_1 L_2 R_L + \omega^3 C M^2 R_L + \omega L_1 R_L + \omega L_1 R_2 + \omega R_1 (L_2 + C R_2 R_L)\right) \end{pmatrix}}$$

$$\underline{U}_2 = \frac{j\omega k \sqrt{L_1 L_2} \underline{U}_1 R_L}{\begin{pmatrix} \omega^2 \cdot \left(L_1 L_2 (k^2 - 1) - C R_L (L_1 R_2 + L_2 R_1)\right) + R_1 (R_L + R_2) \\ +j \cdot \left(\omega^3 C L_1 L_2 R_L (k^2 - 1) + \omega \left(L_1 (R_L + R_2) + R_1 (L_2 + C R_2 R_L)\right)\right) \end{pmatrix}} \qquad [0.2]$$

The absolute value $|\underline{U}_2|$ is:

$$|\underline{U}_2| = \frac{\omega k \sqrt{L_1 L_2} R_L |\underline{U}_1|}{\sqrt{\begin{pmatrix} \left(\omega^2 \cdot \left(L_1 L_2 (k^2 - 1) - C R_L (L_1 R_2 + L_2 R_1)\right) + R_1 (R_L + R_2)\right)^2 \\ + \left(\omega^3 C L_1 L_2 R_L (k^2 - 1) + \omega \left(L_1 (R_L + R_2) + R_1 (L_2 + C R_2 R_L)\right)\right)^2 \end{pmatrix}}}$$

By introducing the auxiliary variables D, E, F, G and H, $\left|\underline{U}_2\right|$ is expressed with:

$$|\underline{U}_2| = \frac{\omega D}{\sqrt{(\omega^2 E + F)^2 + (\omega^3 G + \omega H)^2}} \qquad [0.3]$$

In order to obtain the resonance circular frequency, $\left|\underline{U}_2\right|$ is differentiated with respect to ω.

$$\frac{d\left|\underline{U_2}\right|}{d\omega} = \frac{D\sqrt{(\omega^2E+F)^2+(-\omega^3G+\omega H)^2} - \omega D\frac{(\omega^2E+F)2\omega E + 3\omega^2G(\omega^3G+\omega H)}{\sqrt{(\omega^2E+F)^2+(\omega^3G+\omega H)^2}}}{(\omega^2E+F)^2+(\omega^3G+\omega H)^2}$$

$$\frac{d\left|\underline{U_2}\right|}{d\omega} = \frac{D((\omega^2E+F)^2+(\omega^3G+\omega H)^2) - \omega D\big((\omega^2E+F)2\omega E + 3\omega^2G(\omega^3G+\omega H)\big)}{((\omega^2E+F)^2+(\omega^3G+\omega H)^2)^{\frac{3}{2}}} \quad [0.4]$$

Now equating it to zero results in [0.5].

$$\frac{d\left|\underline{U_2}\right|}{d\omega} = 0 = (\omega^2E+F)^2+(\omega^3G+\omega H)^2 - \omega\big((\omega^2E+F)2\omega E + 3\omega^2G(\omega^3G+\omega H)\big)$$

$$0 = \omega^4E^2 + 2\omega^2EF + F^2 + \omega^6G^2 + 2\omega^4GH + \omega^2H^2 - 2\omega^4E^2 - 2\omega^2EF - 3\omega^6G^2 - 3\omega^4GH$$

$$0 = \omega^6(-2G^2) + \omega^4(-E^2 - GH) + \omega^2(H^2) + F^2 \quad [0.5]$$

By taking a look at the orders of magnitude listed in the table below, it gets clear that no simplifications of equation [0.5] can be made in order to solve it for ω.

Variables	Order of magnitude
L_2	$4 \cdot 10^{-6}$
C	$3 \cdot 10^{-11}$
R_2	3
R_L	10000
R_1	50
L_1	$5 \cdot 10^{-7}$
k	10^{-1}
ω_0	$9 \cdot 10^{7}$

2 10mm Distance Measurement Results

In this chapter, the 10mm distance measurement results are stated without giving information about the measurements background and the procedure itself. This was already done in chapter 5

2.1 B-RFID-A Measurement Results

2.1.1 R_1 and L_1 of coupling coil

Measured with magnetically uncoupled B-RFID-A reader coil.

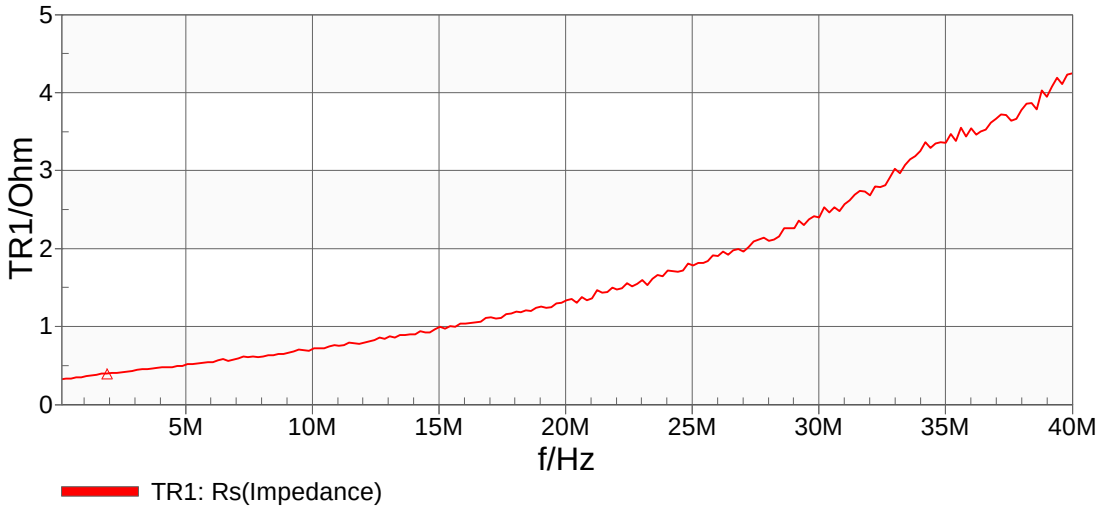

Illustration A: Series Resistance of B-RFID-A Coupling Coil

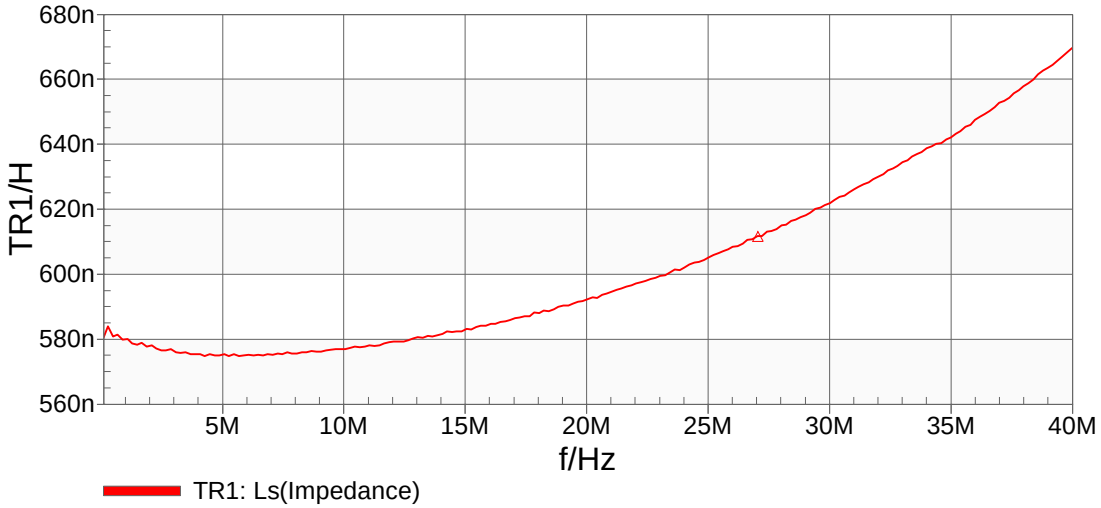

Illustration B: Series Inductance of B-RFID-A Coupling Coil

2.1.2 Resonance frequency measurement

The dashed trace is the obtained result while measuring with a $8dBm$ signal and the solid line was measured with a $-22dBm$ signal. For the measurement result the red line is considered.

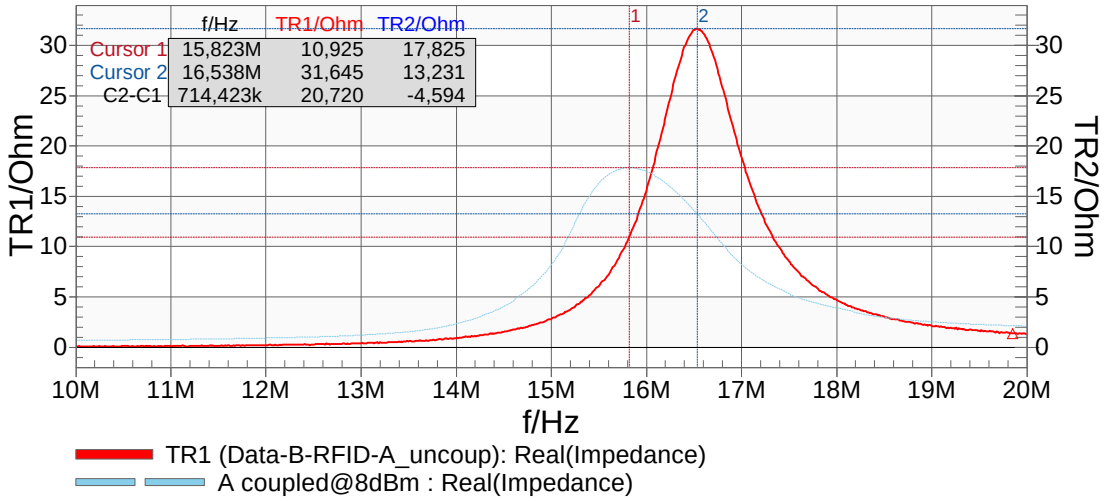

Illustration C: B-RFID-A resonance frequency measurement and influence of dBm level on the result

The obtained resonant frequency f_0 is 16.538MHz.

2.1.3 Quality factor measurement

2.1.3.1 Resonance Frequency to Bandwidth Ratio Definition

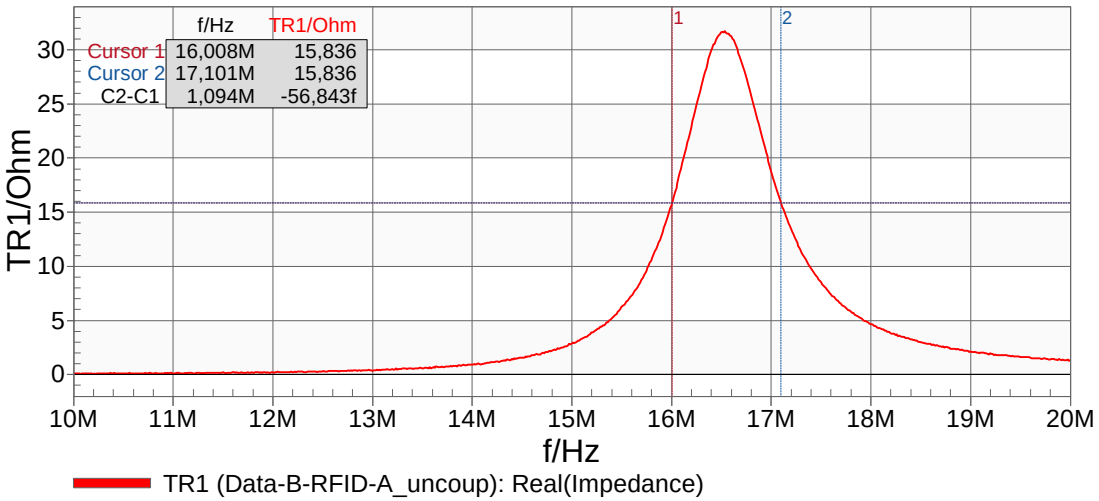

Illustration D: Q Measurement According to the Resonance Frequency to Bandwidth Ratio Definition using the Resistance of $\underline{Z}'$

According to the obtained results stated in Illustration D, the quality factor Q is:

$$Q = \frac{16{,}538MHz}{1{,}094MHz} = 15{,}12$$

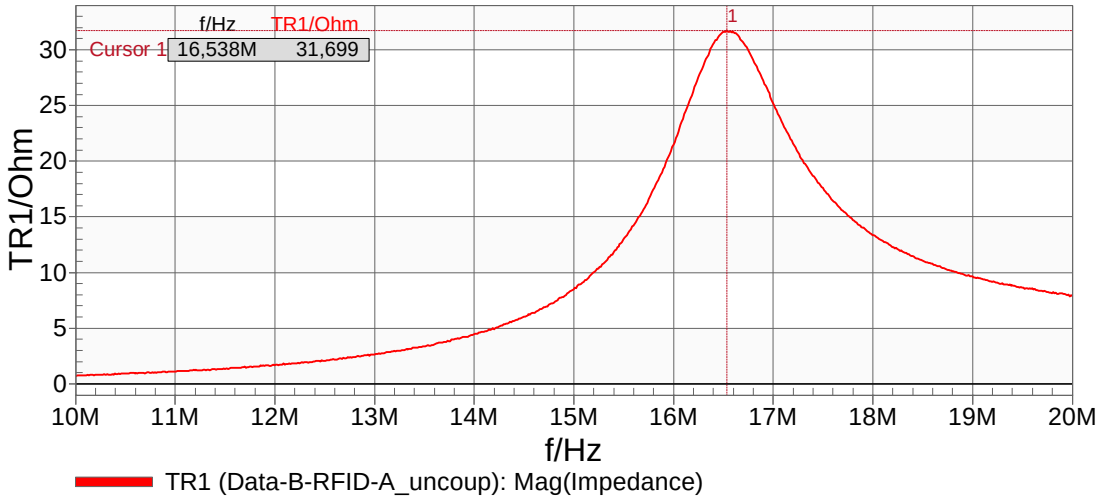

Illustration E: Impedance of Coupled B-RFID-A Coupling Coil

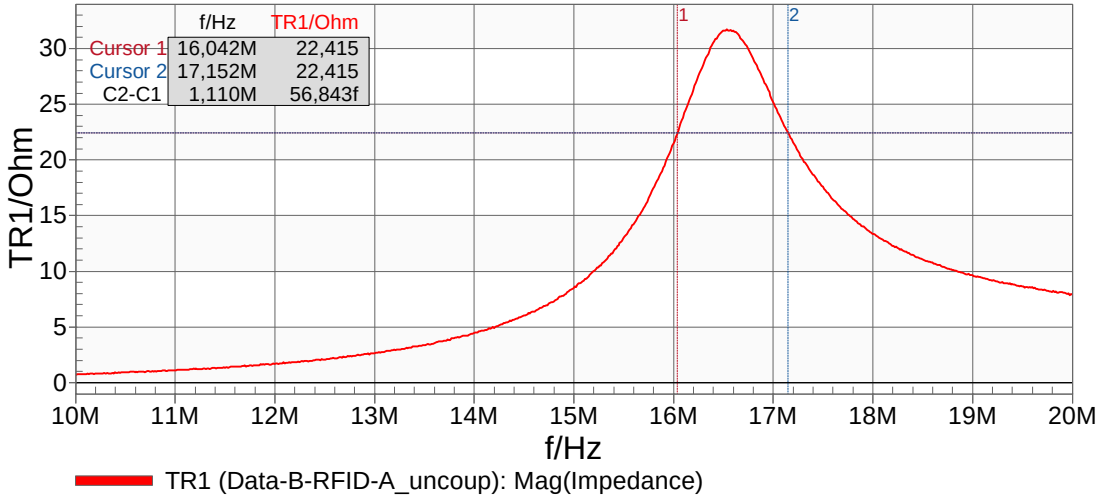

Illustration F: Transformed impedance $\underline{Z}'$ used for Q factor measurement

The Q factor is calculated with $Q = \frac{16{,}538MHz}{1{,}11MHz} = 14{,}9$.

2.1.3.2 Energy Ratio Definition

Now, the Q factor measurement is conducted according to the energy ratio definition stated in section 3.6.1. The mathematical background of this measurement is discussed in section 5.3.2.

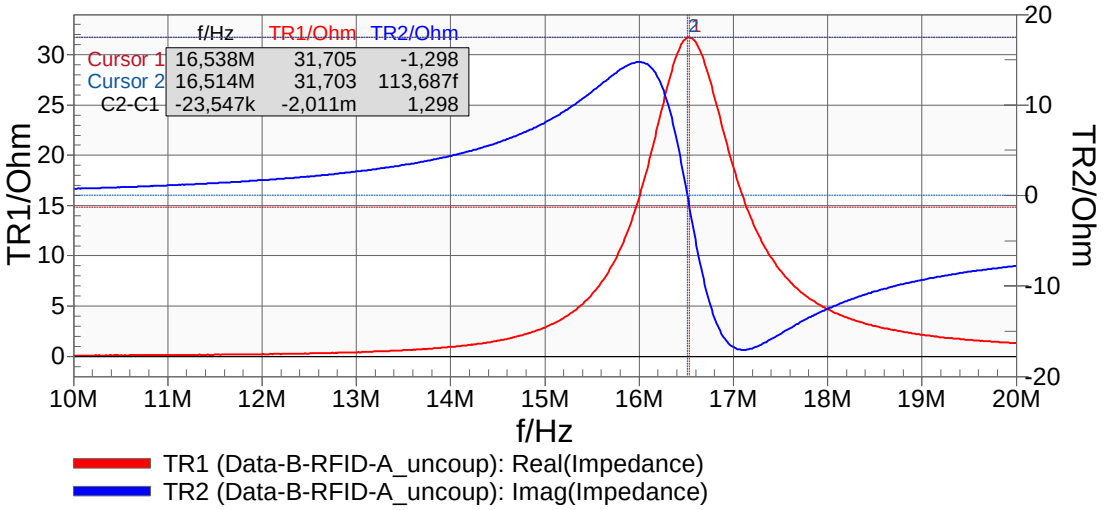

Illustration G: Q Factor Measurement with Resistance and Reactance According to the energy ratio definition.

$$Q = \sqrt{\frac{1}{1 - \left(\frac{16{,}514MHz}{16{,}538MHz}\right)^2}} = 18{,}57$$

2.2 B-RFID-B measurement results

2.2.1 R_1 and L_1 of coupling coil

Measured with magnetically uncoupled B-RFID-B reader coil.

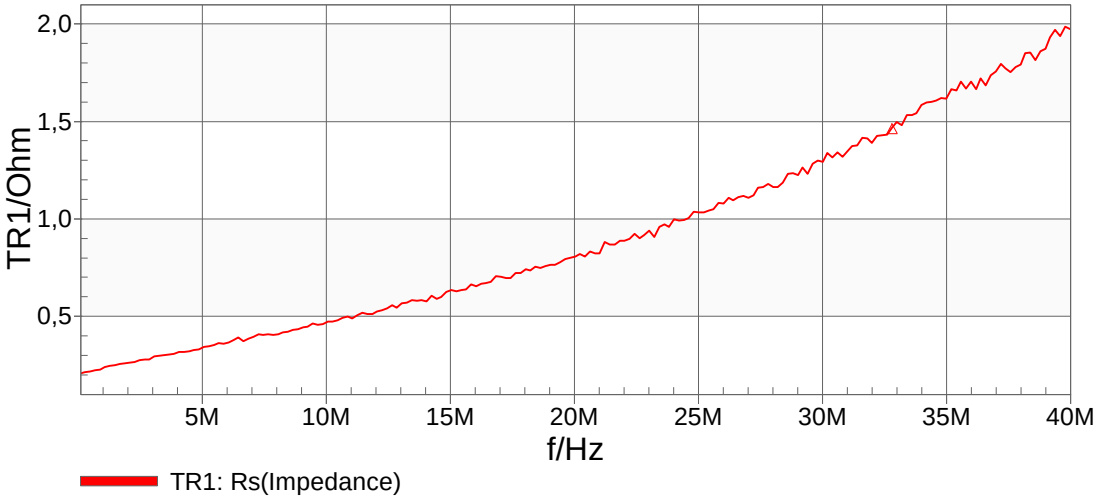

Illustration H: Series Resistance of B-RFID-B Coupling Coil

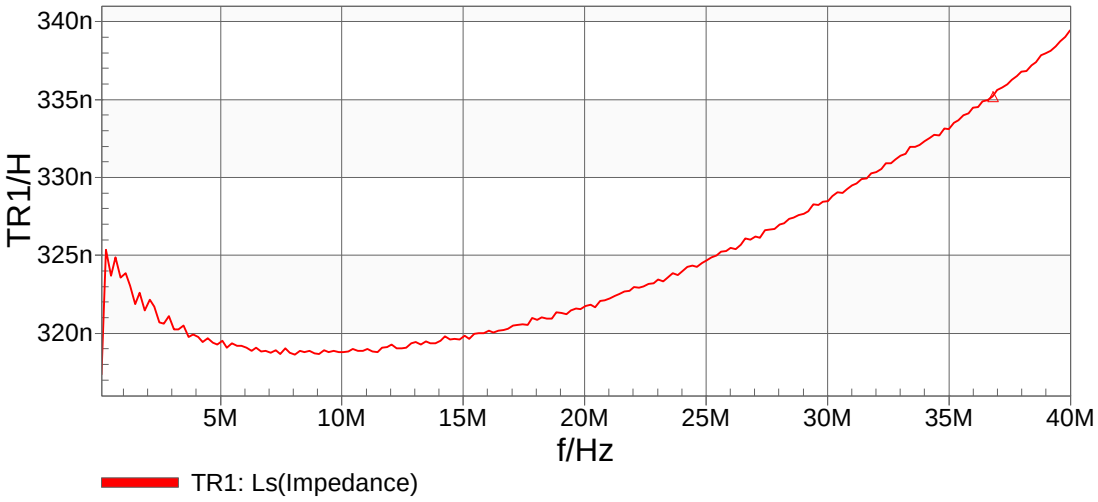

Illustration I: Series Inductance of B-RFID-B Coupling Coil

2.2.2 Resonance frequency measurement

The measurement was conducted with a power level of $-14dBm$. By decreasing the signal power level to this value, it is ensured that the transponder's chip does not get sufficient power to operate, and therefore, it is not influencing the measurement. Illustration J shows the resonant frequency measurement. The obtained resonant frequency is $f_0 = 16.550MHz$.

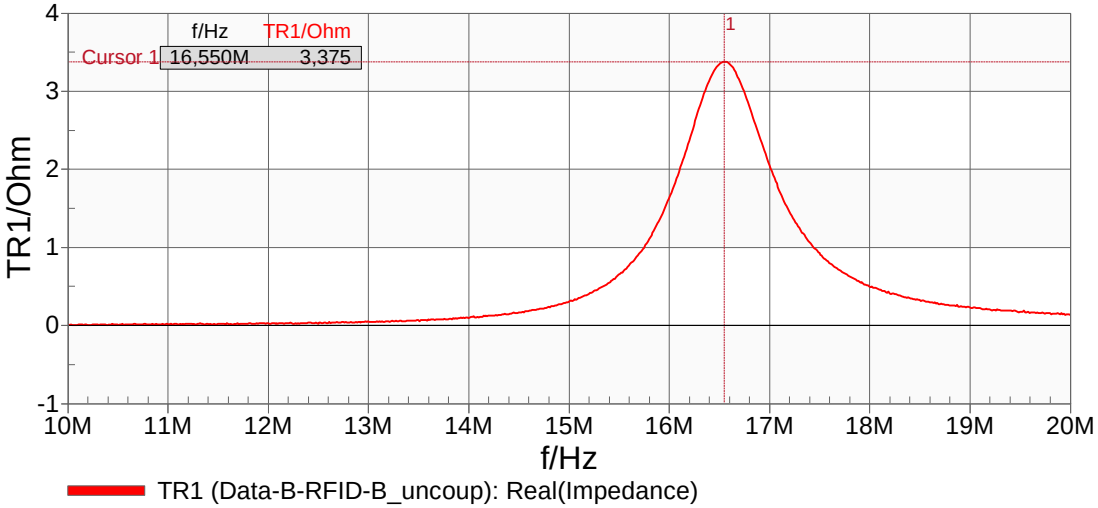

Illustration J: B-RFID-B Resonance Frequency Measurement

2.2.3 Q-factor measurement

2.2.3.1 Resonance Frequency to Bandwidth Ratio Definition

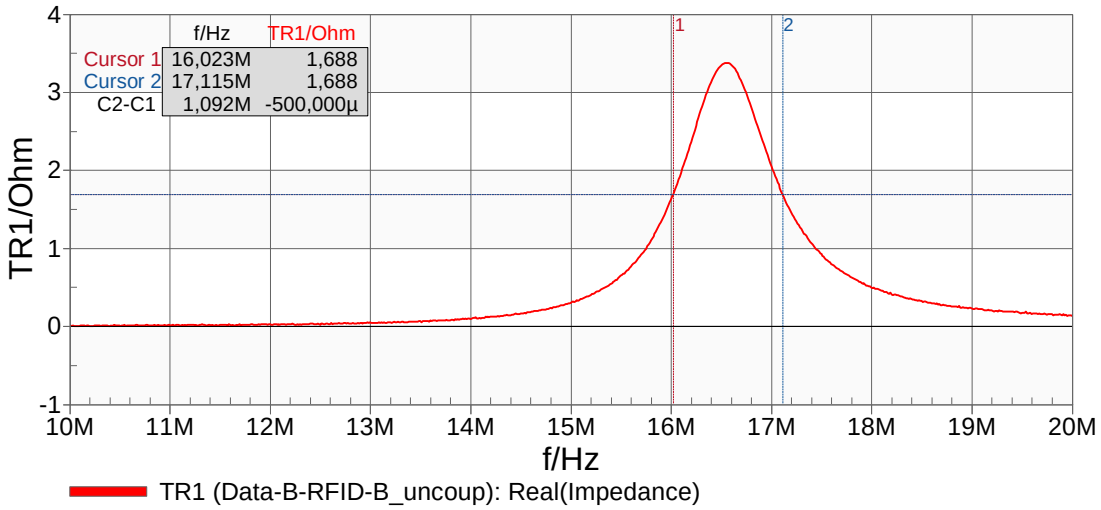

Illustration K: Q Measurement According to the Resonance Frequency to Bandwidth Ratio Definition, using the Resistance of $\underline{Z}'$

The obtained quality factor, according to the resonance frequency to bandwidth ratio, measured via resistance of the transformed impedance $\underline{Z}'$, is $Q = \frac{16{,}550MHz}{1{,}092MHz} = 15{,}15$.

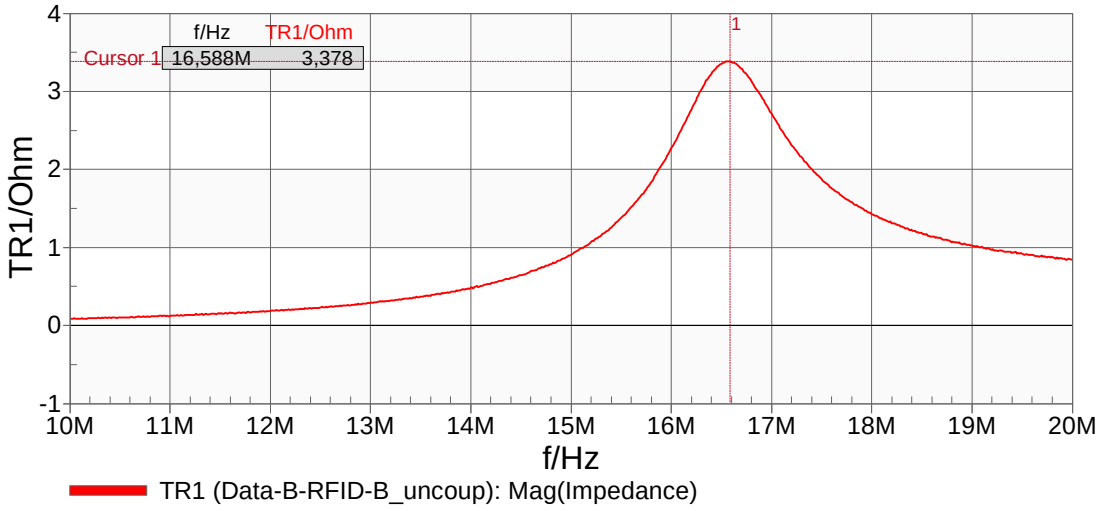

Illustration L: Impedance of Coupled RFID-B Coupling Coil

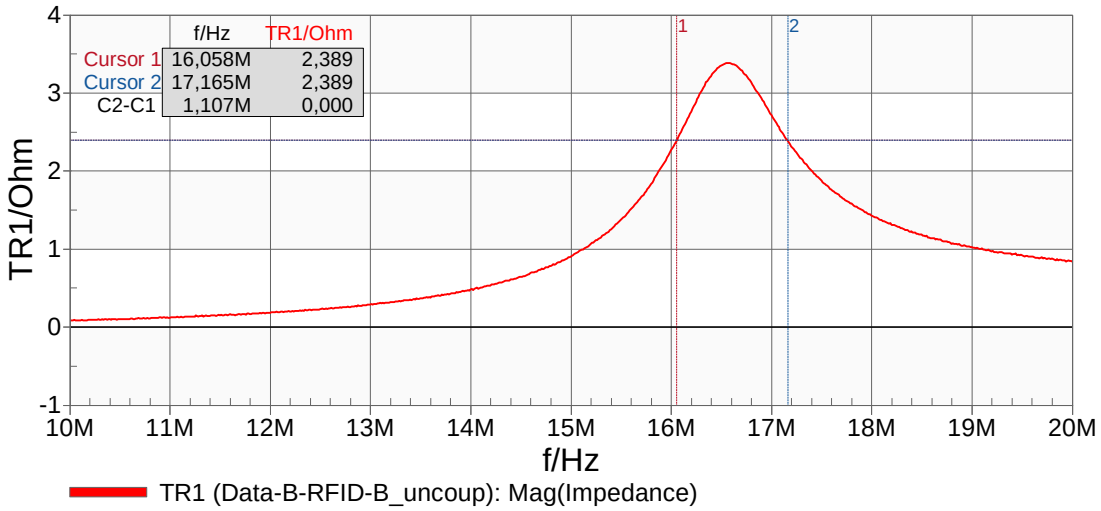

Illustration M: Transformed Impedance $\underline{Z}'$ used for Q Factor Measurement

The obtained quality factor according the resonance frequency to bandwidth ratio definition, measured via the impedance $\underline{Z}'$, is $Q = \frac{16{,}588MHz}{1{,}107MHz} = 14{,}98$.

2.2.3.2 Energy Ratio Definition

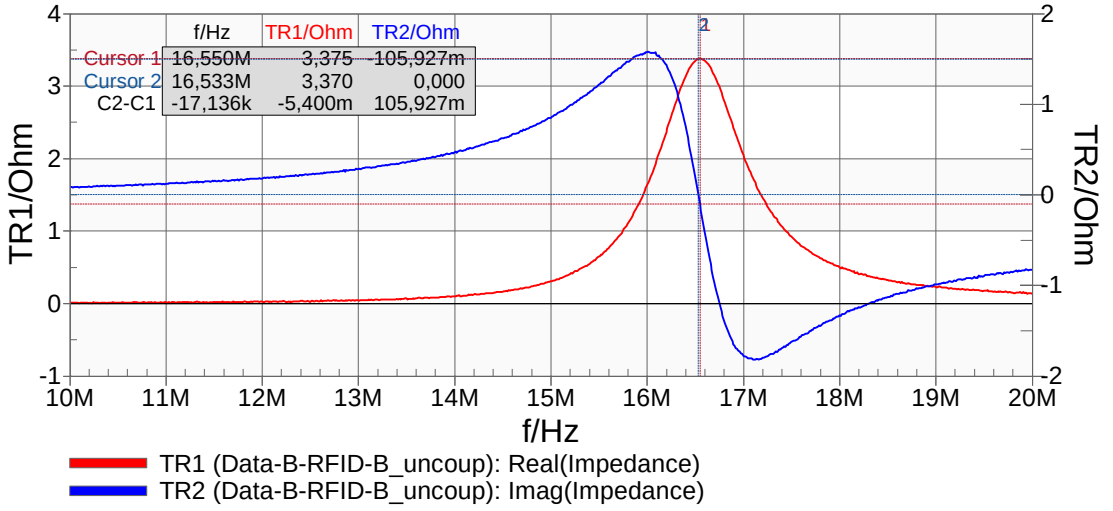

Illustration N: Q Factor Measurement with Reactance and Resistance According to the Energy Ratio Definition

The obtained quality factor according to the energy ratio is $Q = \sqrt{\frac{1}{1-\left(\frac{16{,}533MHz}{16{,}55MHz}\right)^2}} = 22{,}07$.

2.3 B-RFID-C measurement results

2.3.1 R_1 and L_1 of coupling coil

Measured with magnetically uncoupled B-RFID-C reader coil.

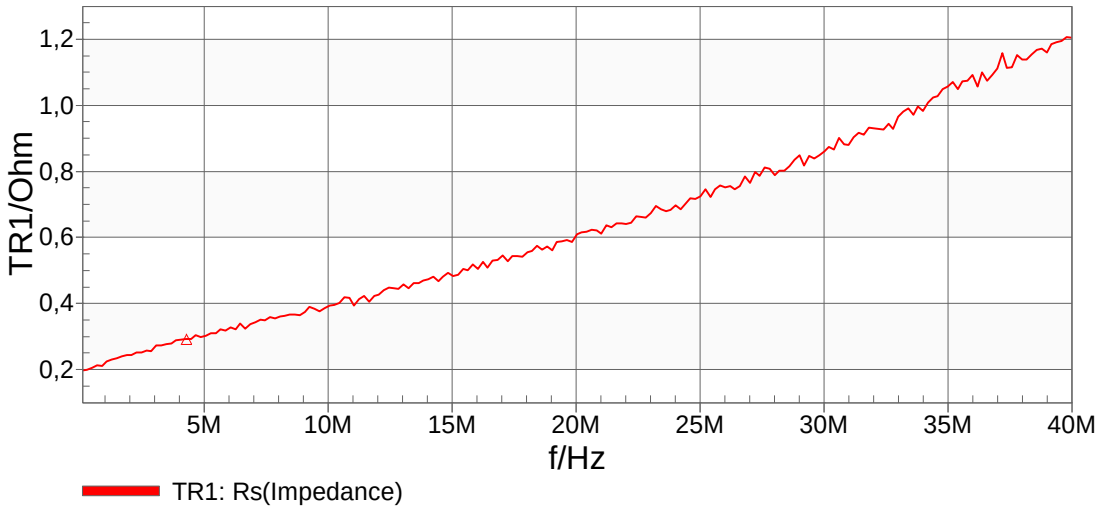

Illustration O: Series Resistance of B-RFID-C Coupling Coil

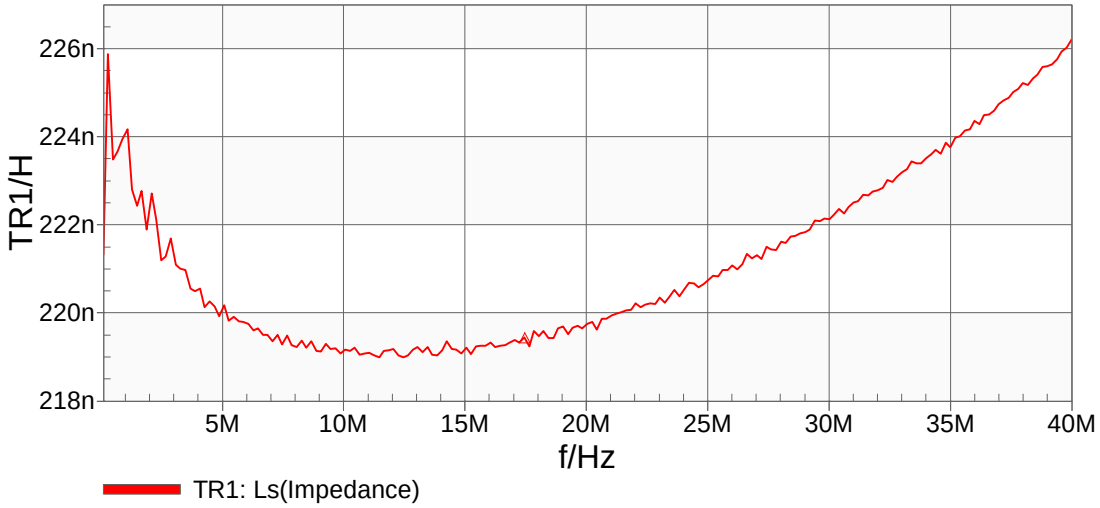

Illustration P: Series Inductance of B-RFID-C Coupling Coil

2.3.2 Resonance frequency measurement

The measurement was conducted with a signal power level of $-4dBm$. According to the measurement stated in Illustration Q, the resonance frequency f_0 is 16.513MHz.

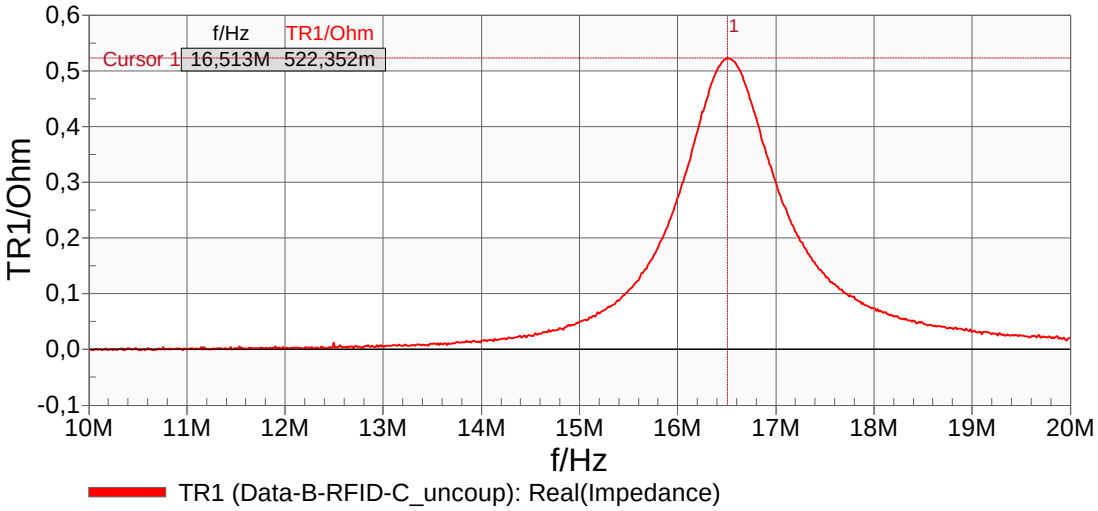

Illustration Q: B-RFID-C Resonance Frequency Measurement

2.3.3 Q-factor measurement

2.3.3.1 Resonance Frequency to Bandwidth Ratio Definition

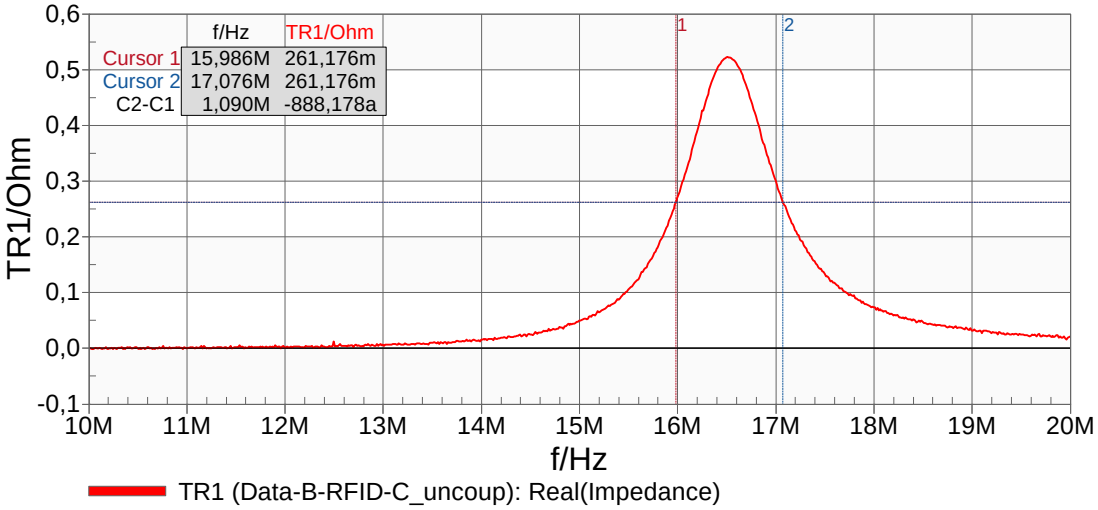

Illustration R: Q Measurement According to the Resonance Frequency to Bandwidth Ratio Definition, using the Resistance of $\underline{Z}'$

The resulting Q factor is $Q = \frac{16{,}513MHz}{1{,}090MHz} = 15{,}15$.

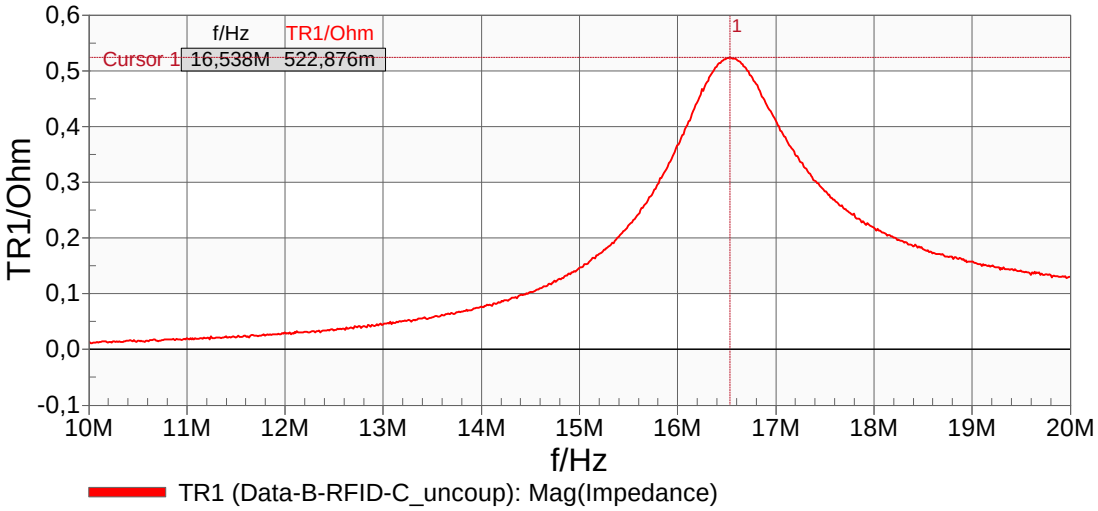

Illustration S: Impedance of Coupled RFID-C Coupling Coil

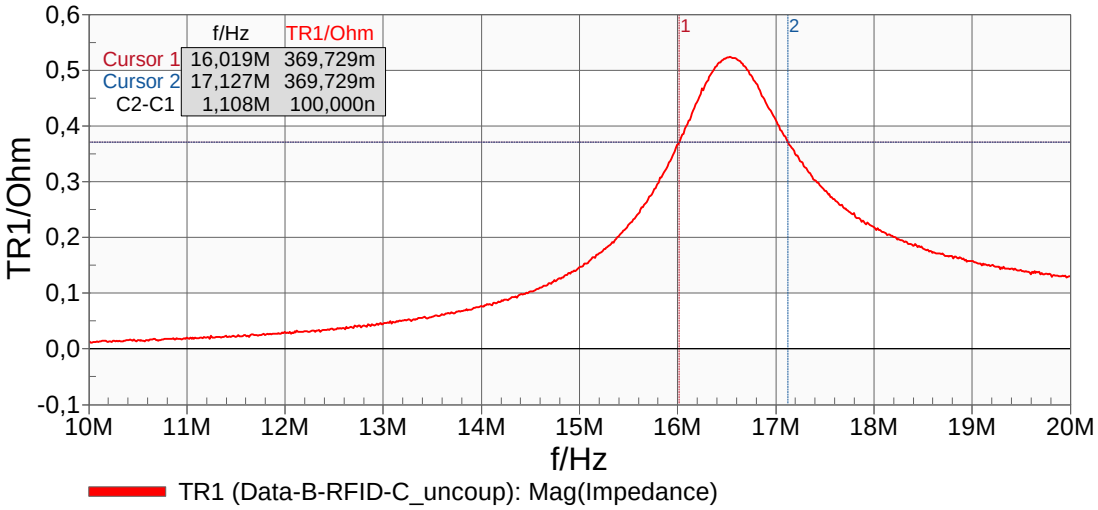

Illustration T: Transformed Impedance Z' used for Q Factor Measurement

The resulting Q factor is $Q = \frac{16{,}538MHz}{1{,}108MHz} = 14{,}93$.

2.3.3.2 Energy Ratio Definition

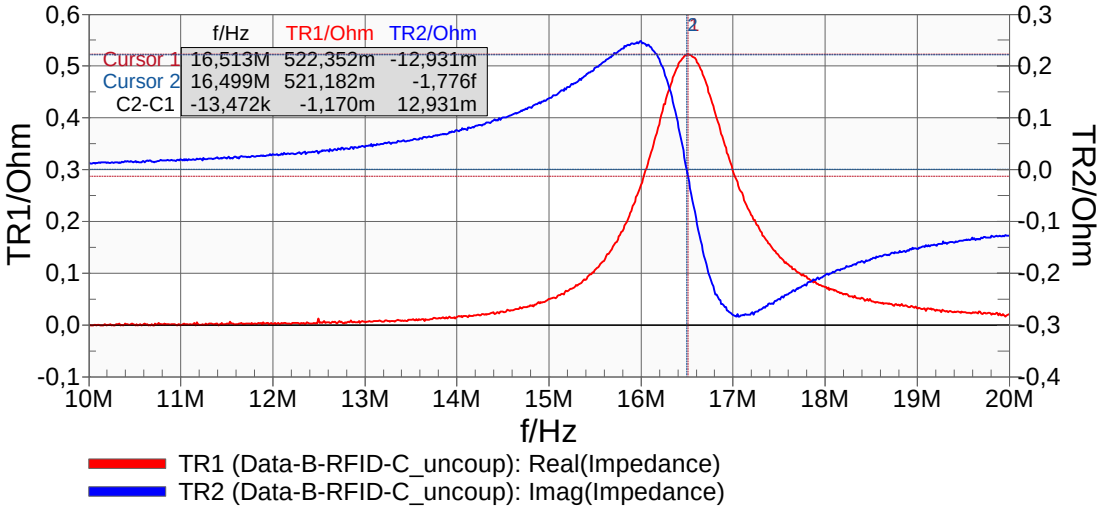

Illustration U: Q Factor Measurement with Reactance and Resistance According to the Energy Ratio Definition

$$Q = \sqrt{\frac{1}{1 - \left(\frac{16{,}499MHz}{16{,}513MHz}\right)^2}} = 26{,}56$$

3 Close Coupled Measurement Results

In this chapter, the close coupled measurement results are stated without giving information about the measurements background and the procedure itself. This was already done in chapter 5

3.1 B-RFID-A measurement results

All measurements stated in this chapter are conducted with the B-RFID-A board. The measurements in this section are conducted with a signal power level of $-18dBm$.

3.1.1 Resonance frequency measurement

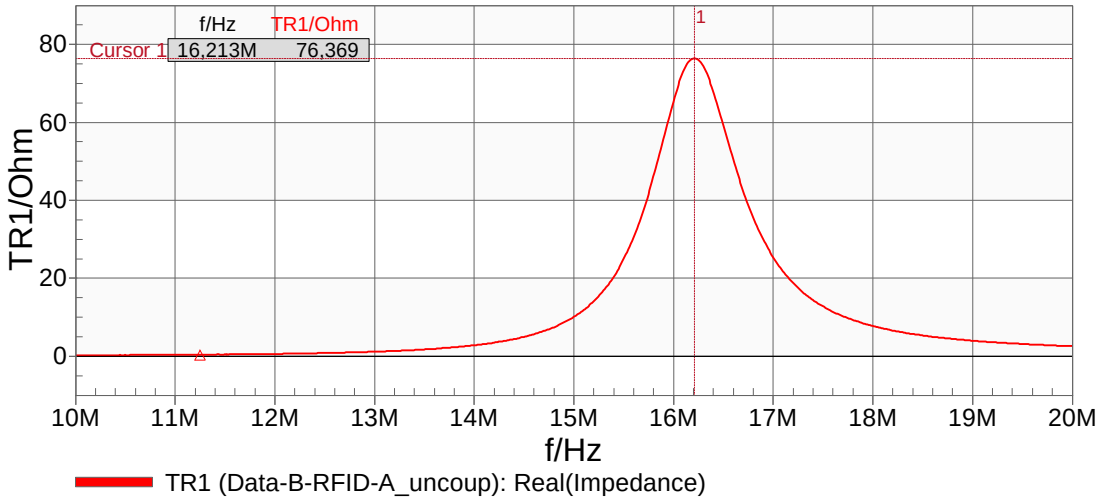

Illustration V: B-RFID-A Resonance Frequency Measurement

For the close coupled measurement, the obtained resonance frequency f_0 is $16{,}213MHz$.

3.1.2 Quality factor measurement

3.1.2.1 Resonance Frequency to Bandwidth Ratio Definition

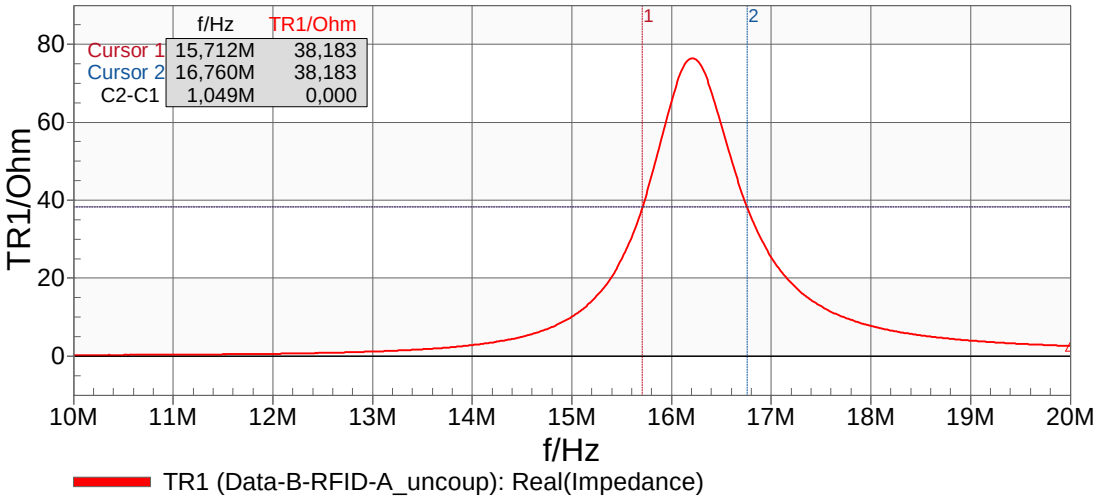

Illustration W: Q Measurement According to the Resonance Frequency to Bandwidth Ratio Definition, using the Resistance of $\underline{Z}'$

$$Q = \frac{16{,}213MHz}{1{,}049MHz} = 15{,}45$$

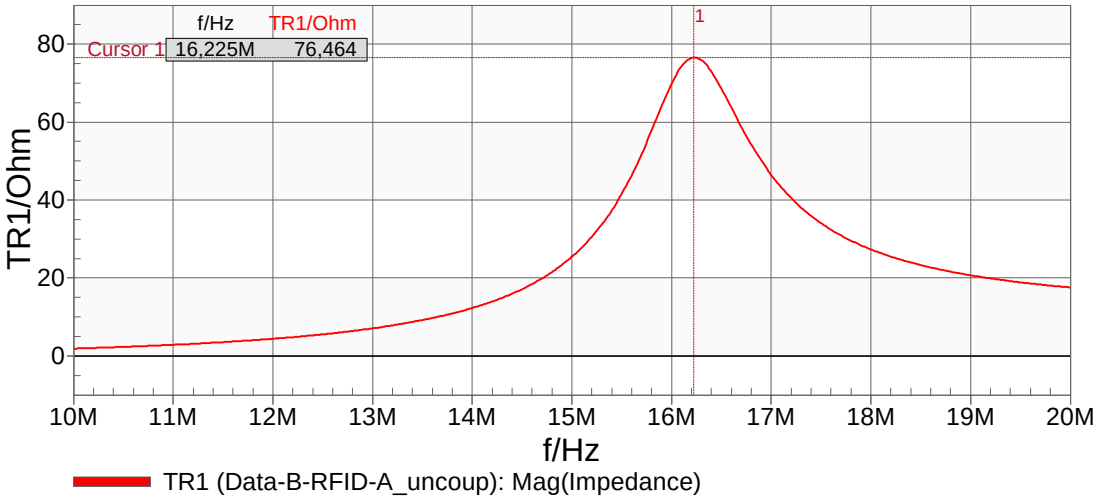

Illustration X: Impedance of Coupled RFID-A Coupling Coil

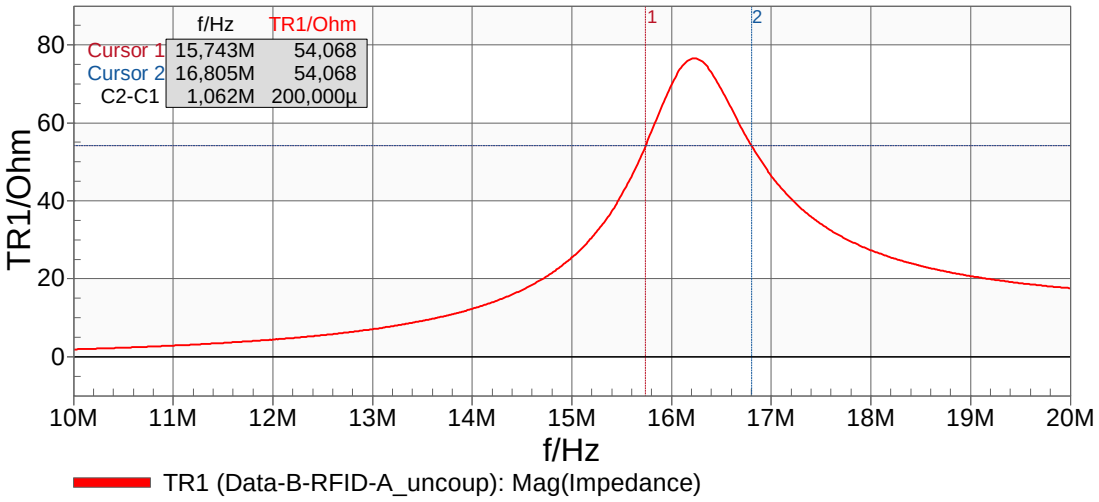

Illustration Y: Transformed Impedance $\underline{Z}'$ used for Q Factor Measurement

$$Q = \frac{16{,}225MHz}{1{,}062MHz} = 15{,}28$$

3.1.2.2 Energy Ratio Definition

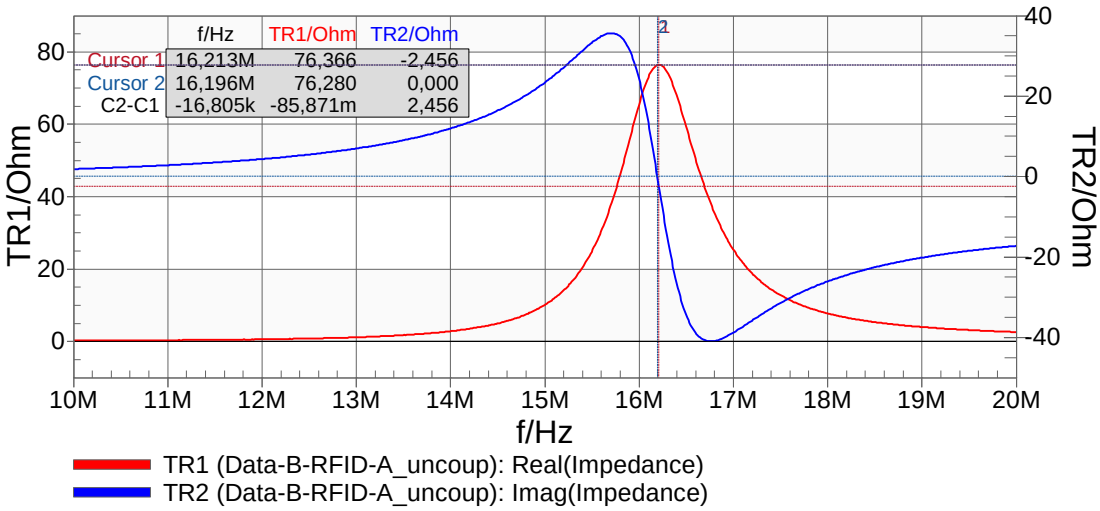

Illustration Z: Q Factor Measurement with Reactance and Resistance According to the Energy Ratio Definition

$$Q = \sqrt{\frac{1}{1 - \left(\frac{16{,}196MHz}{16{,}213MHz}\right)^2}} = 21{,}84$$

3.2 B-RFID-B measurement results

All measurements stated in this chapter are conducted with the B-RFID-B board. The measurements in this section are conducted with a signal power level of $-14dBm$.

3.2.1 Resonance frequency measurement

For the close coupled measurement, the resonance frequency f_0 is $16{,}250MHz$.

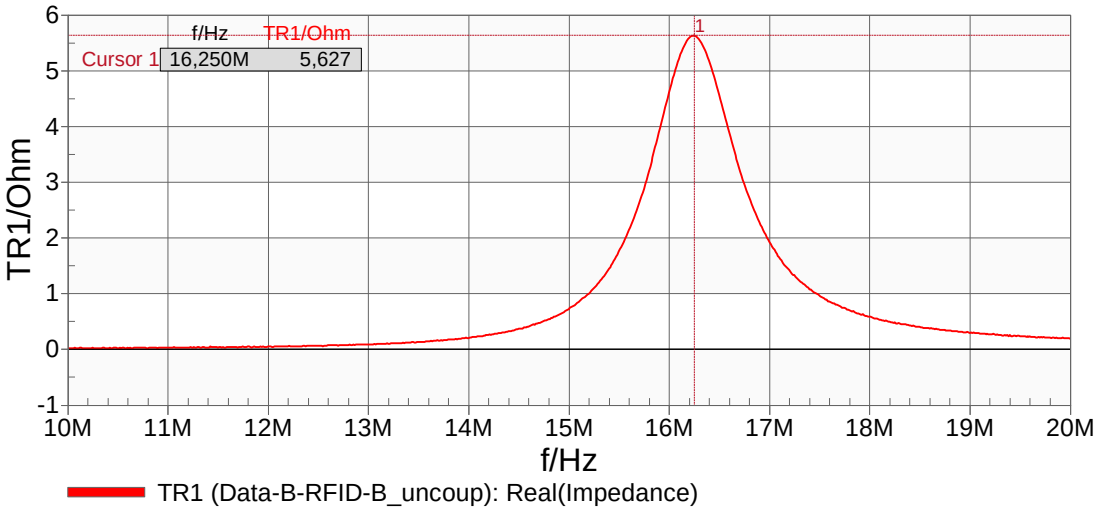

Illustration AA: B-RFID-B Resonance Frequency Measurement

3.2.2 Quality factor measurement

3.2.2.1.1 Resonance Frequency to Bandwidth Ratio Definition

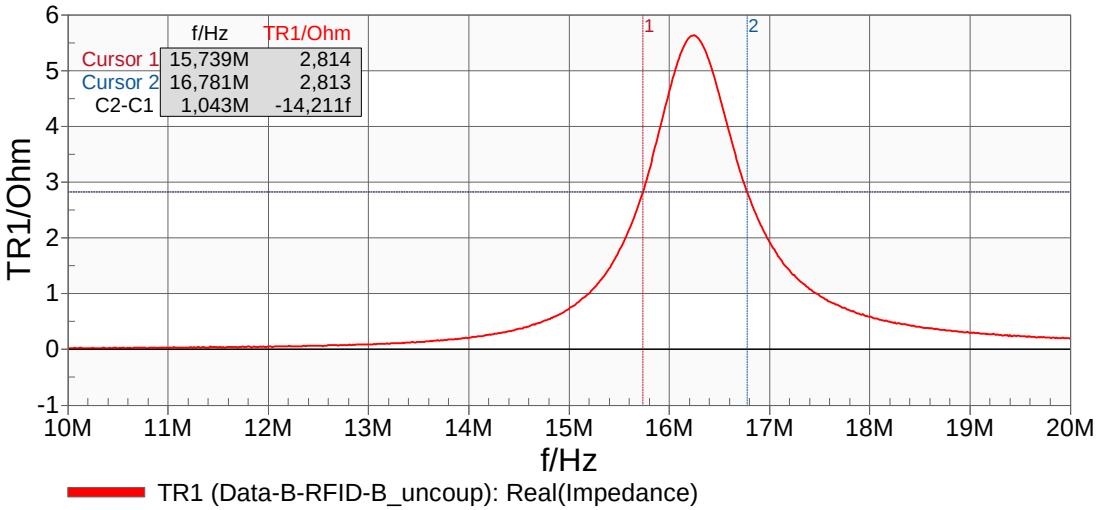

Illustration BB: Q Measurement According to the Resonance Frequency to Bandwidth Ratio Definition, using the Resistance of $\underline{Z}'$

$$Q = \frac{16{,}250MHz}{1{,}043MHz} = 15{,}58$$

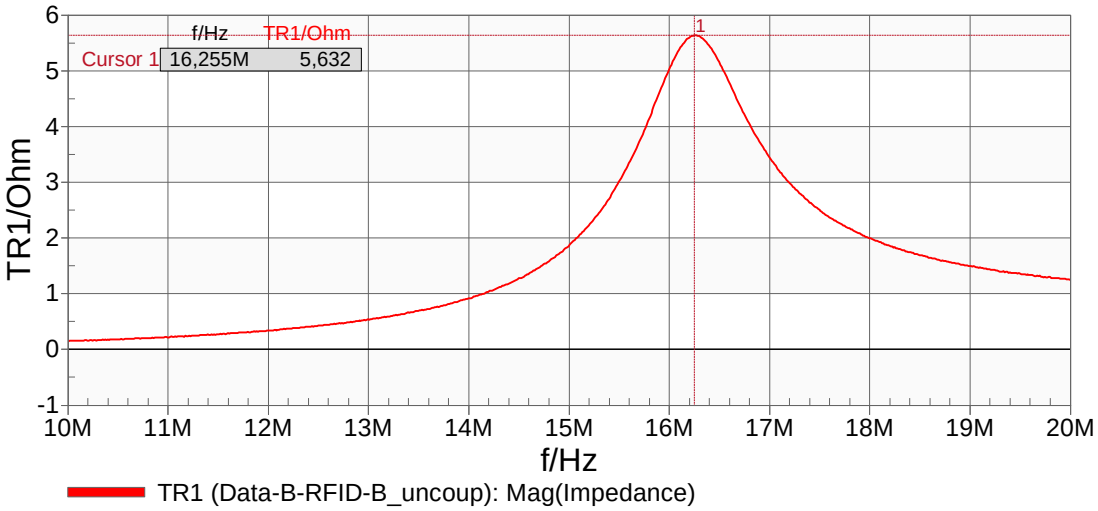

Illustration CC: Impedance of Coupled RFID-B Coupling Coil

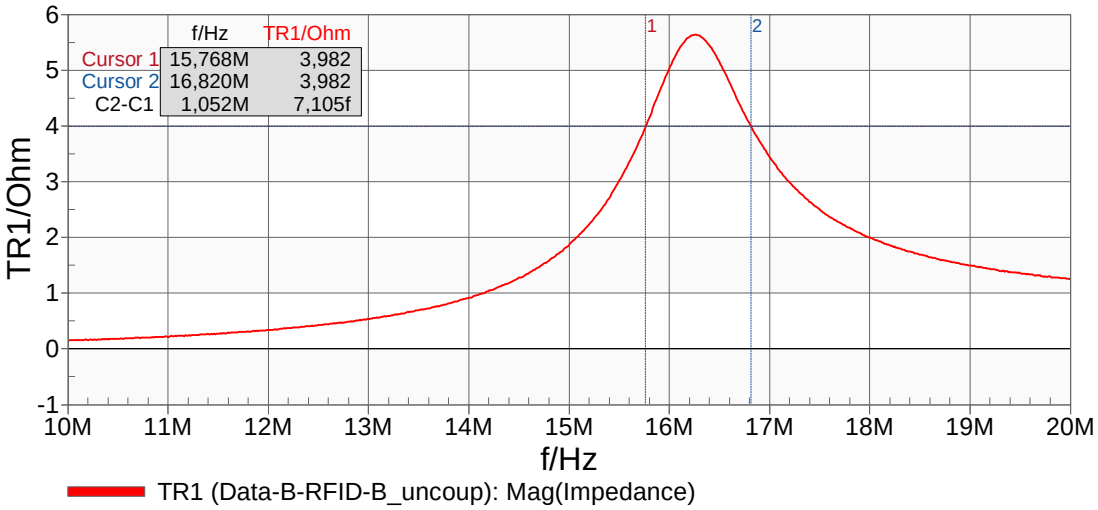

Illustration DD: Transformed Impedance $\underline{Z}'$ used for Q Factor Measurement

$$Q = \frac{16{,}255MHz}{1{,}052MHz} = 15{,}45$$

3.2.2.2 Energy Ratio Definition

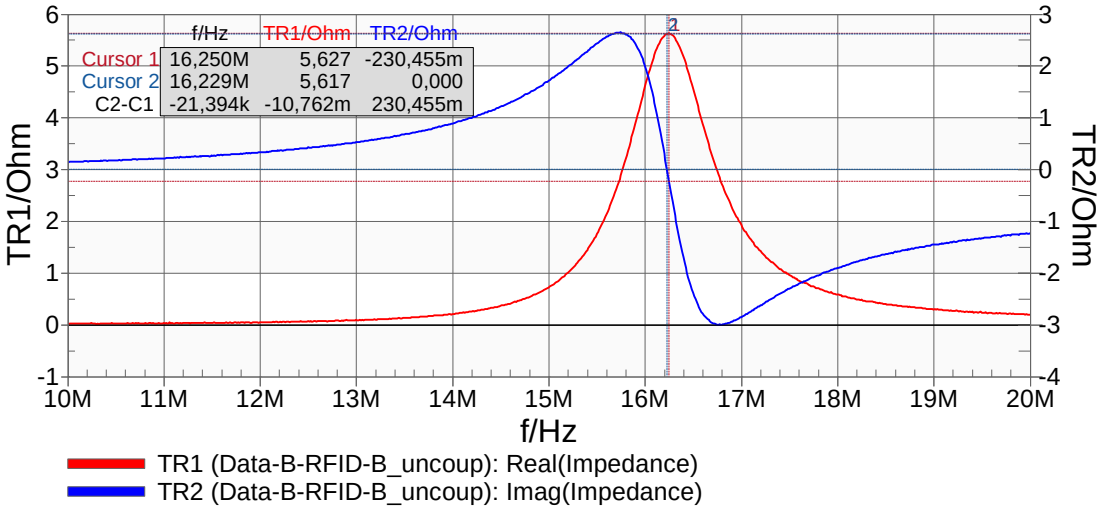

Illustration EE: Q Factor Measurement with Reactance and Resistance According to the Energy Ratio Definition

$$Q = \sqrt{\frac{1}{1-\left(\frac{16{,}229MHz}{16{,}250MHz}\right)^2}} = 19{,}68$$

3.3 B-RFID-C measurement results

All measurements stated in this chapter are conducted with the B-RFID-C board. The measurements in this section are conducted with a signal power level of $-6dBm$.

3.3.1 Resonance frequency measurement

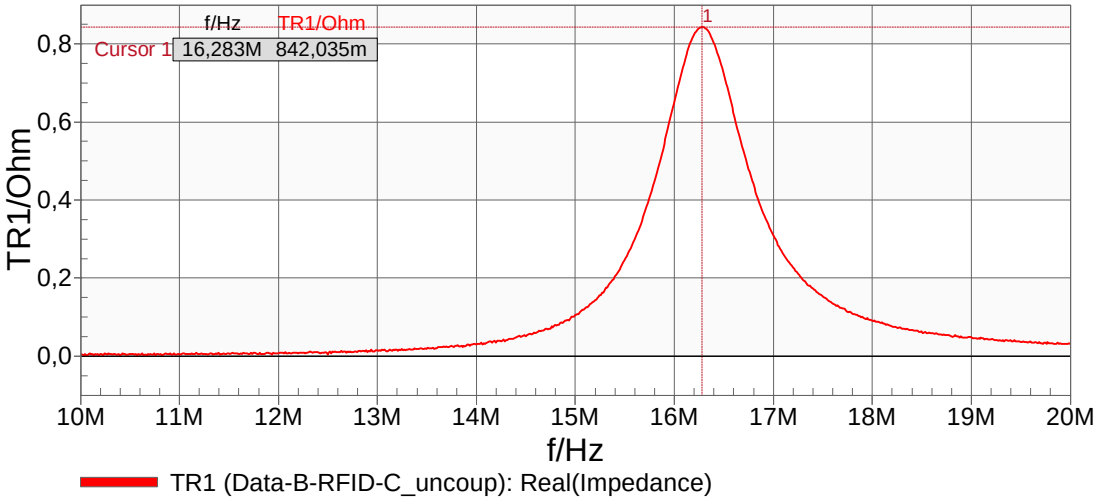

Illustration FF: B-RFID-C Resonance Frequency Measurement

3.3.2 Quality factor measurement

3.3.2.1 Resonance Frequency to Bandwidth Ratio Definition

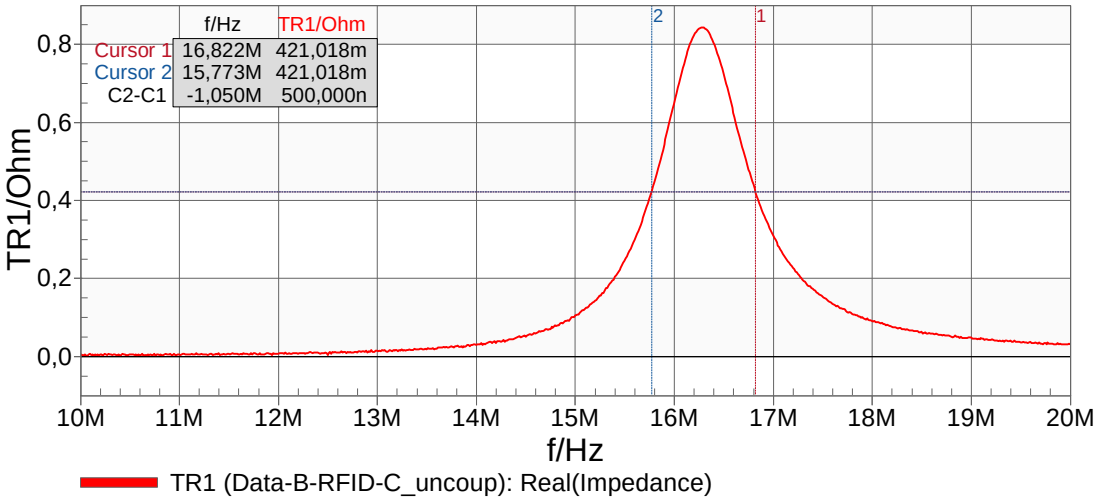

Illustration GG: Q Measurement According to the Resonance Frequency to Bandwidth Ratio Definition, using the Resistance of $\underline{Z}'$

$$Q = \frac{16{,}283MHz}{1{,}050MHz} = 15{,}5$$

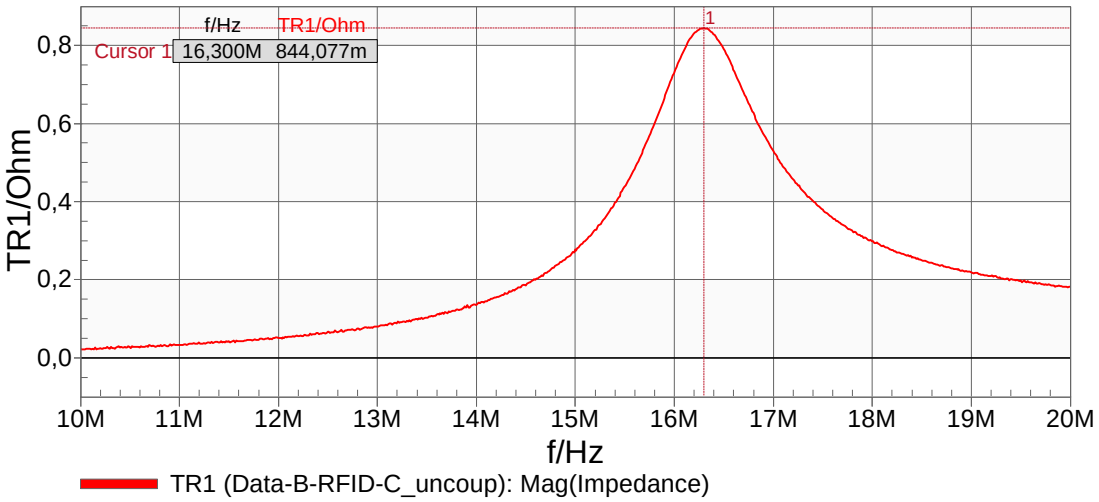

Illustration HH: Impedance of Coupled B-RFID-C Coupling Coil

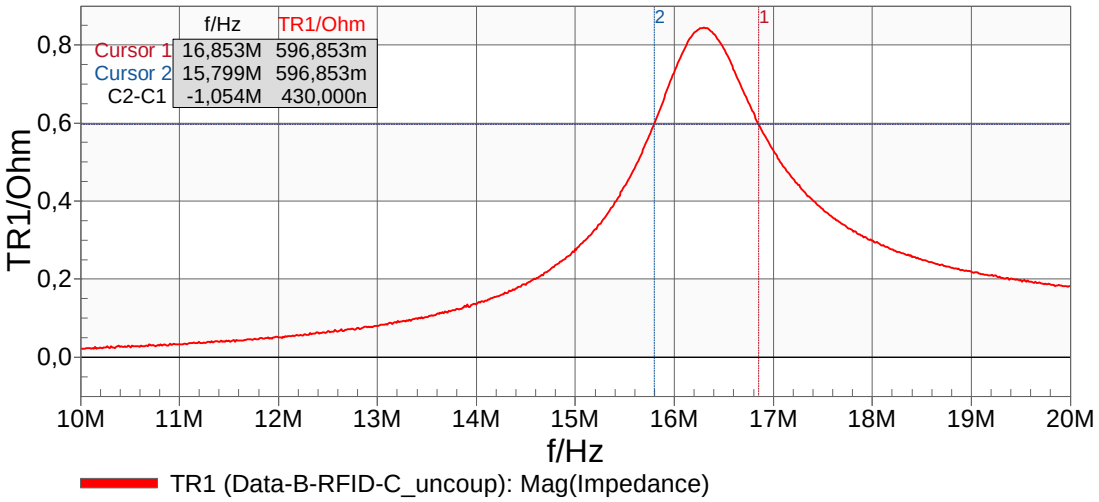

Illustration II: Transformed Impedance $\underline{Z}'$ used for Q Factor Measurement

$$Q = \frac{16{,}3MHz}{1{,}054MHz} = 15{,}46$$

3.3.2.2 Energy Ratio Definition

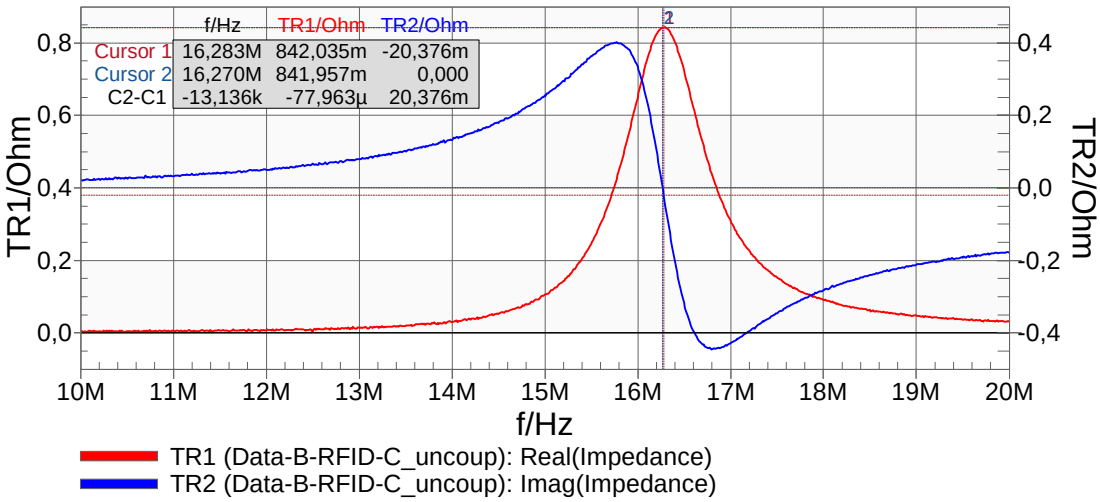

Illustration JJ: Q Factor Measurement with Reactance and Resistance According to the Energy Ratio Definition

$$Q = \sqrt{\frac{1}{1 - \left(\frac{16{,}270MHz}{16{,}283MHz}\right)^2}} = 24{,}9$$

Statement of Affirmation

I hereby declare that all parts of this thesis were exclusively prepared by me, without using resources other than those stated above. The thoughts taken directly or indirectly from external sources are appropriately annotated. This thesis or parts of it were not previously submitted to any other academic institution and have not yet been published.

Dornbirn, 18.06.2016 Martin Dietmar Bitschnau